Bidirectional Akt and Notch1 signaling triggers CLL toward Richter's Transformation

INAUGURAL – DISSERTATION

zur Erlangung des Doktorgrades
der Mathematisch-Naturwissenschaftlichen Fakultät
der Heinrich-Heine-Universität Düsseldorf

vorgelegt von

Vivien Kohlhaas

aus Witten

Düsseldorf, März 2021

Teile dieser Arbeit wurden veröffentlicht:

Kohlhaas, V, Blakemore, SJ, Al-Maarri, M, (2020), **Active Akt signaling triggers CLL toward Richter transformation *via* overactivation of Notch1**. *Blood*. 137 (5):646–660.

Cox, EM, El Behi, M, (submitted), **AKT activity orchestrates marginal zone B cell development in mouse and human**. *Journal of Experimental Medicine.*

Contents

List of Figures

List of Tables

List of Abbreviations

ABC   activated B cell

ACN   Acetonitrile

ADAM   A disintegrin and metalloproteinase

AF594,647   AlexaFluor 594, 647

ALL   Acute lymphocytic leukemia

AML   Acute myeloid leukemia

ANOVA   Analysis of Variance

APC   Allophycocyanin

APS   Ammonium persulfate

ATP   Adenosine triphosphate

BAX   BCL2-associated X protein

BBC3   BCL2 Binding Component 3

BCA   Bicinchoninic acid

BCL2   B cell lymphoma 2

BCR   B cell receptor

bp   Base pair

BSA   Bovine serum albumin

BTK   Bruton's tyrosine kinase

BV421   Brilliant Violet 421

CAG   Chicken β-actin promoter coupled to the CMV enhancer

CCL3,4,22   Chemokine (C-C motif) ligand 3,4,22

CD   Cluster of differentiation

CDK4   Cyclin-dependent kinase 4

CDKN1/2A   Cyclin Dependent Kinase Inhibitor 1/2A

CLL	Chronic lymphocytic leukemia
CML	Chronic myeloid leukemia
Cy5, Cy7	Cyanine5, Cyanine7
Cre	Recombinase from phage PI
C_T	Cycle threshold
DAPI	4′,6-diamidino-2-phenylindole
DEPC	Diethyl pyrocarbonate
DLBCL	Diffuse large B cell lymphoma
DLEU2	Deleted in lymphocytic leukemia 1
DLL	Delta-like protein
DNA	Deoxyribonucleic acid
cDNA	Complementary DNA
gDNA	Genomic DNA
Eμ	*IGHV* promoter and *IGH* enhancer
ECL	Enhanced chemiluminescence
EDTA	Ethylenediaminetetraacetic acid
FACS	Fluorescence activated cell sorting
FDC	Follicular dendritic cell
FDR	False discovery rate
FCS	Fetal calf serum
FISH	Fluorescence in situ hybridization
FOXO1	Forkhead box protein O1
FSC	Forward scatter
GEP	Gene expression profiling
GFP	Green fluorescent protein
GO	Gene ontology
GSI	γ-secretase inhibitor
GSK3b	Glycogen synthase kinase 3 beta

h	Hour
ddH$_2$O	double-distilled water
H&E	Hematoxylin and Eosin
H$_2$O$_2$	Hydrogen peroxide
HES	Hairy enhancer of split
HEY	Hairy/enhancer-of-split related with YRPW motif-like
HRP	Horseradish peroxidase
HSP70	Heat shock protein 70
IFN-γ	Interferon gamma
IG	Immunoglobulin
IGHV	Immunoglobulin heavy chain variable region
IL	Interleukin
IKK	IκB kinase
IVC	Individually ventilated cage
JAG	Jagged
kb	Kilo base pairs
KIF11,23	Kinesin family member 11,23
LANUV	"Landesamt für Natur, Umwelt und Verbraucherschutz"
LFQ	Label-free quantification
dNTP	Deoxynucleotide
MACS	Magnetic cell sorting
MCL	Mantle cell lymphoma
MCM3	Minichromosome maintenance 3
MDM2	Mouse double minute 2 homolog
MECP2	Methyl CpG binding protein 2
MYD88	Myeloid differentiation primary response 88
MZ	Marginal zone
NF-κB	Nuclear factor 'kappa-light-chain-enhancer' of activated B cells

NFATC1	Nuclear factor of activated T cells, cytoplasmic 1
NHL	Non-Hodgkin lymphoma
NICD	Notch intracellular domain
NLC	Nurse-like cell
nm	Nanometer
PBS	Phosphate-buffered saline
PCA	Principal component analysis
PCR	Polymerase chain reaction
qPCR	Quantitative real-time PCR
PDCD10	Programmed cell death 10
PDK1	phosphoinositide dependent kinase 1
PE	Phycoerythrin
PFA	Paraformaldehyde
PI3K	Phospatidyl-inositol-3 kinase
PIP$_3$	Phosphatidylinositol (3,4,5)-trisphosphate
PMSF	Phenylmethylsulfonyl fluoride
PP2A	Protein phosphatase 2A
PTEN	Phosphatase and tensin homolog
PVDF	Polyvinylidene fluoride or polyvinylidene difluoride
RBC	Red blood cell
RBPJ	Recombination signal binding protein for immunoglobulin kappa J region
RIPA	Radioimmunoprecipitation assay
RNA	Ribonucleic acid
scRNA-seq	single cell RNA sequencing
ROSA26	Reverse Oriented Splice Acceptor, Clone 26
rpm	Rounds per minute
RT	Richter's transformation
S100A4	S100 calcium-binding protein A4

SDS-PAGE	Sodium dodecyl sulfate polyacrylamide gel electrophoresis
SEM	Standard error of the mean
Ser	Serine
SHP-1	SH2-containing protein tyrosine phosphatase 1
SLO	Secondary lymphoid organs
SSC	Salinesodium citrate, Side scatter
SYK	Spleen tyrosine kinase
T_{reg}	Regulatory T cells
TBS	Tris-buffered saline
TEMED	Tetramethylethylenediamine
TCL1	T cell leukemia/lymphoma protein 1
TFA	Trifluoroacetic acid
Thr	Threonine
TiO_2	Titanium dioxide
TME	Tumor microenvironment
Tris	Tris(hydroxymethyl)aminomethane
mTOR	Mechanistic Target of Rapamycin
WES	Whole exome sequencing
WHO	World Health Organization
WSS	Westphal stop sequence
Wt	Wildtype
XBP1	X-box binding protein 1
n,μ,m	Nano, micro, mili

Zusammenfassung

Chronische lymphatische Leukämie (CLL) ist die am häufigsten auftretende Leukämieform bei Erwachsenen westlicher Länder und ist charakterisiert durch die Akkumulation von reifen, nicht-funktionalen B-Zellen im Blut und Knochenmark. CLL weist eine variable klinische Manifestation auf, welche je nach Mutationsstatus von einer indolenten bis hin zu einer aggressiven Form reicht. Bis zu 10% der CLL Patienten entwickeln im Krankheitsverlauf ein aggressives Lymphom, die sogenannte Richter Transformation (RT), die meist tödlich verläuft. Trotz der spezifischen RT-assoziierten somatischen Mutationen wie in den *TP53* und *NOTCH1* Genen sind die molekularen Veränderungen, die in der Transformation von CLL zu RT involviert sind, bisher kaum verstanden. In dieser Arbeit wurde die Funktion der AKT Kinase im CLL-Verlauf untersucht. Immunohistochemie von RT-Patienten mit bekanntem Mutationsstatus zeigte, dass AKT hauptsächlich in *NOTCH1*-mutierten Biopsien überaktiviert war. Transgen überaktiviertes Akt im Eμ-*TCL1* CLL-Mausmodell führte zur RT, was durch eine bidirektionale Überaktivierung der Akt und Notch1 Signalwege verursacht wurde. Diese onkogene Kooperation in RT-transformierter CLL hängt von der Tumor-Mikroumgebung (TME) der Milz ab. Die Notch1-Aktivierung in den RT-Zellen wird durch Liganden-präsentierende regulatorische T-Zellen stimuliert, welche wiederum von den RT-Zellen animiert werden, vermehrt Notch-Liganden zu produzieren und zellulär zu expandieren. Diese "manipulative" Wirkung der RT-Zellen auf das TME kann als neuer Ansatz zur Entwicklung von effektiveren Therapien gegen diese aggressive Transformation genutzt werden.

Abstract

Chronic lymphocytic leukemia (CLL) represents the most frequent subtype of leukemia in adults of Western countries and is characterized by the accumulation of mature, nonfunctional B cells in peripheral blood and bone marrow. CLL shows highly variable clinical manifestation ranging from indolent disease to aggressive form advanced by somatic aberrations like in *TP53* and *NOTCH1* genes. In line with this, up to 10% of CLL patients rapidly evolve an aggressive form of CLL, termed Richter's transformation (RT). Although RT-related somatic aberrations have been identified, the molecular mechanisms involved in progression from CLL to RT are still insufficiently understood. In this study, function of the Akt kinase has been investigated in transformation from CLL to RT. Immunohistochemistry of human RT biopsies with identified mutational status revealed aberrant AKT activation in *NOTCH1* mutated samples. Transgenic overactivated Akt in the Eμ-*TCL1* CLL mouse model caused RT *via* bidirectional co-overactivation of Akt and Notch1 signaling. This oncogenic cooperation was critically dependent on the splenic tumor microenvironment (TME) where Notch ligand-expressing regulatory T cells stimulate the Notch1 activation in RT cells. *Vice versa*, RT cells instructed regulatory T cells to express Notch ligands and to expand. This 'manipulative' effect of RT cells on the TME might be used to develop novel therapies against this fatal aggressive transformation.

1   Introduction

1.1   Classification of Blood Cancer

Cancer is defined by the National Cancer Institute as a group of diseases in which abnormal cells uncontrolled proliferate and spread to nearby tissues or through the blood and lymph system to other parts of the body (CNI, 2019). Cancer is responsible for 9.6 million deaths in 2018 and therefore globally the second leading cause of death (F. Bray et al., 2018).

Blood or hematologic cancer represents a heterogeneous group of cancer diseases affecting the immune system and can be divided into leukemia (34%), lymphoma (48%), and multiple myeloma (18% of blood cancer, **Fig.1.1**) (Simon, 2020). More than 900,000 people worldwide (5% of cancer) are annually diagnosed with blood cancer (F. Bray et al., 2018). Depending on age and ethnicity, various blood cancer types are prevalent. The type-dependent causes for blood cancer are rarely understood, probably a combination of genetic aberrations and environmental factors. Somatic alterations can trigger cancer based on activated oncogenes or absent tumor suppressors causing dysregulated differentiation, proliferation, and apoptosis. Mutations occur spontaneously or dependent on lifestyle and environmental factors. Smoking, previous radiation- or chemotherapy, oncoviruses, and family history have been identified as risk factors for the development of blood cancer (Charalambous and Vasileiou, 2012; Esau, 2017).
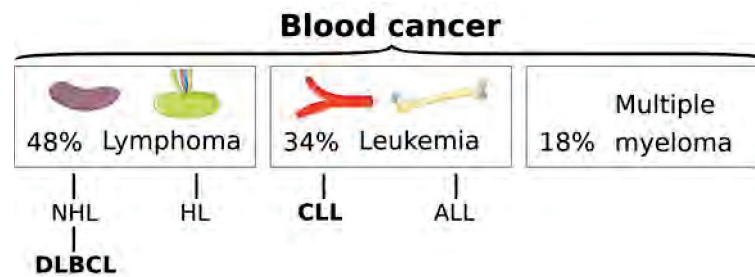
Fig. 1.1: Types and distribution of blood cancer. Blood cancer is divided into lymphoma, leukemia, and multiple myeloma. Lymphomatous cells predominantly affect secondary lymphoid organs including lymph nodes and spleen while leukemic cells affect the bone marrow and blood stream. Cancer cells of lymphoma and leukemia are distinctive leukocytes. A selection of lymphoma and leukemia subtypes that are relevant in this thesis are listed here. ALL: acute lymphocytic leukemia, CLL: chronic lymphocytic leukemia, DLBCL: diffuse large B cell lymphoma, HL: Hodgkin lymphoma, NHL: Non-Hodgkin lymphoma.

1.1.1 Leukemia

In general, leukemia and lymphoma are characterized by the uncontrolled proliferation of leukocytes including lymphocytes. In contrast to the main appearance of lymphomatous cells in secondary lymphoid organs (SLOs) like spleen and lymph nodes, leukemic cells usually accumulate in the bone marrow and spill into the blood stream. Leukemia is the most common pediatric malignancy and the leading cause of cancer death in children (Seth and Singh, 2015). Nevertheless, more cases occur in adults. In epidemiological studies involving 184 countries, the highest incidence rates of leukemia were reported for Australia, the United States, and Europe with a slight prevalence for males (Miranda-Filho et al., 2018). In the GLOBOCAN 2020 statistics report, 6,807 new cases and 2,822 deaths due leukemia are estimated to occur in Germany per year (World Health Organization, 2020).

Leukemia is mainly classified into acute lymphocytic leukemia (ALL), chronic lymphocytic leukemia (CLL), acute myeloid leukemia (AML), and chronic myeloid leukemia (CML) depending on cell type and rate of growth. The incidence of leukemia subtypes varies considerably by age. ALL is the main pediatric leukemia by contributing to 76%

of leukemia patients and 43% of all deaths (Howlader et al., 2012). For adults, the distribution of leukemia is more diverse. However, CLL is the most frequently diagnosed subtype in developed countries. The number of diagnosed cases has more than doubled globally between 1990 and 2017 (Dong et al., 2020). In the United States, CLL is estimated to be the second most common leukemia-related cause of death for 2021 (Siegel et al., 2021). For this reason, further research on CLL is vitally needed to improve therapies and to minimize the proportion of CLL-related deaths.

1.2 Chronic Lymphocytic Leukemia (CLL)

The definition of chronic lymphocytic leukemia (CLL) has changed over the past decades. The World Health Organization (WHO) classification of hematopoietic neoplasias currently describes CLL as a Non-Hodgkin lymphoma (NHL) of mature-appearing, monoclonal B cells with a leukemic progress including the accumulation of cancer cells in peripheral blood and bone marrow (Caligaris-Cappio et al., 1993; Swerdlow et al., 2016). In accordance with a German study, CLL is the most frequent leukemia subtype in developed countries and accounts for approximately 30% of adult leukemia variants as well as 25% of NHLs (Wendtner et al., 2012; Simon, 2020). More than 85% of all countries worldwide exhibit an increase in the age-standardized incidence rate of CLL (Dong et al., 2020). Thereby, CLL is prevalent in aged humans (mean age of diagnosis: 73 years) but rarely found in adults under age 40 and children (Tresckow et al., 2019).

1.2.1 Pathogenesis of CLL

CLL cells are long-lived neoplastic B cells with small cell sizes and the appearance of mature lymphocytes (Rozman and Monserrat, 1995). It is postulated that genetic mutations accumulating with age highly contribute to the outbreak of CLL (Kikushige and

T. Miyamoto, 2014). Using whole exome sequencing (WES), Landau *et al* showed that the loss or addition of large amounts of chromosomal material like *del(11q)*, *del(13q)*, *del(17p)*, and *trisomy 12* may initiate CLL in many cases (Dan A Landau et al., 2015). During CLL progression, further mutations can occur with impact on pathogenesis and prognosis. For instance, mutations in *TP53* and *NOTCH1* genes can contribute to therapy resistance and the transformation of CLL into a more aggressive form, such as Richter's transformation (RT, **Fig.1.2**) (Rossi, Spina, Deambrogi, et al., 2011; Fabbri, Rasi, et al., 2011).
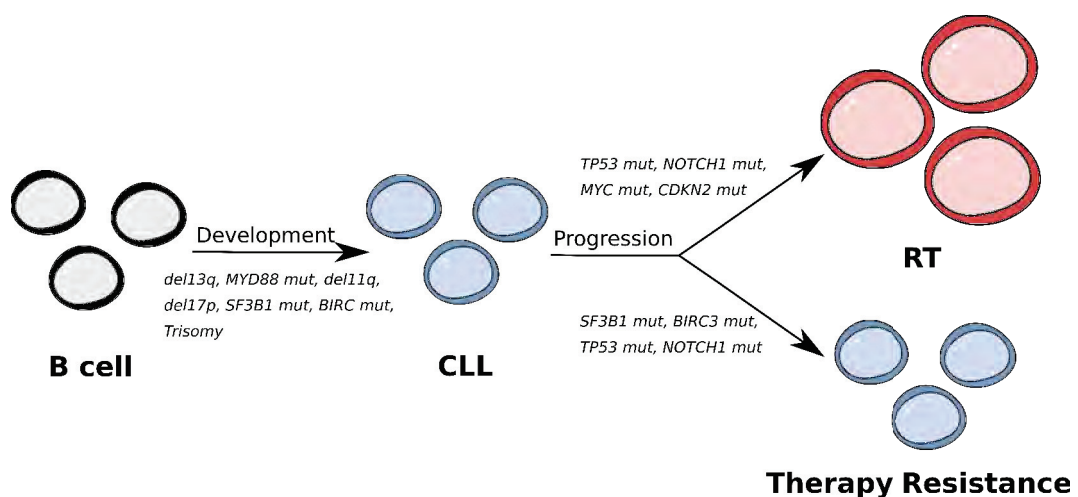
Fig. 1.2: CLL pathogenesis and its frequently involved somatic mutations. A variety of somatic mutations have been identified as being involved in CLL development including *del11q*, *del13q*, and *del17p*. Several mutations are reported to be associated with an aggressive CLL course, such as RT, and therapy resistance including *TP53 mut* and *NOTCH1 mut*. The illustration is done based on the publication of Fabbri *et al* (2016). CLL: chronic lymphocytic leukemia, RT: Richter's transformation.

Individual leukemia cases proceed heterogeneously showing multiple populations of CLL subclones with various somatic mutations, supported by the tumor microenvironment (TME) (see chapter 1.2.4). Dependent on this, CLL subclones evolve through competition based on enhanced survival or reduced apoptosis (Dan A. Landau et al., 2013). Despite the variety of identified genomic abnormalities, neither single nor combined mutations are monitored in all CLL patient consequently causing heterogeneous outcome (Fabbri and Dalla-Favera, 2016). However, determined CLL-specific alter-

ations often affect signaling pathways essential for cell proliferation and apoptosis, such as B cell receptor (BCR), P53, and NOTCH1 signaling (Jan A. Burger and Chiorazzi, 2013; Campo et al., 2018; Rosati et al., 2018).

1.2.2 Richter's Transformation (RT)

Due to its heterogeneity, CLL shows a highly variable clinical manifestation ranging from an indolent disease to an aggressive form. CLL typically features a slow progression compared to other leukemia subtypes that can last for decades initially without the need of any treatments. Nonetheless, up to 10% of CLL patients rapidly evolve an aggressive form, named Richter's transformation (RT), showing a low median survival of approximately 12 months (Y. Wang et al., 2020). RT, initially characterized as a 'reticular cell sarcoma' by Maurice Richter in 1928, defines an uncommon clonal transformation from CLL into an aggressive NHL with histomorphological characteristics of a diffuse large B cell lymphoma (DLBCL) (Richter, 1928; Parikh et al., 2013). RT can occur in all CLL patients unrelated to age, gender or ethnicity. It is often mistakenly assumed that RT represents a late event during CLL course. Instead, studies evidenced that DLBCL-like RT occurs in patients with a short median time of 1.8 years from CLL diagnosis (Parikh et al., 2013). Nearly half of the analyzed CLL cases (47%) develops RT before any treatments become necessary (Tadmor et al., 2014).

1.2.3 Prognostic Indicators and Risk Factors of CLL and RT

Diagnosis is typically done by blood tests or biopsies of lymph nodes and bone marrow using histological and immunophenotypic validation corresponding to the clinical stage according to Rai *et al* and Binet *et al* (Binet et al., 1981; Rai et al., 1975). As histomorphological hallmark, CLL cells of indolent cases are medium-sized neoplastic B cells

with low proliferation rates and prolonged cell survival. Furthermore, leukemic cells are morphologically and immunophenotypically defined as mature lymphocytes. As distinctive characteristic, CLL cells are predominantly identified by consistent co-expression of the common T cell marker CD5 and pan B cell markers like CD19 and CD23 (Hallek et al., 2018; Al-Sawaf, Eichhorst, and Hallek, 2020).

Since RT shows properties of DLBCL, it can be distinguished from CLL by histomorphological changes, such as the diffuse accumulation of large, pleomorphic B cells with increased proliferative capacities. Rapidly enlarged lymph nodes and extranodal sites including splenomegaly are further DLBCL-typical characteristics of RT (Allan and Furman, 2018). Although several molecular indicators like CD5 appear in CLL and RT, single markers specifically predict RT. For instance, ZAP-70 expression (Wąsik-Szczepanek et al., 2018) as well as stereotyped BCR (Rossi, Spina, Cerri, et al., 2009) are approved as indicators for an aggressive course.

In addition, multiple RT-related mutations have been identified as risk factors by several laboratories in recent years. Genomic abnormalities contributing to the progression to RT mainly include *TP53* disruption (Campo et al., 2018), *MYC* or *NOTCH1* activation (Fonseka and Tirado, 2015; Rosati et al., 2018), and *CDKN2A* loss (Martel et al., 1997). Some somatic aberrations are frequently found as clusters. For example, half of RT-transformed CLL patients features somatic alterations of *TP53*, *MYC*, and *CDKN2A* genes or a combination thereof whereas *NOTCH1* mutations correlate with *trisomy 12* in some cases (**Fig.1.3**) (Dan A Landau et al., 2015; Rossi, Spina, Deambrogi, et al., 2011).
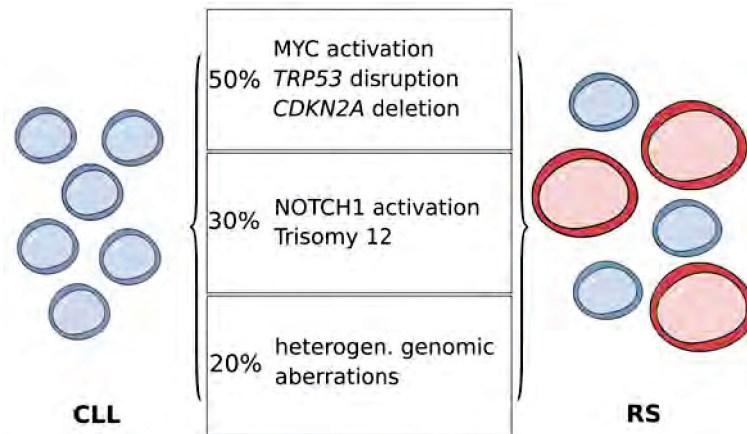
Fig. 1.3: RT-associated somatic aberrations. RT-promoting mutations occur alone or in combination with certain other mutations. Half of the analyzed RT patients show mutations in the *TP53*, *MYC* and *CDKN2A* genes or a combination thereof. *NOTCH1* mutations, *trisomy 12* or both occur in about 30% of RT patients. The other 20% of patients display heterogeneous somatic aberrations. The illustration is done based on Rossi *et al* (2011). CLL: chronic lymphocytic leukemia. RT: Richter's transformation.

1.2.4 Tumor Microenvironment (TME) as Supportive Structure in CLL and RT

The tumor microenvironment (TME) is defined as the surrounding of cancer cells, including various normal cells, blood vessels, and signaling molecules. Cancer progression is influenced by bidirectional communication between cancer and TME cells through several crosstalk mechanisms. Thereby, TME cells affect cell survival, proliferation, migration, and metastasis of cancer cells and further release extracellular signals to favor their own clonal expansion. On the other hand, cancer cells modify the tissue-specific TME to create a favorable surrounding for disease progression (Quail and Joyce, 2013; Hacken and Jan A. Burger, 2016).
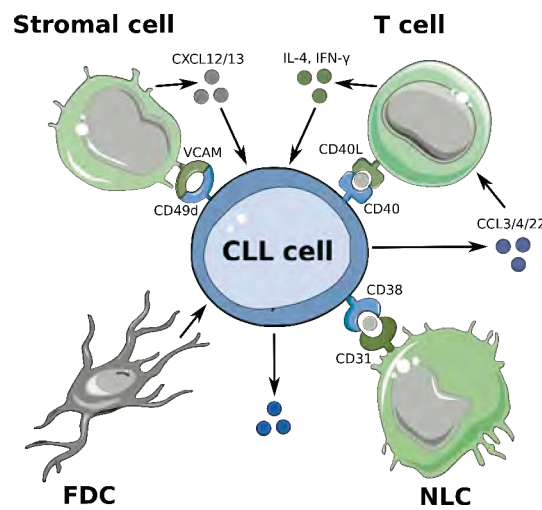
Fig. 1.4: Tumor microenvironmental (TME) cells involved in CLL. Marrow and splenic TME - CLL interactions include FDCs, NLCs, stromal cells as well as T cells and involve a complex network of many pathways. The illustration shows selected interactions and was created using Servier Medical Art. CCL: C-C motif chemokines, CD: cluster of differentiation, CLL: chronic lymphocytic leukemia, CXCL: chemokine (C-X-C motif) ligand, FDC: follicular dendritic cell, IFN-γ: interferon gamma, IL-4: interleukin 4, NLC: nurse-like cell, VCAM: vascular cell adhesion protein.

Over the last decade, marrow and SLO-located TME has been recognized as a pivotal player in CLL (Ten Hacken and Jan A. Burger, 2014; M.K. et al., 2017). There, CLL cells undergo apoptosis until their survival is forced by TME-specific stimuli (Herishanu, Katz, et al., 2013). Cellular and molecular interactions between CLL and TME cells mainly result in the activation of the BCR signaling and its downstream kinases like phospatidyl-inositol-3 kinase (PI3K)/AKT to enhance cell homing and survival of leukemic cells (Oppezzo and Dighiero, 2013). Reported CLL-promoting TME cells include follicular dendritic cells (FDCs) (Heinig et al., 2014), monocyte-derived nurse-like cells (NLCs) (J. A. Burger et al., 2000; Boissard et al., 2015), stromal cells (Kurtova et al., 2009; Lutzny et al., 2013), and diverse T cell subsets (Bagnara et al., 2011) (**Fig.1.4**). For instance, several groups discovered abnormalities in T cell frequencies in blood and SLOs in human and murine CLL (Mackus et al., 2003; Hofbauer et al., 2011; Roessner and Seiffert, 2020). *Inter alia*, accumulation of regulatory T (T_{reg}) cells is confirmed in SLO-derived biopsies of CLL patients and correlates with progressive outcome and

unfavorable genetics (Beyer et al., 2005; Weiss et al., 2011; Biancotto et al., 2012). Numerous proteins and molecules are involved in the communication of CLL cells with the environment, such as chemokines (Jan A. Burger, 2010), interleukins (Dancescu et al., 1992; Francia Di Celle et al., 1996), membrane receptors (Pascutti et al., 2013), and microvesicles or exosomes containing RNA, proteins, and metabolites (Ghosh et al., 2010; Yeh et al., 2015). The communication of T cells with surrounding CLL cells is rarely understood but includes secretion of interleukin 4 (IL-4) (Dancescu et al., 1992) and interferon gamma (IFN-γ) (Buschle et al., 1993) as well as direct interactions by membrane proteins, such as CD40/CD40L (Kitada et al., 1999; Wierda et al., 2000).

1.2.5 Eμ-*TCL1* Transgenic Mouse Model for CLL Investigations

Due to high similarities on genetic and physiological levels, mouse models that mimic human diseases are crucial for medical investigations to understand the underlying pathogenic mechanisms and to develop novel therapies. For CLL studies, mouse models with genetic changes have been generated showing aberrations of CLL-associated genes. Especially the first developed CLL-like mouse model, the Eμ-*TCL1* transgenic mouse line, highly resembles the human malignancy.

Eμ-*TCL1* mice are characterized by exogenous overexpression of the human *T cell leukemia/lymphoma protein 1 (TCL1)* gene under the control of the *IGHV* promoter and *IGH* enhancer (Eμ) causing its expression in immature and mature B cells (Bichi et al., 2002). Upregulated *TCL1* is detected in about 90% of CLL patients with intratumoral heterogeneity at which strong *TCL1* expression correlates with poor prognosis (M. Herling et al., 2006; Marco Herling et al., 2009). The pathogenic mechanism underlying overexpressed *TCL1* remains unsolved, probably a combination of transcriptional and epigenetic alterations initiated by TME-specific stimuli (Yuille et al., 2001; French et al., 2003). In CLL, TCL1 is reported to function *inter alia* as activator of the serine/threo-

nine kinase AKT (Laine et al., 2000; Y. Pekarsky, 2000) and the nuclear factor 'kappa-light-chain-enhancer' of activated B cells (NF-κB) pathway (Gaudio et al., 2012; Yuri Pekarsky et al., 2008) or as inhibitor of DNA (cytosine-5)-methyltransferases (DNMT3A and DNMT3B) (Palamarchuk et al., 2012; Biran et al., 2019). As consequence, TCL1 promotes proliferation and survival of malignant B cells.
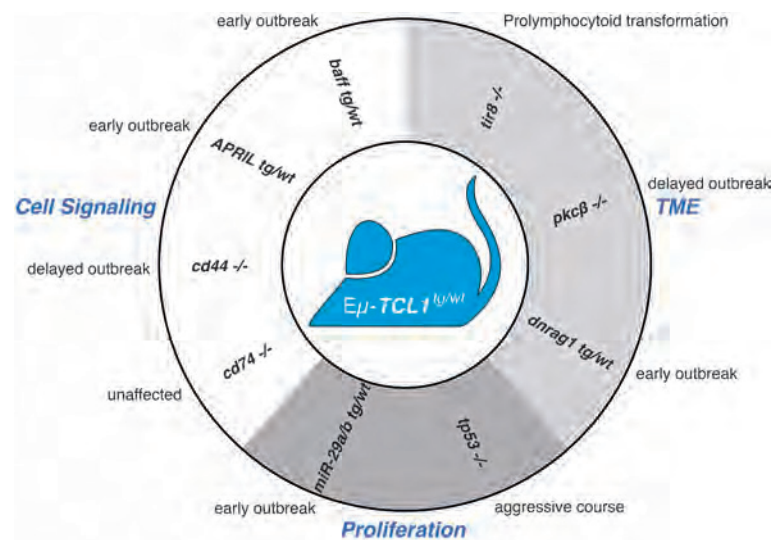
Fig. 1.5: Overview of mouse models for CLL investigations based on Eµ-*TCL1* transgenic mice. Additional mouse models were generated to investigate pathogenic pathways in TCL1-driven B cell malignancies involved in cell signaling, proliferation, and tumor microenvironment (TME). This illustration was created based on Simonetti *et al* (2014). -: deletion, tg: transgenic, wt: wildtype.

The Eµ-*TCL1* mouse model is widely used for investigations of TCL1-driven mature B cell malignancies. In the last decade, novel mouse models with additional genetic changes have been generated based on Eµ-*TCL1* mice to elucidate specific pathogenic mechanisms in the onset of CLL and progression to RT *in vivo* (**Fig.1.5**). These studies provide new insights into CLL pathogenesis, in particular in the dysregulation of proliferation or apoptosis, altered trafficking, and TME. In this study, the Eµ-*TCL1* transgenic mouse model was utilized to investigate the involvement of Akt and Notch1 signaling in CLL progression to RT.

1.3   B Cell Receptor (BCR) Signaling

B cells are necessary for the adaptive immune response to fight against bacterial and viral infection mainly through the BCR signaling. BCR is the most numerous membrane-bound receptor on B cells with between 100,000 to 200,000 complexes per cell (Yang and Reth, 2015). B cells generate an unique, high-affinity BCR during maturation that is activated either in an antigen-dependent ('activated') or -independent ('tonic') fashion in SLOs. Active BCR induces activation of Src family kinases, such as LYN and Bruton's tyrosine kinase (BTK), as well as PI3K, especially PI3Kδ (Gauld and Cambier, 2004; Werner, Hobeika, and Jumaa, 2010). Active PI3K generates the second messenger phospatidylinositol-3,4,5-triphosphate (PIP_3) to turn on calcium mobilization (Scharenberg et al., 1998), AKT (Osaki, Oshimura, and Ito, 2004; Fresno Vara et al., 2004), and the NF-κB signaling (M. W. Mayo et al., 2002). Combined PI3K/AKT and BTK actions coordinate proliferation, survival, DNA repair, and migration of mature B cells by the formation of a signalosome including a complex network of signaling cascades. The outcome of BCR signaling is determined by the state of B cell maturation, bound antigen, signal duration, and modulator proteins. BCR abnormalities can lead to a lack of humoral immune response or autoimmunity (Rawlings et al., 2017). Loss-of-function mutations of BCR or downstream kinases like BTK result in impaired B cell development, *inter alia* the absence of mature B cells, and cause immunodeficiency, termed X-linked agammaglobulinemia (XLA) (Takata and Kurosaki, 1996; Ferrari et al., 2007).

1.3.1   AKT Kinase as Key Regulator in Mature and Malignant B Cells

The serine/threonine protein kinase AKT regulates multiple cellular processes, such as activation, apoptosis, cell survival, and proliferation of mature B cells. AKT consists of three isoforms, AKT1 to AKT3, conserved in mammalian genomes with high

homology and similar structures. AKT1 and AKT2 are the dominant isoforms in mature B cells (Calamito et al., 2010; Zhu et al., 2019). Several studies confirm that AKT isoforms have overlapping but also specialized functions in development and physiology contributing to the diversity of AKT activities (Gonzalez and McGraw, 2009). AKT is activated through sequential phosphorylation at threonine 308 (Thr308) and serine 473 (Ser473) catalyzed by mechanistic target of rapamycin complex 2 (mTORC2) (Sarbassov et al., 2005), membrane-localized phosphoinositide dependent kinase 1 (PDK1) (Stokoe et al., 1997; Gold et al., 1999), and PI3K (Alessi, James, et al., 1997).
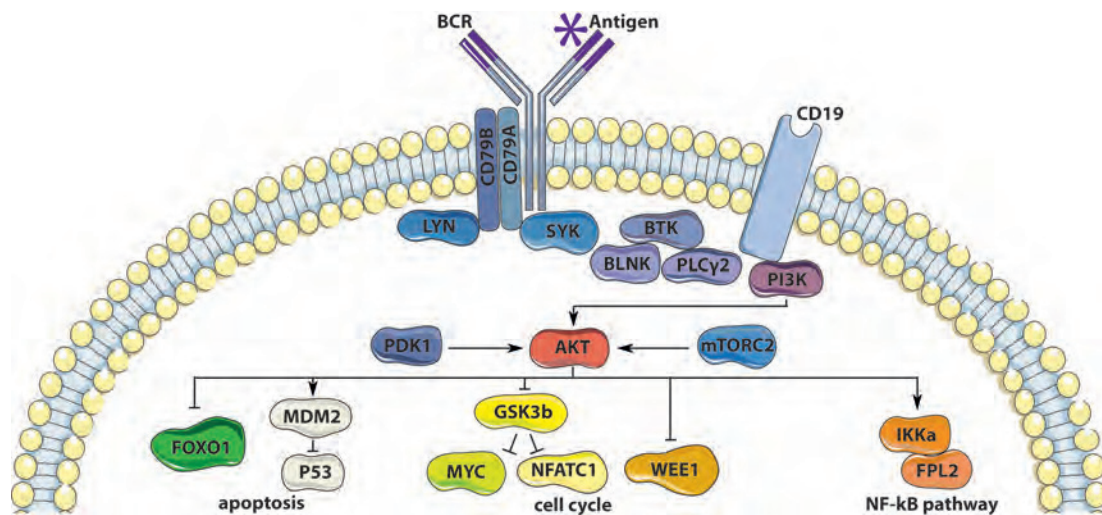
Fig. 1.6: **Downstream actions of AKT kinase in B cells.** AKT is mainly activated by mTORC2, PDK1, and PI3K *via* sequential phosphorylation at Thr308 and Ser473. In B cells, AKT kinase regulates numerous downstream proteins by phosphorylation involved in proliferation, apoptosis, and differentiation. A selection of AKT actions is presented. The illustration was created using Servier Medical Art. BCR: B cell receptor, BLNK: B cell linker, BTK: Bruton's tyrosine kinase, CD: cluster of differentiation, FOXO1: Forkhead box protein O1, GSK3b: glycogen synthase kinase 3 beta, IKKa: IκB kinase, MDM2: mouse double minute 2 homolog, mTORC2: mechanistic target of rapamycin complex 2, NF-κB: nuclear factor 'kappa-light-chain-enhancer' of activated B cells, NFATC1: nuclear factor of activated T cells, cytoplasmic 1, PDK1: phosphoinositide dependent kinase 1, PI3K: phosphoinositide 3-kinases, PLCγ2: phospholipase C gamma 2, SYK: spleen tyrosine kinase.

AKT regulates a multitude of downstream proteins. Currently, over one hundred AKT substrates linked to cell physiology and disease have been identified (**Fig.1.6**). Glycogen synthase kinase 3 beta (GSK3b) was the first discovered substrate (Alessi, Caudwell, et al., 1996). AKT-mediated inhibition of GSK3b promotes nuclear accumulation

of multiple transcription factors including MYC (Gregory, Qi, and Hann, 2003) and nu-
clear factor of activated T cells, cytoplasmic 1 (NFATC1) (Moon et al., 2012). Further-
more, AKT regulates apoptosis and cell cycle by indirect inhibition of P53 through phos-
phorylated mouse double minute 2 homolog (MDM2) (L. D. Mayo and Donner, 2001;
Ogawara et al., 2002) and the nuclear exclusion of the phosphorylated transcription
factor Forkhead box protein O1 (FOXO1) (Biggs et al., 1999; Brunet et al., 1999). AKT
actions are terminated by phosphatases. For instance, protein phosphatase 2A (PP2A)
inactivates AKT by dephosphorylation at Thr308 in lymphoid cells (Kuo et al., 2008)
whereas PH domain leucine-rich repeat protein phosphatases (PHLPP1 and PHLPP2)
dephosphorylates AKT at Ser473 (Brognard, Sierecki, et al., 2007; Brognard and New-
ton, 2008). In addition, phosphatase and tensin homolog (PTEN) indirectly represses
AKT actions by dephosphorylating PIP_3 (Stambolic et al., 1998). Since the loss of these
phosphatases causes overactivated AKT, their expression is repressed or lost in many
cancer types (Q. Zhang and Claret, 2012; Álvarez-Garcia et al., 2019).

An involvement of AKT in CLL is assumed since AKT inhibition results in apoptosis of
human CLL cells (Zhuang et al., 2010; Hofbauer et al., 2011). Nevertheless, muta-
tions of the PI3K/AKT pathway are rarely found. The molecular mechanisms causing
PI3K/AKT activation are still debated but might include BCR stimulation (Schrader et al.,
2014; Zurli et al., 2017), overexpression of protein tyrosine phosphatase, non-receptor
type 22 (PTPN22) (Negro et al., 2012), and microRNA-22 (Palacios et al., 2015). Par-
ticularly in CLL, BCR signaling has been reported as the most prominent pathogenic
signaling to empower survival and growth of leukemic B cells (Herishanu, Pérez-Galán,
et al., 2011). Thereby, BCR stimulation occurs heterogeneously and partly controver-
sial with an enhanced involvement in aggressive CLL (Stevenson et al., 2011). How-
ever, PI3K/AKT downstream actions and their involvement in the suggested progressive
course of CLL remain uncertain.

1.4   NOTCH Signaling

The ligand-mediated NOTCH signaling is an evolutionary highly conserved pathway that regulates a wide spectrum of cell types. In vertebrates, the signaling system consists of four homologous NOTCH receptors (NOTCH1-4) which are activated by Jagged (JAG1, JAG2) or Delta-like proteins (DLL1, DLL3, and DLL4).
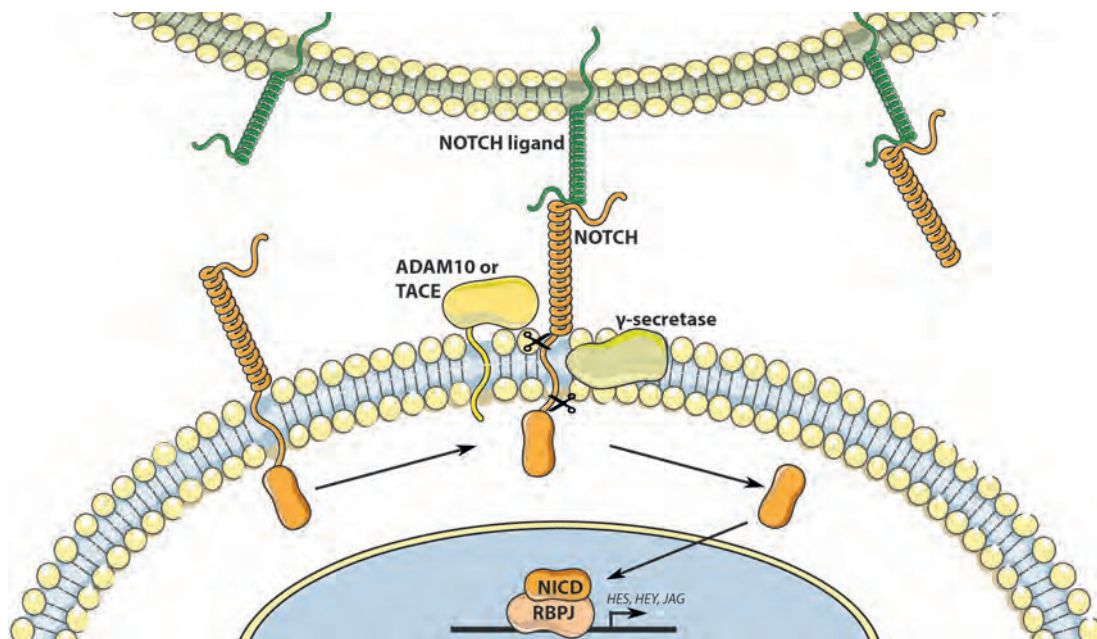
Fig. 1.7:   NOTCH signaling. NOTCH ligands activate NOTCH receptor by initiating the release of its active moiety, termed NOTCH intracellular domain (NICD). Activated NICD translocates into the nucleus to activate the transcription of target genes as coactivator of RBPJ. ADAM10: a disintegrin and metalloproteinase 10, HEY: hairy/enhancer-of-split related with YRPW motif protein, HES: hairy and enhancer of split; JAG: jagged, TACE: tumor necrosis factor-α converting enzyme. The illustration was created using Servier Medical Art.

The NOTCH receptor is activated after ligand-binding of neighboring cells by the release of the active moiety, the NOTCH intracellular domain (NICD), from the full-length receptor catalyzed by ADAM-family metalloproteases and γ-secretase complex (Bozkulak and Gerry Weinmaster, 2009). Thereby, the short-lived NICD can enter the nucleus to form a complex with the recombination signal binding protein for immunoglobulin kappa J region (RBPJ) to activate transcription of target genes (**Fig.1.7**) (S. J. Bray, 2006; Castel et al., 2013). Despite the simplicity of the direct and irreversible NOTCH

activation without the need of secondary messengers, the regulation of NOTCH path-way is of importance and complex including glycosylation of receptor and ligand (Panin et al., 2002), endocytosis (Yamamoto, Charng, and Bellen, 2010), and corepressor complexes (Kao et al., 1998; Hsieh et al., 1999).

1.4.1 NOTCH Signaling in Mature and Malignant B Cells

NOTCH signaling displays various context-specific functions ranging from apoptosis, differentiation, and proliferation to migration. In B cells, NOTCH signaling regulates several cell fate decisions. In general, *NOTCH1* and *NOTCH2* are the most frequently expressed members in B cells (Bertrand et al., 2000). During B cell development, NOTCH signaling promotes the differentiation toward marginal zone (MZ) B cells. As consequence, conditional *Notch2* knock out in murine B cells leads to the specific defi-ciency of MZ B cells (Saito et al., 2003). Conversely, B cell-specific overexpression of a constitutively active Notch2 enhances the accumulation of MZ B cells at the expense of follicular B cells (Hampel et al., 2011). In addition, NOTCH signaling is an impor-tant mediator for B cell activation and terminal differentiation toward antibody-secreting cells (Thomas et al., 2007; Santos et al., 2007). Kang *et al* demonstrated that Notch1 increases cell survival and proliferation in murine B cells. In accordance, *Notch1* dele-tion markedly reduces B cell activation and antibody secretion (Kang, Kim, and Park, 2014).

Due to various interventions of NOTCH signaling in B cell development, abnormal NOTCH activity is associated with diverse B cell malignancies. In CLL, *NOTCH1* is frequently mutated whereas it mostly consists of 2-bp (CT) frameshift deletions caus-ing a premature stop codon. Thereby, *NOTCH1* mutations affect the C-terminal PEST domain (approximately 80% of cases) that regularly initiates the proteasomal degrada-tion of activated NICD (Ianni et al., 2009; Rosati et al., 2018). As consequence, the

truncated PEST domain prolongs half-life of NICD (Blain et al., 2017). In human CLL biopsies, gain-of-function mutations of *NOTCH1* occur in 6 to 12% at initial diagnosis of CLL and approximately 30% of RT cases (Fabbri, Rasi, et al., 2011; Lionetti et al., 2014). For this reason, *NOTCH1* is the most RT-promoting mutation. Although numerous studies confirm the correlation between RT and *NOTCH1* mutations, studies are still missing but vitally needed to pinpoint the function of activated NOTCH1 in B cell transformation.

1.5 Objective

CLL is the most frequently diagnosed leukemia subtype in adults of developed countries, accounting for approximately 30% of leukemia variants (Simon, 2020). The majority of CLL patients reveals an indolent course of disease whereas up to 10% of patients manifest an aggressive course like RT (Jain and O'Brien, 2012). The occurrence of certain somatic aberrations promotes RT progression as risk factors, such as *TP53* and *NOTCH1* mutations (Rossi, Spina, Deambrogi, et al., 2011; Dan A Landau et al., 2015).

Despite the correlation between high-risk mutations and RT development, molecular alterations of pathways are poorly understood. However, several studies suggest the involvement of AKT kinase in pathogenesis by promoting cell proliferation and survival (Zhuang et al., 2010; Hofbauer et al., 2011). For this reason, this study aimed to analyze downstream effectors of AKT in progression from CLL to RT.

2 Materials and Methods

2.1 Chemicals & Materials

2.1.1 Consumables

Chemical/Material	Supplier
Acetonitrile (ACN)	Merck KGaA, Darmstadt, Germany
Agarose	Peqlab, Erlangen, Germany
Ammonium chloride	Sigma-Aldrich, Seelze, Germany
Ammonium persulfate (APS)	Sigma-Aldrich, Seelze, Germany
AutoMACS Rinsing Solution	Miltenyi Biotec, Bergisch Gladbach, Germany
β-mercaptoethanol	Applichem, Darmstadt, Germany
Bovine serum albumin (BSA)	Sigma-Aldrich, Seelze, Germany
Breeding diet	ssniff, Soest, Germany
Chloroform	Merck KGaA, Darmstadt, Germany
Deoxyribonucleoside triphosphate (dNTPs)	Amersham, Freiburg, Germany
Dithioreitol (DTT)	Applichem, Darmstadt, Germany
DMEM plus Glutamax	Gibco BRL, Eggenstein, Germany

Dream Taq DNA polymerase	ThermoFisher Scientific, Schwerte, Germany
DreamTaq buffer 10x	ThermoFisher Scientific, Schwerte, Germany
Enhanced chemiluminescence (ECL) Western Blotting Substrate	ThermoFisher Scientific, Schwerte, Germany
Entellan	Merck KGaA, Darmstadt, Germany
Eosin	Merck KGaA, Darmstadt, Germany
Ethanol, absolute	Applichem, Darmstadt, Germany
Ethidium bromide	Sigma-Aldrich, Seelze, Germany
Ethylendiamine tetraacetate (EDTA)	Applichem, Darmstadt, Germany
Fetal calf serum (FCS) (10%)	Biochrom, Berlin, Germany
Formaldehyde	Applichem, Darmstadt, Germany
Glycerol	Serva, Heidelberg, Germany
Glycine	Applichem, Darmstadt, Germany
4–(2-hydroxyethyl)-1-piperazineethanesulfonic acid (HEPES)	Applichem, Darmstadt, Germany
Horseradish peroxidase (HRP)	PerkinElmer, Inc., Massachusetts, U.S.
Hydrogen peroxide (H_2O_2)	Merck KGaA, Darmstadt, Germany
Indole-3-acetic acid (IAA)	Sigma-Aldrich, Seelze, Germany
Laemmli-sample buffer	Bio-Rad Laboratories, Inc., California, U.S.
MACS BSA Stock Solution	Miltenyi Biotec, Bergisch Gladbach, Germany
Maintenance diet	ssniff, Soest, Germany
Mayer's Haematoxylin solution	Sigma-Aldrich, Seelze, Germany

Methanol	Roth, Karlsruhe, Germany
Microbeads (Cd19, Cd90.2)	Miltenyi Biotec, Bergisch Gladbach, Germany
Milk powder	Applichem, Darmstadt, Germany
Nitrogen (liquid)	Linde, Pullach, Germany
PageRuler Prestained Protein Ladder	ThermoFisher Scientific, Schwerte, Germany
Paraffin	Merck KGaA, Darmstadt, Germany
Paraformaldehyde (PFA)	Sigma-Aldrich, Seelze, Germany
PCR primer	Eurogentec, Cologne, Germany
PeqGreen	VWR, Erlangen, Germany
Phenylmethylsulfonylfluoride (PMSF)	Sigma-Aldrich, Seelze, Germany
Phosphate buffered saline (PBS)	Gibco BRL, Eggenstein, Germany
PhosphoSTOP	Sigma-Aldrich, Seelze, Germany
2-Propanol (Isopropanol)	Roth, Karlsruhe, Germany
Proteinase K	Sigma-Aldrich, Seelze, Germany
PVDF membrane	Bio-Rad, Munich, Germany
Qiazol	Qiagen, Hilden, Germany
RIPA buffer	Cell Signaling, Danvers, USA
Sodium azide	Sigma-Aldrich, Seelze, Germany
Sodium chloride (NaCl)	Applichem, Darmstadt, Germany
Sodium dodecyl sulfate (SDS)	Applichem, Darmstadt, Germany
Sodium pyruvate	Gibco BRL, Eggenstein, Germany
Strainer 30 µm	Sysmex, Noderstedt, Germany
SuperSignal West Dura ECL substrate	Applied Biosystems/Thermo Fisher Scientific, Darmstadt, Germany

Taq-polymerase	Applied Biosystems/Thermo Fisher Scientific, Darmstadt, Germany
Tetraethylethylenediamine (TEMED)	Sigma-Aldrich, Seelze, Germany
Trifluoroacetic acid (TFA)	Sigma-Aldrich, Seelze, Germany
Trishydroxymethylaminomethane (Tris)	Applichem, Darmstadt, Germany
Tris(hydroxymethyl)aminomethane acetate (Tris AcOH)	Sigma-Aldrich, Seelze, Germany
Tris(hydroxymethyl)aminomethane hydrochloride (Tris HCl)	Sigma-Aldrich, Seelze, Germany
Triton-X-100	Applichem, Darmstadt, Germany
Tween 20	Applichem, Darmstadt, Germany
Xylol	Merck KGaA, Darmstadt, Germany
Western Blocking reagent	Roche, Mannheim, Germany

Tab. 1: **Consumables and their suppliers.**

2.1.2 Kits

Kit	Supplier
Agilent RNA 6000 Nano Kit	Agilent, Santa Clara, USA
cDNA reverse transcription kit, high capacity	Applied Biosystems/Thermo Fisher Scientific, Darmstadt, Germany
eBiosciece^{TM} Foxp3 Transcription factor staining kit	Applied Biosystems/Thermo Fisher Scientific, Darmstadt, Germany
LIVE/DEAD Fixable Aqua Dead Cel Stain Kit	Applied Biosystems/Thermo Fisher Scientific, Darmstadt, Germany
High Fidelity PCR Master	Merck KGaA, Darmstadt, Germany
High-Select^{TM} TiO$_2$ Phosphopeptide Enrichment Kit	Applied Biosystems/Thermo Fisher Scientific, Darmstadt, Germany
Pierce^{TM} BCA Protein Assay Kit	Applied Biosystems/Thermo Fisher Scientific, Darmstadt, Germany
RNase-free DNase Set	Qiagen, Hilden, Germany
RNeasy Mini Kit	Qiagen, Hilden, Germany
TSA Signal Amplification Kit	PerkinElmer, Waltham, US

Tab. 2: **Kits and their suppliers.**

2.2 Patient Ethics

All human samples were obtained with informed consent and with approval of the ethical commission of the medical faculty of the University of Cologne (reference no. 13–091). The diagnosis of CLL, DLBCL, MCL, and RT was based on standard morphological and immunophenotypic criteria. Tumor tissue sections were received by biopsies and characterized for genetic aberrations as previously published (Vollbrecht et al., 2015; Frenzel et al., 2011).

2.3   Animal Care and Breeding

2.3.1   Animal Ethics and Housing

All experiments were performed with the approval of the ethics of LANUV with identification numbers 84-02.04.2013.A146 and 84-02.04.2019.A009: "Development of personalized therapy strategies by cancer" (Bezirksregierung Cologne, Germany). Mice (*mus musculus*) were kept in the pathogen-free animal facility of the Experimental Medicine and Anatomy at the University Hospital of Cologne with a 12-hour-12-hour light-dark cycle and a temperature of 22-24 °C. Mice were housed in single ventilated cages (IVCs, TypII long) at groups of two to five mice with *ad libitum* access to food and water. Breeding was started on a 1:1 or 1:2 (male:female) basis. Pups were weaned and ear-marked after 21 days.

Mice were monitored twice a week in absence or daily in presence of noticeable health conspicuousness to prevent suffering of mice. Based on a previously prepared score sheet, mice were categorized into different states of burden. Mice were sacrificed if they reached a certain score calculated by their general health state including weight, behavior, and tumor formation. In absence of health complications, mice were scored until an age of 20 months or organ collection. The experimental cohorts randomly represented both females and males.

2.3.2   Animal Breeding

The common investigated CLL mouse model, the Eµ-*TCL1* transgenic mice (The Jackson Laboratory, Stock No: 010511), was generated by Bichi *et al* (Jefferson Medical College) (Bichi et al., 2002). The *Cd19-Cre* mouse model (The Jackson Laboratory, Stock No: 006785) was generated by Rickert *et al* (Max Delbruck Centre for Molec-

ular Medicine) (Rickert, Roes, and Rajewsky, 1997). Eµ-*TCL1* transgenic CLL and *Cd19-Cre* mice were ten times backcrossed toward C57/BL6 background. R26-fl-*Akt-C* mouse line was previously generated in the Wunderlich lab (MPI for Metabolism Research) (Kohlhaas et al., 2020). R26-fl-*FoxO1ADA* and R26-fl-*MycT58A* mice were generated by Nakae *et al* (Columbia University) (Nakae, Barr, and Accili, 2000) and Wang *et al* (Oregon Health and Sciences University) (X. Wang et al., 2011) while James R Woodgett is the donating investigator (Mount Sinai Hospital) of Gsk3b^{S9A} mice (The Jackson Laboratory, Stock No: 029592) (Patel et al., 2008). Furthermore, R26-fl-*Notch1-IC* mice were ordered by The Jackson Laboratory (Stock No: 008159) with Murtaugh *et al* (Harvard University) as donating investigator (Murtaugh et al., 2003). All R26-based knockin mice were interbreed with *Cd19-Cre* and partly with Eµ-*TCL1* mice to study hematologic malignancies.

2.4   Organ Collection and Cell Preparation

2.4.1   Dissection of Organs

Euthanasia of mice was performed according to ethical license either by cervical dislocation or by carbon dioxide overdose if blood was collected. Breathing and reflexes of both hind paws were tested to guarantee death of mice. All required organs were isolated and directly used for extraction of primary cells for *ex vivo* examinations (see chapter 2.4.2). Parts of organs were immediately fixed in 4% paraformaldehyde (PFA) and stored at room temperature protected from light until embedding in paraffin (**Tab. 3**).

Blood samples were taken monthly from the lateral tail vein or by cardiac puncture (end of experiment). For this reason, tails of mice were shortly warmed up under continuous control of temperature under red light to extend blood vessels. The tail vein was punc-

tured using Microlance Cannula 20 G (*Becton Dickinson*). Up to a maximum of 40 μl blood was collected in EDTA coated K2 microvettes (*Sarstedt*) and stored on ice until further processing.

Buffer	Component	Amount
Paraformaldehyde (4%)	37% Paraformaldehyde	10.8 ml
	PBS	89.2 ml

Tab. 3: Buffer used for tissue fixation.

2.4.2   Isolation of Primary Murine Cells and Peripheral Blood Mononuclear Cells

To receive primary murine immune cells, spleen was homogenized in a gentleMACS C Tube (*Miltenyi Biotec*) filled with 5 ml autoMACS Rinsing buffer (*Miltenyi Biotec*) containing BSA (FACS buffer, **Tab. 4**) *via* gentleMACS Octo Dissociator (pre-saved program: spleen_4). Bone marrow was isolated from the mouse thigh. After removing the surrounding muscle tissue and incising the bone, the bone marrow was received by injecting FACS buffer into the bone. Peripheral blood mononuclear cells (PBMCs) and splenic as well as bone marrow-derived immune cells were isolated by red blood cell (RBC) lysis to remove RBCs (**Tab. 4**). 5 ml RBC lysis buffer was added to the sample with occasional inverting until the solution turned clear. Lysis was stopped with 5 ml FACS buffer. After harvest of cells by centrifugation (300 g, 10 min, at 4 °C), cell suspension was filtered through 30 μm strainers to prevent clotting of cells.

Buffer	Component	Amount
FACS buffer	MACS BSA Stock Solution	5%
	autoMACS Rinsing Solution	95%
RBC lysis buffer	NH_4Cl	139.5 mM
	Tris-HCl (pH 7.65)	10 mM

Tab. 4: Buffer used for cell preparation.

2.4.3   Magnetic Cell Sorting (MACS) Technology

B cells and T cells were purified out of single cell suspension of spleen using the MACS®-technology (*Miltenyi Biotec*). In principle, cells were magnetically labeled with MACS MicroBeads and added to a magnetic column placed in a MACS separator. While unlabeled cells pass through the magnetic field, magnetically labeled cells were retained within the column. Afterwards, the column was removed from the separator to elute labeled cells.

Cells were labeled with murine Cd19 (B cells) or Cd90.2 (T cells) MicroBeads after total cells were counted by the MACSQuant 10 (*Miltenyi Biotec*). 10 µl beads were added per 10^7 total cells and incubated in the dark for 20 min at 4 °C. Cells were washed twice with FACS buffer and 10^8 total cells were resuspended in 500 µl FACS buffer. Magnetic separation was performed using the autoMACS Separator (*Miltenyi Biotec*) or LS Columns (*Miltenyi Biotec*) placed to the MACS MultiStand (*Miltenyi Biotec*). Columns were washed twice with 5 ml FACS buffer before labeled cells were eluted in 5 ml FACS buffer. Using the autoMACS Separator, the program "Possel" was chosen. Purity of B or T cell suspensions were determined by anti-mouse Cd19-BV421 (*BioLegend*) or anti-mouse Cd90.2-APC/Cy7 (*BioLegend*) positivity of Aqua negative cells as a live/dead marker *via* flow cytometry (**Tab. 11**, see chapter 2.6.1.1). Isolated cell samples with a purity of at least 90% of total cells were used for further examination.

2.5   DNA and RNA Analysis

2.5.1   Isolation of DNA and Genotyping

2.5.1.1   DNA Isolation

To receive the genotype of weaned mice, genomic DNA (gDNA) was isolated out of ear cuts and analyzed by polymerase chain reactions (PCR). After addition of 500 µl tail lysis buffer containing Proteinase K (1 mg/ml), biopsies were digested at 56 °C and 500 rpm for at least 3 h preferably over night (**Tab. 7**). 500 µl 100% isopropanol was added to precipitate and pellet DNA by centrifugation (17,000 g, 10 min, room temperature). DNA was washed once with 200 µl 70% ethanol and air-dried at 37 °C. Finally, the pellet was resuspended in 50 µl TE buffer containing RNAse overnight at room temperature before use.

2.5.1.2   Polymerase Chain Reaction (PCR)

Amplification of DNA fragments was done by PCR using the PCR mastermix (**Tab. 7**) with gene-specific primers binding to the gene of interest (**Tab. 5**). The amplification was performed using *Taq*-polymerase (named after the thermophilic bacterium *Thermus aquaticus*) by *in vitro* enzymatic replication using the Flex Cycler[2] (*Analytik Jena*).

Gene of interest	Primer Sequence (5' - 3')	Band Size
TCL1	GCC GAG TGC CCG ACA CTC CAT CTG GCA GCA GCT CGA GAC AAA ACT CCT GAG GCC ATA TTG CTG ATC CAC ATC TGC TG	490 wt, 300 fl
R26-fl-*Notch1-IC*	ACA CCG GCC TTA TTC CAA G CAG GAC AAC GGC CAC ACA TGG TAT GCC TGA CAC TCA CC AAG GGA GCT GCA GTG GAG TA	241 wt, 300 tg
R26-fl-*Akt-CA*	TGTCGCAAATTAACTGTGAATC GATATGAAGTACTGGGCTCTT AAAGTCGCTCTGAGTTGTTATC	590 wt, 390 tg
Cd19-Cre	CTGCAGTTCGATCACTGGAAC AAAGGCCTCTACAGTCTATAG TCCAATTTACTGACCGTACA TCCTGGCAGCGATCGCTATT	550 wt, 450 tg

Tab. 5: Gene-specific primer sequences (5'-3') for genotyping.

For each gene-specific primer pair, an adapted PCR protocol was chosen (**Tab. 6**).

Step	Eμ-*TCL1*	R26-fl-*Akt-CA*, R26-fl-*Notch1-IC*	*Cd19-Cre*
1	94 °C, 10 min	94 °C, 3 min	94 °C, 5 min
2	94 °C, 30 s	94 °C, 30 s	94 °C, 30 s
3	62 °C, 30 s	56 °C, 45 s	58 °C, 45 s
4	72 °C, 1 min	72 °C, 1 min	72 °C, 1 min
5	repeat 30x Step 2-4	repeat 30x Step 2-4	repeat 30x Step 2-4
6	72 °C, 5 min	72 °C, 10 min	72 °C, 10 min
7	12 °C	12 °C	12 °C

Tab. 6: PCR protocols.

PCR products were analyzed by horizontal agarose gel electrophoresis to separate and prove DNA fragments depending on size. 1x TAE buffer was boiled with the aimed amount of agarose (usually 2% agarose gel) and blended with the DNA intercalating PeqGreen (1:20,000, *VWR Chemicals*) to visualize DNA (emission maximum: 530 nm, **Tab. 7**). The gel chamber with comb was filled with boiled gel which polymerized by cooling down. 20 μl of PCR product was loaded on gel and run in 1x TAE buffer at

150 V.

Buffer and Mastermix	Component	Amount
Tail Lysis Buffer	Tris-HCl, pH 8.5	100 mM
	EDTA, pH 8.0	5 mM
	SDS	0.2%
	NaCl	200 mM
	Proteinase K	1x
TAE Buffer	40 mM	Tris-AcOH (pH 8.0)
	1 mM	EDTA (pH 8.0)
TE Buffer	10 mM	Tris-HCl (pH 8.5)
	1 mM	EDTA (pH 8.5)
TE/RNase A Buffer	Tris-HCl, pH 8.5	100 mM
	EDTA, pH 8.0	5 mM
	RNase A	100 mg/ml
PCR Mastermix (100x)	H_2O	2085 µl
	DreamTaq Buffer	250 µl
	dNTPs	20 µl
	per primer	25 µl

Tab. 7: Buffer and mastermix used for DNA isolation and PCR.

2.5.2   RNA Isolation and Analysis of Gene Expression

2.5.2.1   RNA Isolation

To analyze transcriptional levels of the gene of interest, RNA was isolated and expression was analyzed by quantitative real-time PCR (qPCR). Total RNA was isolated from MACS-sorted Cd19$^+$ and Cd90.2$^+$ lymphocytes out of spleen with RNeasy Mini Kit (*Qiagen*). Cell pellets were lysed in 500 µl QIAzol (*Qiagen*) before 100 µl chloroform was added and vortexed for 30 s. After centrifugation (12,000 g, 25 min, at 4 °C), samples were separated into three phases: an colorless aqueous phase containing RNA, a white interphase with DNA as well as cell debris and a red organic phase containing proteins. The aqueous phase was transferred to a new tube and RNA as well as DNA was precipitated by addition of the same volume of 70% ethanol. After incubation for 2 min, samples were transferred into RNeasy spin columns. During centrifugation (10,000 g,

15 s, room temperature), nucleic acids bound to the membrane of the spin columns. Column-bound nucleic acids were washed using 350 µl RW1 buffer. Bound DNA was digested using the RNase-free DNase Set (*Qiagen*) by adding 70 µl RDD buffer with 10 µl DNase I directly onto the membrane and incubating for 15 min. Digested DNA was washed off with 350 µl RW1 buffer. RNA was washed with 500 µl RPE buffer. Spin columns were placed onto new collection tubes and membrane was dried by centrifugation (10,000 g, 2 min, room temperature). RNA was eluted with 30 µl RNase-free water by centrifugation (10,000 g, 3 min, room temperature). RNA concentration was determined using NanoDrop (*Thermo Fisher Scientific*).

2.5.2.2   cDNA Synthesis

RNA was reverse transcribed with the High Capacity cDNA RT Kit (*Applied Biosystems*). RNA was diluted to a concentration of 100 ng/µl. RNA samples and 2x cDNA mastermix were mixed with a 1:1 ratio (**Tab. 8**). Transcription was performed by the Flex Cycler[2] (*Analytik Jena*) at 37 °C for 2 h. Afterwards, the reverse transcriptase was inactivated by incubation for 5 min at 85 °C. cDNA was diluted with RNase-free water to a final concentration of 12.5 ng/µl.

Component	Volume/reaction [µl]
10x RT Buffer	2,0
25x dNTP Mix	0,8
10x RT Random Primers	2,0
Multiscribe Reverse Transcriptase	1,0
total	5,8

Tab. 8: Mastermix used for cDNA synthesis.

2.5.2.3   Quantitative Real-Time PCR (qPCR)

Gene expression were analyzed by qPCR using the TaqMan Gene Expression Master Mix (**Tab. 9**). qPCR assay was prepared and analyzed in 384-well plates using the QuantStudio™ 6 Flex Real-Time PCR System (*Thermo Fisher Scientific*).

Component	Volume/reaction [µl]
TaqMan Mastermix	5,0
specific TaqMan probe (FAM-MGB)	0,3
reference TaqMan probe (VIC-MGB)	0,3
H_2O	0,4
total	6,0

Tab. 9: **Mastermix used for qPCR.**

50 ng cDNA was mixed with TaqMan Gene Expression Master Mix to a final volume of 10 µl. Probes from *Thermo Fisher Scientific* shown in **Tab. 10** were choosen. *Tbp* was used as reference gene.

Gene	Catalog number	Gene	Catalog number
Akt1	Mm01331624_m1	*Jag1*	Mm00496902_m1
Bax	Mm00432050_m1	*Jag2*	Mm01325629_m1
Bbc3	Mm00519268_m1	*Mdm2*	Mm00487657_m1
Bcl2	Mm00477631_m1	*Notch1*	Mm00435245_m1
Cdkn1a	Mm01303209_m1	*Notch2*	Mm00803077_m1
Dll1	Mm01279269_m1	*Notch3*	Mm00435270_m1
Dll3	Mm00432854_m1	*Notch4*	Mm00440525_m1
Dll4	Mm00444619_m1	*Pdcd10*	Mm00479023_m1
Dtx1	Mm00492297_m1	*Ppm1d*	Mm00450393_m1
Fas	Mm01204974_m1	*Pten*	Mm00477208_m1
Heyl	Mm00516555_m1	*s100a4*	Mm00803372_g1
Hes1	Mm00468601_m1	*Tbp*	Mm00446973_m1
Hes5	Mm00439311_g1	*Trp53*	Mm01731290_g1

Tab. 10: **qPCR probes of gene of interest and reference gene.**

2.6 Protein Analysis

2.6.1 Flow Cytometry

Flow cytometry provides a method to study cells based on specific light scattering and fluorescent characteristics of single cells. Expression of either surface, intracellular or nuclear proteins can further be detected by staining cells with fluorochrome-conjugated antibodies (**Tab. 11**) whereas cells expressing endogenous fluorescent proteins like eGFP can be directly detected. For flow cytometry, primary cells out of peripheral blood, spleen, and bone marrow were isolated and analyzed. All centrifugation steps were performed at 300 g, 4 °C for 10 min.

2.6.1.1 Staining of Extracellular Proteins

Primary murine cells were stained against various antibody panels listed in **Tab. 11** and **Tab. 12**. Dilutions of antibodies were used as recommended by the manufacturer or adjusted by titration experiments. Cells were pelleted by centrifugation before being resuspended in 50 µl staining solution composed of FACS buffer, TruSain fcX^{TM} anti-mouse Cd16/32 antibody (*BioLegend*) as blocking solution, and fluorochrome-labeled antibodies of interest.

Antibody	Fluorochrome	Dilution	Company	Panel No.
Cd4 (GK1.5)	BV421	1:100	BioLegend	VI
Cd5 (53-7.3)	PE/Cy5	1:150	BioLegend	I, II, III
Cd8 (53-6.7)	APC	1:60	BioLegend	VI
Cd19 (6G5)	BV421	1:100	BioLegend	I, II, III
Cd90.2 (30-H12)	APC/Cy7	1:60	BioLegend	I, II, III, VI
Dll1 (HMD1-3)	PE	1:100	BioLegend	II, IV
F4/80 (BM8)	PE/Cy7	1:50	BioLegend	II, III
Jag1 (E-12)	PE	1:100	BioLegend	III
-	Aqua	1:250	Thermo Fisher	all

Tab. 11: Antibodies used for extracellular staining analyzed by flow cytometry. APC: Allophy-cocyanin, BV421: Brilliant Violet 421, Cy5: Cyanine5, Cy7: Cyanine7, PE: Phycoerythrin.

Cells were incubated with extracellular antibodies (**Tab. 11**) for 15 min at room temperature protected from light. Cells were washed twice with 1 ml FACS buffer before being resuspended in 200 µl FACS buffer. Stained samples were analyzed immediately by MACSQuant 10. Additionally, an unstained sample was measured as negative control to reduce effects of autofluorescence. The following gating strategies were applied (**Fig.2.1**).
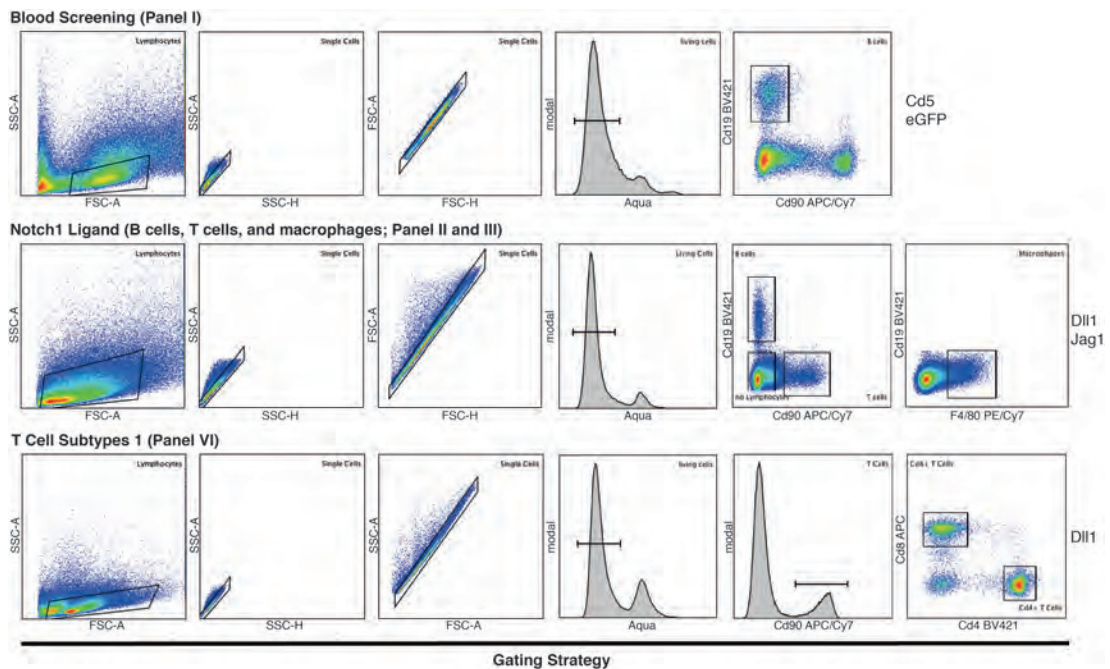
Fig. 2.1: Gating strategy for flow cytometry experiments with extracellular staining. Cells were identified *via* FSC-A vs. SSC-A dot blots and single cells *via* both SSC-H vs SSC-A as well as FSC-H vs FSC-A dot blots. Apoptotic cells were gated out using Live/Dead Aqua staining. APC: Allophycocyanin, BV421: Brilliant Violet 421, Cy5: Cyanine5, Cy7: Cyanine7, FSC-A/H: forward scatter-area/height, PE: Phycoerythrin, SSC-A/H: side scatter-area/height.

2.6.1.2 Staining of Intracellular Proteins

For intracellular staining, the eBioscienceTM Foxp3/Transcription Factor Staining Buffer Set (*Thermo Fisher Scientific*) was used. Cells were fixed after extracellular staining (see chapter 2.6.1.1) by 500 µl Foxp3 Fixation/Permeabilization solution. Cells were incubated for 1 h on ice protected from light. Afterwards, cells were directly perme-

abilized using 1 ml 1x Permeabilization buffer and centrifuged (600 g, 15 min, room temperature). After washing, 50 µl intracellular staining solution was added for at least 30 min at room temperature protected from light (**Tab. 12**).

Antibody	Fluorochrome	Dilution	Company	Panel No.
Cd4 (GK1.5)	BV421	1:100	BioLegend	V
Cd5 (53-7.3)	AF647	1:100	BioLegend	VII, VIII
Cd19 (GD5)	AF594	1:100	BioLegend	VII, VIII
Cd19 (GD5)	BV421	1:100	BioLegend	IX
Cd90.2 (30-H12)	FITC	1:150	BioLegend	V
Dll1 (HMD1-3)	PE	1:100	BioLegend	V
Foxp3 (FJK-16s) *	APC	1:150	Thermo Fisher	V
Ki-67 (11F6) *	BV421	1:100	BioLegend	VII
Notch1 (HMN1-12) *	BV421	1:100	BioLegend	VIII
p53 (1C12) *	AF647	1:100	Cell Signaling	IX
-	Aqua	1:250	Thermo Fisher	all

Tab. 12: Antibodies used for intracellular staining analyzed by flow cytometry. Marked (*) antibodies were stained after fixation and permeabilization. AF594: AlexaFluor 594, AF647: AlexaFluor 647, APC: Allophycocyanin, BV421: Brilliant Violet 421, FITC: Fluorescein isothiocyanate, PE: Phycoerythrin.

Cells were washed twice and resuspended in 200 µl FACS buffer. Samples were stored at 4 °C until measurement by MACSQuant 10 and MACSQuant VYB *via* flow cytometry. The following gating strategies were applied for extracellular staining (**Fig.2.2**).
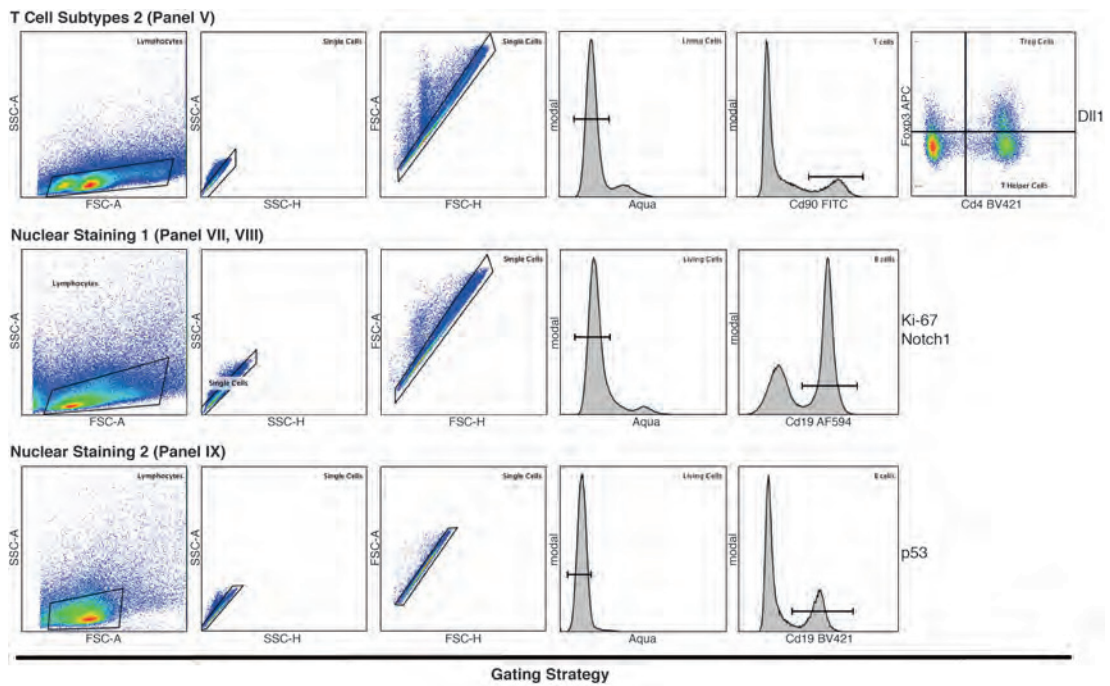
Fig. 2.2: Gating strategy for flow cytometry experiments with intracellular staining. Lymphocytes were identified *via* FSC-A vs. SSC-A dot blots and single cells *via* both SSC-H vs SSC-A as well as FSC-H vs FSC-A dot blots. Apoptotic cells were gated out using Live/Dead Aqua staining. APC: Allophycocyanin, BV421: Brilliant Violet 421, FITC: Fluorescein isothiocyanate, FSC-A/H: forward scatter-area/height, PE: Phycoerythrin, SSC-A/H: side scatter-area/height.

2.6.2 Western Blot Analysis

2.6.2.1 Protein Isolation

Western blot analysis allows to detect and relatively quantify specific proteins and phosphoproteins from cell lysates. Cell samples were incubated in 50 µl 1x RIPA buffer supplemented with phenylmethylsulfonyl fluoride (PMSF) and PhosphoSTOP for 1 h at 4 °C to lyse cells. Cell debris were harvested by centrifugation (17,000 g, 10 min, at 4 °C) at which the through-over contains proteins. Protein concentration was determined by Nanodrop (*Thermo Fisher Scientific*) and Pierce™ BCA Protein Assay Kit (*Thermo Fisher Scientific*). For the Pierce BCA protein assay, protein samples were 1:100 diluted in DEPC water and mixed with the BCA mastermix. Samples were incubated for 30 min at 37 °C. After cooling down the samples to room temperature, the

absorbance of samples was determined at 562 nm. Protein concentration was calculated using standard curves. Samples were diluted to a final concentration of 20 µg with 1x Laemmli sample buffer supplemented with 10% β-mercaptoethanol.

2.6.2.2   SDS Polyacrylamide Gel Electrophoresis (SDS-PAGE) and Western blot

Sodium dodecyl sulfate polyacrylamide gel electrophoresis (SDS-PAGE) was performed using Mini-PROTEAN® Series (*BioRad*). Samples were boiled for 10 min at 95 °C to denature proteins before being loaded on 10% agarose gel (*BioRad*) together with 15 µl PageRuler Prestained Protein Ladder. The agarose gel run at 150 V. The transfer onto a PVDF-membrane (*BioRad*) was performed using Trans-Blot Turbo Transfer System (program: midi, 7 min, *BioRad*). PVDF-membranes were blocked for 2 h at room temperature in the same blocking solution as used for primary antibodies (**Tab.13**). PVDF-membranes were probed with the appropriate primary antibody added to blocking solution overnight at 4 °C.

Antibody	Species	Ratio	Company	Cat. Number
α Phospho-Akt (Ser473)	rabbit	1:2,000	Cell Signaling	4060
α panAkt	rabbit	1:2,000	Cell Signaling	4685S
α Calnexin, C-Terminal	rabbit	1:10,000	Sigma-Aldrich	208880
α rabbit-HRP	goat	1:2,000	Sigma-Aldrich	A6154

Tab. 13: Antibodies used for Western blot analysis. HRP: horseradish peroxidase.

Unbound antibodies were removed by five washing steps with TBS-T for 5 min each time (**Tab.14**). Immunoreactivity was detected with horseradish peroxidase (HRP)-labeled secondary antibodies (**Tab.13**). PVDF-membranes were incubated into blocking solution containing secondary antibodies for 1 h at room temperature. Proteins were visualized on the FUSION Solo (*Vilber*) using ECL super signal (*Thermo Fisher*

Scientific) as substrate. Images were analyzed and proteins were relatively quantified using ImageJ software. If necessary, PVDF-membranes were stripped in Stripping buffer containing 2% β-mercaptoethanol at 56 °C for 30 min for further protein analysis.

Buffer	Component	Amount
Blocking solution	10% (v/v)	10x Western Blocking
	90% (v/v)	Reagen TBS-T
Blocking solution (BSA)	5% (v/v)	BSA
	95%	TBS-T
Blocking solution (milk powder)	5% (v/v)	Milk powder
	95%	TBS-T
SDS-running buffer	Tris	25 mM
	Glycin	200 mM
	SDS	0.1%
Stripping buffer	SDS	2%
	Tris	625 mM
	β-mercaptoethanol	0.8%
TBS	1.47 M	NaCl
	0.2 M	Tris (pH 7.5)
TBS-T	Tris	50 mM
	NaCl	140 mM
	Tween20	0.05%

Tab. 14: Buffer used for Western blot analysis.

2.6.3 Proteomics and Phosphoproteomics

Proteomics and phosphoproteomics were used to analyze the proteome including protein levels as well as their phosphorylation states. Cd19$^+$ purified B cells (2.4.3) were dissolved in 200 µl Urea/Thiourea buffer (**Tab.15**). The reducing agent dithiothreitol (1 mM) was added to samples and incubated for 1 h at room temperature. Indole-3-acetic acid (5.5 mM) was added and incubate for 45 min at room temperature in the dark. 800 µg of total proteins were digested two times with LysC (0,5 ng/µl) with a 1:100 ratio at room temperature overnight. For desalting of samples, samples were acidified using trifluoroacetic acid (TFA, 1%). The supernatant was collected after centrifugation (full speed, 10 min, room temperature). A C$_{18}$ column (*Thermo Fisher Scientific*) was

activated with 2 ml 100% acetonitrile (ACN). After washing with 1 ml 0.1% TFA, samples were loaded on column. The column was washed three times with 1 ml 0.1% TFA. Peptides were eluted with elution buffer (**Tab.15**). A quarter of samples were taken for proteome analysis by mass spectrometry (*Bruker Daltonics*).

Desalted samples were enriched using the High-Select TiO_2 Phosphopeptide Enrichment Kit (*Thermo Fisher Scientific*) to receive phosphoproteins. For TiO_2 extraction, dried peptide samples were suspended in 150 µl Binding/Equilibration buffer. 200 µl Wash buffer was added to TiO_2 spin tip before centrifugation (3,000 g, 2 min, room temperature). 20 µl Binding/Equilibration buffer was added to spin tip and centrifuged (3,000 g, 2 min, room temperature). To bind phosphopeptides, 150 µl suspended peptide samples were added to the spin tip and centrifuged (1,000 g, 5 min, room temperature). Column was washed two times with 20 µl Binding/Equilibration buffer and centrifuged (3,000 g, 2 min, room temperature). 20 µl LC-MS grade water was added to column and centrifuged (3,000 g, 2 min, room temperature). Phosphopeptides were eluted using 50 µl Phosphopeptide Elution buffer and centrifuged (1,000 g, 5 min, room temperature). To enhance phosphopeptide concentration, the elution step was repeated. Eluted phosphopeptide samples were immediately dried in a speed vacuum concentrator to remove Phosphopeptide Elution buffer and resuspended in 15 µl 5% FA and 2% ACN. Prepared proteomic and phosphoproteomic samples were measured *via* mass spectrometry (*Bruker Daltonics*) by Dr. Janica Wiederstein (Krüger lab, CECAD).

Buffer	Component	Amount
Urea/Thiourea buffer	Urea	6 M
	Thiourea	2 M
	Hepes pH 7.4	500 M
Elution buffer	ACN	60%
	FA	0.1%

Tab. 15: Buffer used for proteomics and phosphoproteomics.

2.7   Immunohistochemical and Immunofluorescent Staining

Murine spleen was fixed in 4% paraformaldehyde (PFA) for at least 3 days at room temperature. Paraffin-embedded samples were deparaffinized and stained after retrieval.

2.7.1   H&E Staining

For H&E staining of murine samples, sections were incubated in Mayer's Haematoxylin solution for 2 min. Excess staining was washed off with water and further incubated in tap water for 15 min. Sections were washed using ddH$_2$O and incubated in Eosin for 15 min. Stained sections were washed with tap water for five times. Samples were incubated in 75% ethanol for 1 min, in 90% ethanol for 1 min, in isopropanol for 1 min and in xylol for 1 min for dehydration. Finally, samples were mounted using Entellan and imaged with AxioVision 4.2 (*Carl Zeiss MicroImaging*) using bright field microscopy.

2.7.2   Immunofluorescent Staining

For immunofluorescent staining of human biopsies and murine spleens, deparaffinized sections after retrieval were added to Tris-buffered saline (TBS) buffer for 10 min and three time to TBS buffer with 0.05% Tween-20 for 5 min. Sections were blocked in 1% hydrogen peroxide (H$_2$O$_2$) and incubated three time in TBS buffer with 0.05% Tween-20 for 5 min. Samples were blocked in TNB buffer (*PerkinElmer*) for 20 min. First antibodies in blocking buffer were incubated overnight on room temperature in the dark (**Tab.16**). Antibodies were washed off using TBS buffer with 0.05% Tween-20 three times for 5 min. Samples were incubated in horseradish peroxidase (HRP, 1:100) for 30 min at room temperature protected from light. Samples were washed three time using TBS buffer with 0.05% Tween-20 for 5 min. Using TSA Signal Amplification Kit

(*PerkinElmer*), Cyanine 3 was incubated on sections as fluorochrome with a 1:100 ratio and washed three time in TBS buffer with 0.05% Tween-20 for 5 min. Finally, samples were counterstained with DAPI (1:1,000, *Hoechst*) and mounted. Sections were imaged with AxioVision 4.2 (*Carl Zeiss MicroImaging*).

Antibody	Species	Ratio	Company	Cat. Number
α pAKT Ser473	anti-rat	1:100	Cell Signaling	#3787

Tab. 16: Antibodies used for immunofluorescent staining.

2.8   Statistical Analysis

Mice of indicated genotype were randomly assigned to groups, regardless of gender but taking age (weeks) at organ collection into account. All mouse studies were performed in a blinded fashion. GraphPad Prism software package was used for statistical analysis and illustration. Proteomics and phosphoproteomics were illustrated and calculated using Instant Clue software (Nolte et al., 2018). Gene Ontology (GO) Enrichment Analysis (n=20 terms, P-value cutoff (FDR) < 0.05) was performed using ShinyGO v0.61 software. P values were determined with a unpaired Student's t-test or a two-tailed unpaired Student's t-test with an One- or Two-way Analysis of Variance (ANOVA) followed by Fisher Least Significant Difference (LSD) (see Figure legends). P values below 0.05 were considered significant, *$p \leq 0.05$, **$p \leq 0.01$, and ***$p \leq 0.001$.

3   Results

3.1   Human RT Biopsies Display Overactivated AKT

The BCR pathway is required for the proliferation, activation, and survival of mature B cells and was proven as the most prominent signaling particularly in CLL (Herishanu, Pérez-Galán, et al., 2011). It was hypothesized that BCR stimulation and its downstream pathways including PI3K/AKT and IKK/NF-κB, correlates with worse prognosis of CLL (Jan A. Burger and Chiorazzi, 2013). CLL reveals a variable clinical outcome ranging from indolent disease to aggressive forms, such as RT. RT describes a clonal transformation from CLL into an aggressive NHL with the histomorphological characteristics of a DLBCL (Richter, 1928; Parikh et al., 2013). Despite the suggested involvement of PI3K/AKT signaling in an aggressive course of CLL, this correlation had never been studied in RT patients. This might be due to the fact that RT rarely contains activating PI3K/AKT or PTEN null mutations (Schrader et al., 2014).

To fill the gap in knowledge, human CLL (n=8), DLBCL (n=12), and RT (n=19) sections were immunohistochemically analyzed for steady-state levels of activated AKT using Ser473 phosphorylation antibody. Active AKT was detected in 12.5% of CLL and 16.7% of DLBCL tumor biopsies. Contrarily, the majority of RT patients (52.6%) stained positive for active AKT (**Fig.3.1A**). Mantle cell lymphoma (MCL, n=9) sections were used as positive control due to the widely accepted, constitutive activation of AKT involved

in pathogenesis (**Fig.3.1C**) (Rudelius et al., 2006; Col et al., 2008).
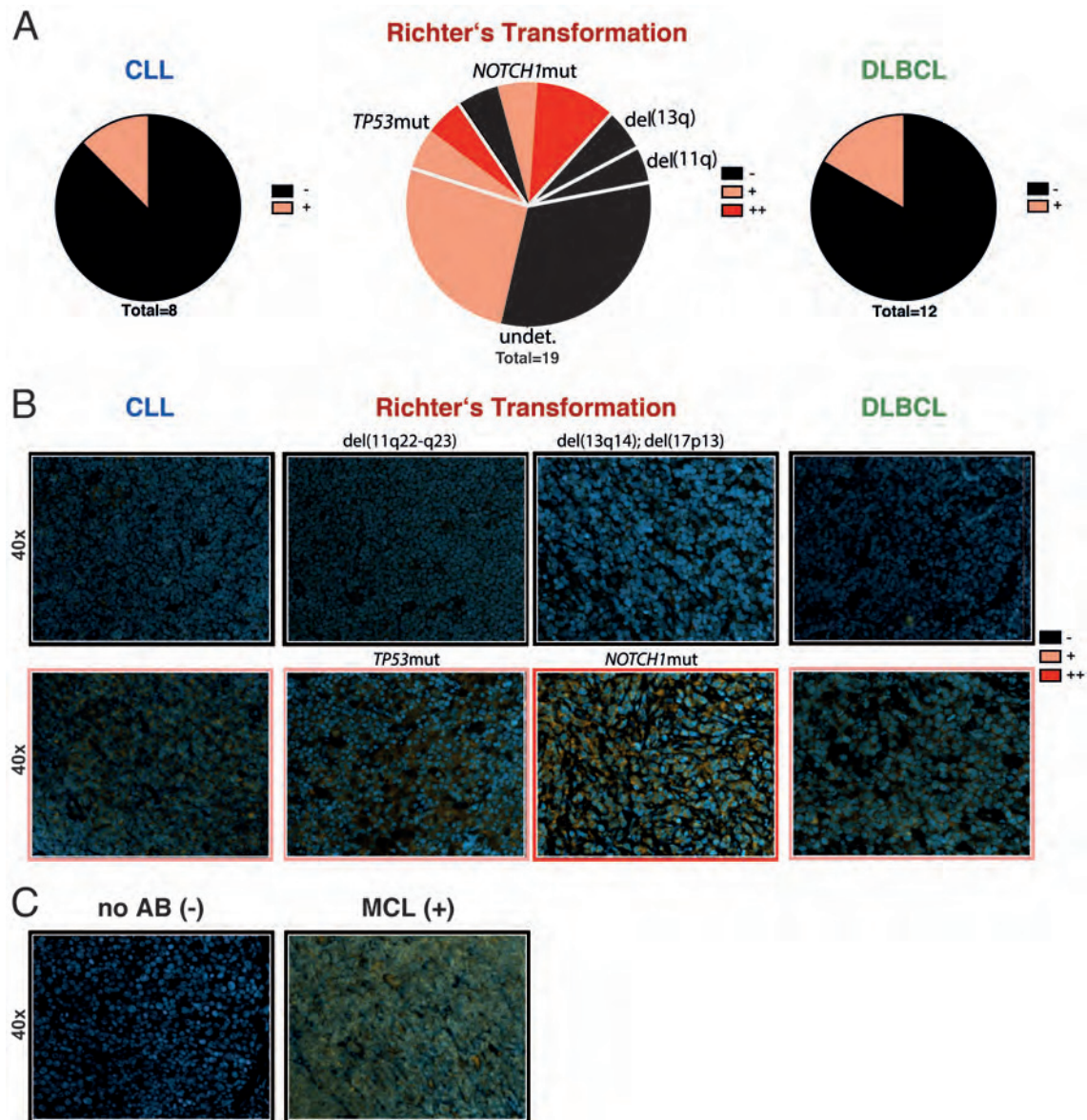
Fig. 3.1: **Active Akt in human RT tumor biopsies with *Notch1* or *TP53* mutations. A** Ratio of CLL (n=8), RT (n=19), and DLBCL (n=12) patients without (-, black), with (+, light red), and with excessive (++, red) signal for pAKT (Ser473) *via* immunohistochemistry. The classification of pAKT (Ser473) signal was independently decided upon by five project-unrelated assessors without any information about samples. **B** Immunohistochemical representatives (magnification: 40-times) for human tumor biopsies without (-, outlined in black), with (+, outlined in light red), and with excessive (++, outlined in red) signal for pAKT (Ser473) used for **A**. **C** Immunohistochemical representatives of controls. Human MCL samples were used as positive control. The negative control was only incubated with the secondary but not with the primary pAKT (Ser473) antibody. AB: antibody, CLL: chronic lymphocytic leukemia, DLBCL: diffuse large B cell lymphoma, MCL: mantle cell lymphoma; yellow: pAKT (Ser473), blue: DAPI.

Moreover, various strengths of phosphorylated AKT were determined for RT sections. RT patients harboring somatic mutations in *NOTCH1* or *TP53* genes exhibited moderate to high levels of active AKT whereas activated AKT was absent in RT patients possessing *del(11q)*, the site of the *ATM* gene and the *miR34b/c* cluster (Stankovic and Skowronska, 2014), or *del(13q)* aberrations including *DLEU2, MIR15A,* and *MIR16-1* genes (**Fig.3.1A,B**) (Cimmino et al., 2005; Klein et al., 2010). These results correlate with Western blot data of Dr. Mona al-Maarri showing a high variability of steady state levels of activated AKT in primary, human CLL samples. While most CLL samples showed low levels of active AKT, samples with mutations approved to be present in progressive cases, mainly *NOTCH1* and *TP53* mutations, revealed augmented activation of AKT by Ser473-phosphorylation (Kohlhaas et al., 2020). Collectively, RT and progressive CLL patients display enhanced AKT activation, especially in presence of *NOTCH1* and *TP53* somatic mutations.

3.2   B Cell-Specific *Akt-C* Expression in Eµ-*TCL1* Transgenic CLL Mice Drives RT

3.2.1   Generation of the Eµ-*TCL1* CLL Mouse Model with B Cell-Specific *Akt-C* Expression

To study the relevance and function of activated Akt kinase in the progression of CLL *in vivo*, a common CLL mouse model, the Eµ-*TCL1*$^{tg/wt}$ (termed Eµ-*TCL1*) mice (Bichi et al., 2002), was characterized in the presence of B cell-specific constitutive active Akt. For this purpose, a ROSA26 (R26) mouse line was generated in which a loxP-flanked stop cassette prevents the expression of a N-terminal myristoylation tagged murine *Akt1* gene, named *Akt-C*, and the reporter gene *eGFP* (enhanced green fluo-

rescent protein, **Fig.3.2A**). The N-terminal myristoylation tag directs Akt-C to the cell membrane to initiate its continuous activation through phosphorylation at Thr308. Akt is fully activated by further phosphorylation at Ser473 (Liao and Hung, 2010).
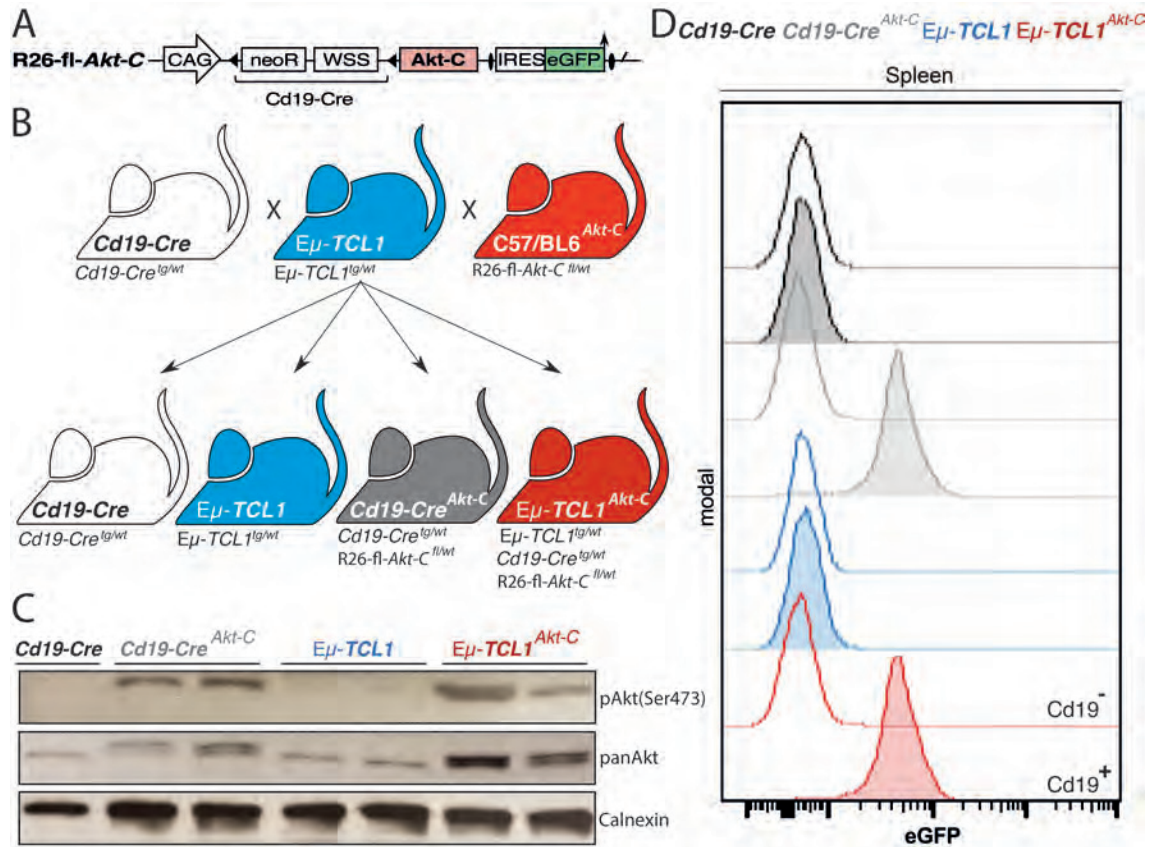
Fig. 3.2: **Validation of the Akt-C construct expressed in B cells.** **A** Scheme of the *Akt-C* construct. **B** Scheme of the breeding strategy to receive experimental Eµ-*TCL1*$^{Akt-C}$ mice. **C** Representative Western blot of pAKT (Ser473) and total Akt in splenic B cells of indicated mice at 7-8 months age. Calnexin was used as loading control. **D** Representative blot of eGFP in Cd19⁻ (uncolored) and Cd19⁺ (colored) splenocytes of indicated mice at 7-8 months age *via* flow cytometry. Data were previously gated for living (Aqua staining), single cells (FSC-A vs. FSC-H, SSC-A vs. SSC-H). Akt-C: constitutive active Akt, CAG: cytomegalovirus early enhancer/chicken β actin, eGFP: enhanced green fluorescent protein, IRES: internal ribosomal entry site, neoR: neomycin resistance, WSS: Westphal stop sequence.

To investigate the impact of Akt-C in CLL, R26-fl-*Akt-C*$^{fl/wt}$ mice were intercrossed with *Cd19-Cre*$^{tg/wt}$ (termed *Cd19-Cre*) mice yielding *Cd19-Cre*$^{tg/wt}$; R26-fl-*Akt-C*$^{fl/wt}$ (termed *Cd19-Cre*$^{Akt-C}$) mice to express *Akt-C* specifically in Cd19⁺ B cells. *Cd19-Cre*$^{Akt-C}$ mice were further intercrossed with the Eµ-*TCL1* transgenic CLL mouse model to obtain experimental Eµ-*TCL1*$^{tg/wt}$; *Cd19-Cre*$^{tg/wt}$; R26-fl-*Akt-C*$^{fl/wt}$ (termed Eµ-*TCL1*$^{Akt-C}$) mice

(**Fig.3.2B**). While Eµ-*TCL1* mice display a B cell-restricted overexpression of human *TCL1*, Eµ-*TCL1*$^{Akt-C}$ mice additionally express the constitutive active *Akt1* variant in B cells. The specificity of *Akt-C* expression was validated by the B cell-restricted eGFP expression in both *Cd19-Cre*$^{Akt-C}$ and Eµ-*TCL1*$^{Akt-C}$ mice (**Fig.3.2D**). The overactivation of Akt was detected by phosphorylation on the activating residue Ser473 in splenic B cells of *Cd19-Cre*$^{Akt-C}$ and Eµ-*TCL1*$^{Akt-C}$ mice. Both the endogenous and the N-terminal myristoylation tagged Akt protein were monitored in B cells of *Cd19-Cre*$^{Akt-C}$ and Eµ-*TCL1*$^{Akt-C}$ mice causing two bands with different molecular weights (**Fig.3.2C**).

3.2.2   B Cell-Specific *Akt-C* Expression in Eµ-*TCL1* Transgenic CLL Mice Causes a Decreased Survival Capacity

CLL cells are predominantly identified by the expression of Cd5, a common T cell surface receptor and marker for B-1a cells, on Cd19$^+$ B cells. The CLL course was monitored by monthly screening of Cd5$^+$ B cells in peripheral blood *via* flow cytometry. CLL cells occurred in Eµ-*TCL1* mice at 4-5 months age and in Eµ-*TCL1*$^{Akt-C}$ mice at 6-7 months age. Despite the various ages of incidence, the course of CLL proceeded similarly in both mouse models (**Fig.3.3B**). The median survival of Eµ-*TCL1* mice amounted 11.6 months whereas survival decreased markedly in Eµ-*TCL1*$^{Akt-C}$ mice to a median survival of 7.6 months independent of gender. Almost all Eµ-*TCL1*$^{Akt-C}$ mice (96%) died until 10 months of age whereas 67% of Eµ-*TCL1* mice survived this time point (**Fig.3.3A**). This confirms a rapidly evolving, aggressive outcome of CLL in Eµ-*TCL1*$^{Akt-C}$ mice.
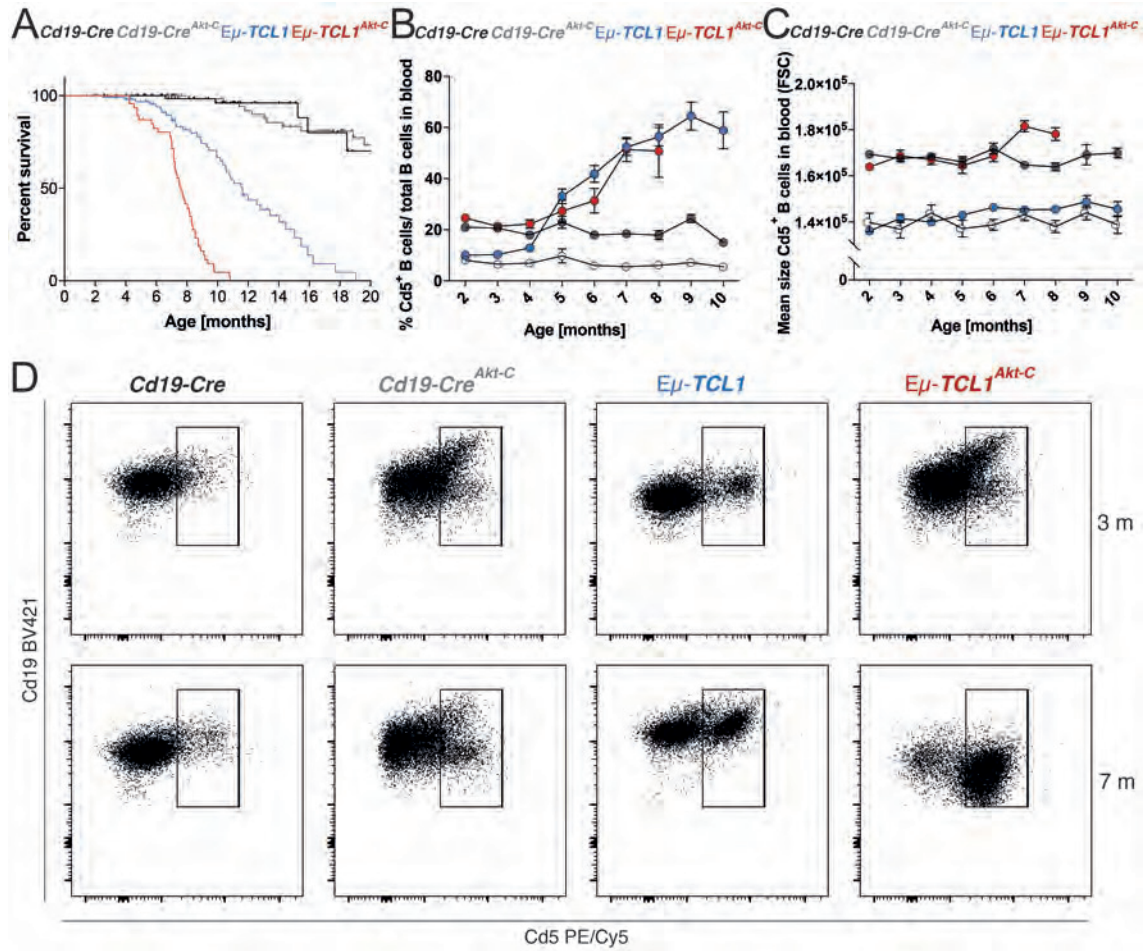
Fig. 3.3: B cell-specific *Akt-C* expression in Eμ-*TCL1* mice promotes progressive CLL.
A Kaplan-Meyer survival curve of indicated mice (n=45-50 mice per genotype). **B** Relative quantification (%) and **C** relative cell size (FSC) of Cd5$^+$ B cells in peripheral blood taken monthly from indicated mice (n=25-30 mice per genotype) *via* flow cytometry. Due to premature death, curve of Eμ-*TCL1*$^{Akt-C}$ mice ends at 8 months age. **D** Representative blots of extracellular Cd5 PE/Cy5 and Cd19 BV421 in blood-derived samples of indicated mice at 3 and 7 months age *via* flow cytometry. The gating to define Cd5$^+$ B cells is shown and used for the quantification in **B** and **C**. Data were previously gated for living (Aqua staining), single cells (FSC-A vs. FSC-H, SSC-A vs. SSC-H). Data are presented as means ± SEM (**B,C**). BV421: Brilliant Violet 421, FSC: forward scatter, PE/Cy5: tandem fluorochrome composed of phycoerythrin (PE) and cyanine 5 (Cy5).

Cd19-Cre and *Cd19-Cre*$^{Akt-C}$ mice revealed neither affected survival capacity nor CLL cells at any age but a constant low level of Cd5$^+$ B cells in peripheral blood (**Fig.3.3B,D**). This assumption is supported by studies showing that the mature B cell selection into B-1a and MZ B cells is compromised in absence of Akt1/Akt2 (Calamito et al., 2010). However, *Cd19-Cre*$^{Akt-C}$ mice featured a B cell-intrinsic phenotype without leukemia/lymphomagenesis at any age (Cox et al, submitted).

3.2.3   B Cell-Specific *Akt-C* Expression in Eµ-*TCL1* Transgenic CLL Mice

Drives RT

RT is characterized as rapid transformation from indolent CLL to an aggressive DL-BCL, advanced by acquired RT-related somatic aberrations. As characteristic, RT cells can be identified by their cell enlargement. Relative cell sizes of Cd5^{+} B cells were determined by the FSC (forward scatter) *via* flow cytometry.
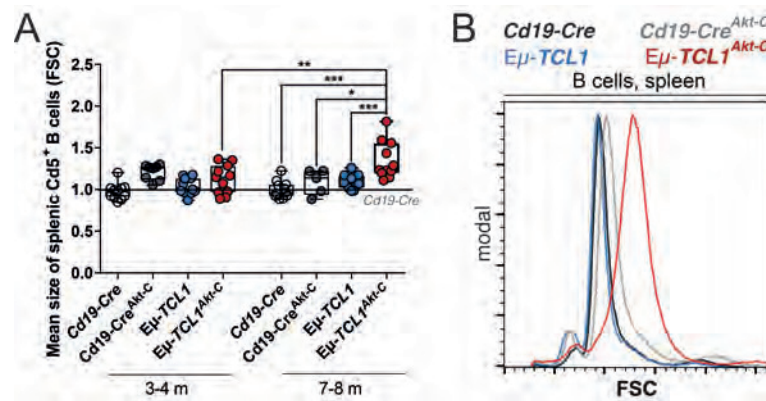
Fig. 3.4: B cell-specific *Akt-C* expression in Eµ-*TCL1* mice causes cancer cell enlargement.
A Relative mean cell size (FSC) of splenic Cd5^{+} B cells of indicated mice at 3-4 and 7-8 months age *via* flow cytometry. **B** Representative blot of FSC of splenic B cells of indicated mice at 7-8 months age. Data were previously gated for living (Aqua staining), single cells (FSC-A vs. FSC-H, SSC-A vs. SSC-H). Data were normalized on 3-4 months old *Cd19-Cre* mice in **A**. Data of mice at 3-4 months age represent the analysis before, at 7-8 months age the analysis after the transformation to RT in Eµ-*TCL1*$^{Akt-C}$ mice. Data are presented as box with whiskers and median (**A**). *p ≤ 0.05, **p ≤ 0.01, and ***p ≤ 0.001. Statistical analyses were performed using Two-Way ANOVA plus Fisher's LSD test (**A**). FSC: forward scatter.

Blood and splenic CLL cells of Eµ-*TCL1* mice displayed unchanged cell sizes over time, similar to *Cd19-Cre* mice. *Cd19-Cre*$^{Akt-C}$ and Eµ-*TCL1*$^{Akt-C}$ mice exhibited larger Cd5^{+} B cells at any age, indicating the capacity of Akt on cell size (Faridi et al., 2003; Latronico et al., 2004). In contrast to the unaltered B cell size of *Cd19-Cre*$^{Akt-C}$ mice throughout life, blood and splenic Cd5^{+} B cells of Eµ-*TCL1*$^{Akt-C}$ mice were enlarged at 6 months of age (**Fig.3.3C, 3.4A,B**).
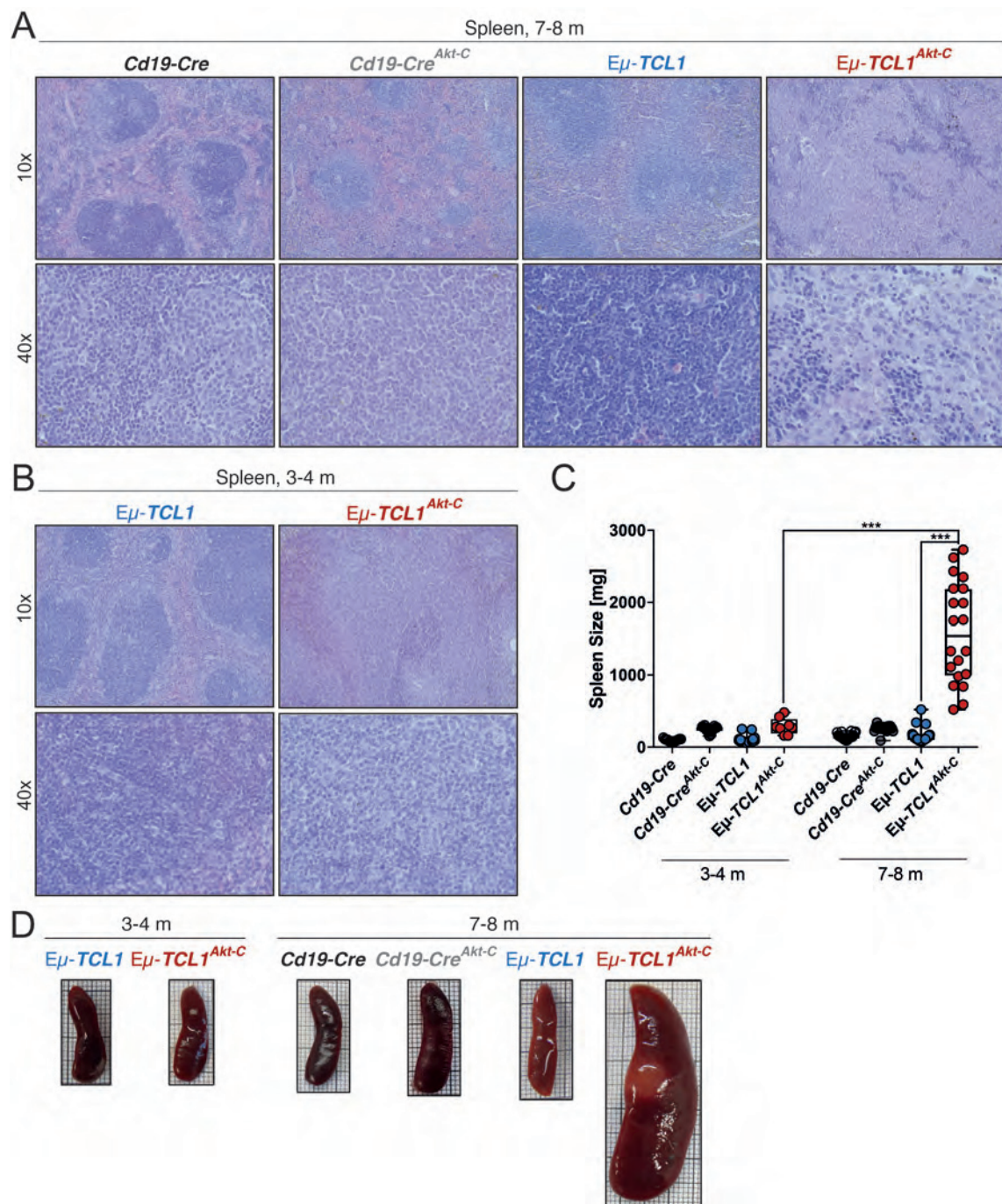
Fig. 3.5: B cell-specific *Akt-C* expression in Eμ-*TCL1* mice drives the progression to RT.
A,B Histological representatives (magnification: 10- and 40-times) of indicated mice at 3-4 and 7-8 months age using H&E staining. **C** Spleen sizes [mg] and **D** representative spleens of indicated mice at 3-4 and 7-8 months age. Data of mice at 3-4 months age represent the analysis before, at 7-8 months age the analysis after the transformation to RT in Eμ-*TCL1*$^{Akt-C}$ mice. Data are presented as box with whiskers and median (**C**). ***p ≤ 0.001. Statistical analyses were performed using Two-Way ANOVA plus Fisher's LSD test (**C**).

Morphological evaluation *via* H&E staining exhibited disrupted splenic histoarchitecture in both Eμ-*TCL1* and Eμ-*TCL1*^{Akt-C} mice at 7-8 months age. Splenocytes of Eμ-*TCL1* transgenic CLL mice displayed normal-sized cells with scant cytoplasm and inconspicuous nucleoli. Contrarily, enlarged, pleomorphic cells with degranulated nuclei and abundant cytoplasm were observed in Eμ-*TCL1*^{Akt-C} mice after transformation (7-8 months of age), thus showing a DLBCL-like histomorphology (**Fig.3.5A**). In contrast, splenocytes of Eμ-*TCL1*^{Akt-C} mice before transformation (3-4 months of age) featured round nucleoplasms with inconspicuous cell sizes (**Fig.3.5B**). *Cd19-Cre* and *Cd19-Cre*^{Akt-C} mice showed ordinary histomorphology at any age. In addition, spleens of *Cd19-Cre*^{Akt-C} and Eμ-*TCL1*^{Akt-C} mice were larger at any age. However, Eμ-*TCL1*^{Akt-C} mice revealed splenomegaly with weights up to 2870 mg (24-times increased) after transformation, a characteristic property of lymphomas. Contrarily, Eμ-*TCL1* mice presented normal-sized spleens at analyzed ages (**Fig.3.5C,D**).
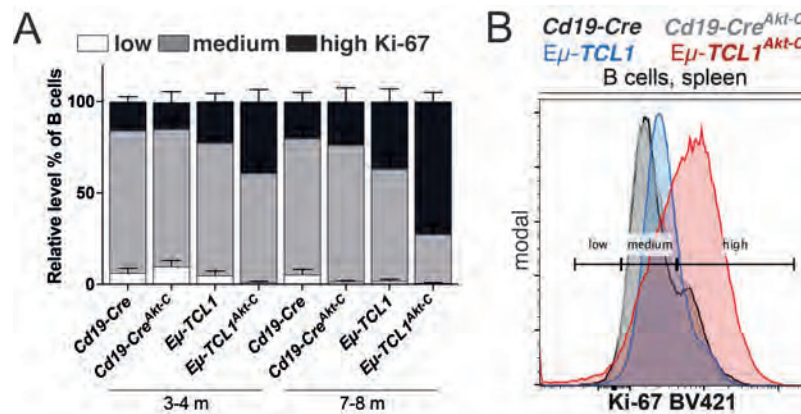
Fig. 3.6: B cell-specific *Akt-C* expression in Eμ-*TCL1* mice demonstrates high proliferative capacity. A Relative level (%) of splenic B cells with low (white), medium (gray) or high (black) levels of nuclear Ki-67 BV421 of indicated mice at 3-4 and 7-8 months age (n=8-12 mice per genotype) *via* flow cytometry. **B** Representative blot of nuclear Ki-67 BV421 in splenic B cells of indicated mice at 7-8 months age *via* flow cytometry. Gating for "medium Ki-67" was defined based on the signal (50% of the maximal amplitude) of nuclear Ki-67 BV421 in *Cd19-Cre* mice. Augmented levels were defined as "high Ki-67", lower levels until the unstained peak (50% of the maximal amplitude) were defined as "low Ki-67". Data were previously gated for living (Aqua staining), single cells (FSC-A vs. FSC-H, SSC-A vs. SSC-H). Data of mice at 3-4 months age represent the analysis before, at 7-8 months age the analysis after the transformation to RT in Eμ-*TCL1*^{Akt-C} mice. Data are presented as box with means ± SEM (**A**). BV421: Brilliant Violet 421.

The proliferative nuclear marker Ki-67 has a strong prognostic value in CLL. The fraction of proliferating cells increases with disease progression (Bruey et al., 2010). Consequently, immoderate proliferative activity was published for RT cases (Giné et al., 2010). The intracellular staining against Ki-67 revealed augmented proliferation rates in splenic B cells of Eµ-TCL1^{Akt-C} mice *via* flow cytometry. Beside equal Ki-67 levels in both 7-8 months old Eµ-TCL1 mice and Eµ-TCL1^{Akt-C} mice before transformation, RT cells of Eµ-TCL1^{Akt-C} mice displayed increased Ki-67 protein, indicating high proliferative capacity and a more progressive disease (**Fig.3.6A,B**). On average, Ki-67 levels were 2.6-times increased in 7-8 months old Eµ-TCL1^{Akt-C} mice compared to *Cd19-Cre* mice. Eµ-TCL1 mice also showed the increase of nuclear Ki-67 protein throughout life but this was small in comparison to Eµ-TCL1^{Akt-C} mice, corresponding to the definition as a low-grade lymphoproliferative disorder (Bosch and Dalla-Favera, 2019). The proliferative capacity of *Cd19-Cre*$^{Akt-C}$ mice resembled that of *Cd19-Cre* mice at any age.
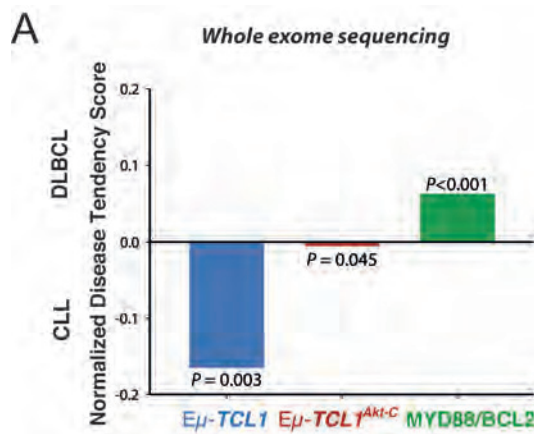
Fig. 3.7: Akt-induced RT cells genetically demonstrate an intermediary form between CLL and DLBCL. A The mean normalized disease tendency score using splenic B cell-derived DNA samples of indicated mice at 7-8 months age *via* whole exome sequencing (WES). Eµ-*TCL1* mice were used as CLL control, MYD88/BCL2 mice as DLBCL control. Data were generated and analyzed by Dr. Stuart Blakemore. P values were calculated *via* binomial testing. CLL: chronic lymphocytic leukemia, DLBCL: diffuse-large B cell lymphoma.

Next, it was investigated whether additional acquired mutations in Eμ-*TCL1*^*Akt-C* mice might drive CLL to RT. In cooperation with the Pallasch lab (CECAD), an intermediary mutational form between CLL and DLBCL has been revealed in splenic RT cells of Eμ-*TCL1*^*Akt-C* mice (n=9) *via* WES (**Fig.3.7A**). This corresponds to the definition of RT by featuring properties of both CLL and DLBCL (Mao et al., 2007). As controls, Eμ-*TCL1* mice pointed out an enrichment of CLL-typical somatic alterations in leukemic cells whereas MYD88/BCL2 mice (Cd19-Cre-driven combined Myd88 and Bcl2 aberrations), a common activated B cell (ABC)-DLBCL mouse model (Knittel et al., 2016), exhibited augmented aberrations characteristically for DLBCL. Thus despite the incidence of RT-typical mutations for individual RT samples including genes of the BCR signaling or *Notch1*, recurrent mutations were absent in RT cells of Eμ-*TCL1*^*Akt-C* mice, suggesting that RT exclusively occurred based on Akt actions as kinase (Kohlhaas et al., 2020). These findings confirm that the continuous B cell-specific activation of Akt kinase in the Eμ-*TCL1* CLL mouse model causes the spontaneous transformation from CLL to RT with a disease penetrance of 100%.

3.2.4   (Phospho)proteomic Profiling Identifies Overexpression of *s100a4* and Reduction of *Pcdc10*, Regulated by Rbpj/Notch

The serine/threonine kinase Akt may function as a central regulator for the transformation from CLL to RT. Akt regulates various metabolic processes involved in cell proliferation, survival, and apoptosis through phosphorylation of *inter alia* Gsk3b (Alessi, Caudwell, et al., 1996), FoxO1 (Biggs et al., 1999; Brunet et al., 1999), and Mdm2 (L. D. Mayo and Donner, 2001; Ogawara et al., 2002) (**Fig.1.6**). To identify relevant downstream actions of Akt arising in RT, alterations on protein levels and their phosphorylation states were investigated using proteomics and phosphoproteomics in collaboration

with the Krüger lab (CECAD). For this, splenic B cell-derived proteins of 7-8 months old

Eμ-*TCL1* (n = 4) and Eμ-*TCL1*$^{Akt-C}$ (n = 4) mice were investigated.
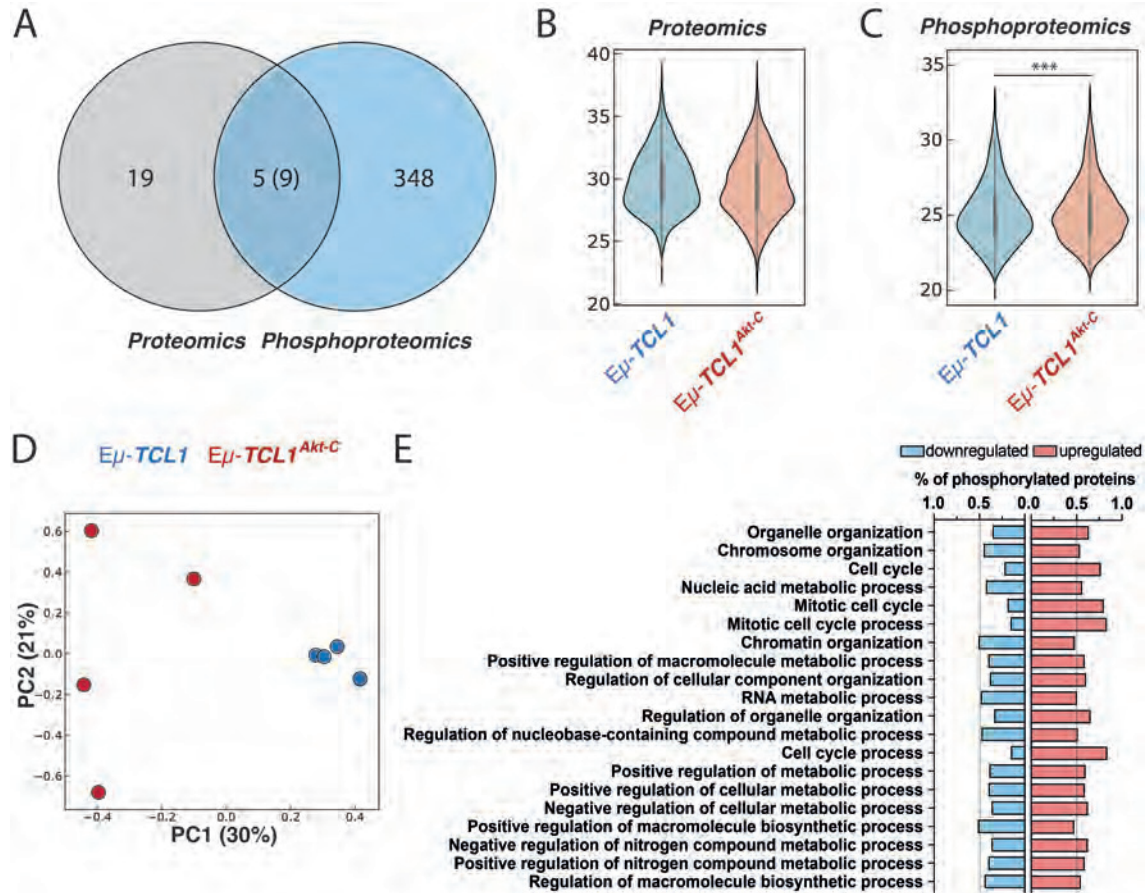
Fig. 3.8: Akt-induced RT cells reveal the enrichment of activating phosphorylation of proteins involved in cell cycle processes. A Venn diagram showing numbers of proteins with different amounts (grey, proteomics) or phosphorylation states (blue, phosphoproteomics) of splenic B cells in comparison between Eμ-*TCL1*$^{Akt-C}$ vs. Eμ-*TCL1* mice. Five proteins with in total nine phosphorylation sites (Akt1, Golm1, Mecp2, Nfatc1, Sp140) were significantly changed in both proteomics and phosphoproteomics. **B,C** Label-free quantification (LFQ) intensity of proteomics and phosphoproteomics of indicated mice. **D** Principal component analysis (PCA) plot of indicated mice. **E** Gene Ontology (GO) Enrichment Analysis of biological processes (n=20 terms, P-value cutoff (FDR) < 0.05) of significantly changed phosphorylation sites (phosphoproteomics) in comparison between Eμ-*TCL1*$^{Akt-C}$ vs. Eμ-*TCL1* mice using ShinyGO v0.61. The measurement of samples on the mass spectrometry was carried out by Dr. Janica Wiederstein (CECAD). ***p ≤ 0.001. PC1,2: principal component 1,2.

Mice with identical genotypes exhibited similar outcome and hence, homogeneous biology of RT or CLL samples (**Fig.3.8D**). Despite the constant total amount of proteins, significantly more phosphorylated proteins were observed in Eμ-*TCL1*$^{Akt-C}$ mice, rep-

resenting the activity of Akt kinase (**Fig.3.8B,C**). Most altered phosphorylation sites were enhanced phosphorylated (70.3%) in Eμ-*TCL1^{Akt-C}* mice. In total, 24 proteins and 357 phosphorylation sites were significantly changed in Eμ-*TCL1^{Akt-C}* mice compared to Eμ-*TCL1* mice. In RT cells, five proteins (Akt1, Golm1, Mecp2, Nfatc1, and Sp140) displayed changes on both protein levels and phosphorylation states (**Fig.3.8A**).

To identify biological processes in which Akt-mediated phosphorylated proteins were involved, Gene Ontology (GO) Enrichment Analysis (n=20 terms, P-value cutoff (FDR) < 0.05) was performed with proteins showing altered phosphorylation using ShinyGO v0.61 software. Changed phosphorylated proteins were involved in an abundance of processes including cell cycle, epigenetic regulation, and biosynthesis (**Fig.3.8E**). While most processes revealed equal levels of up- and downregulated phosphorylation, enhanced phosphorylation (77.2-84.2%) was enriched for proteins involved in cell cycle. Phosphorylation of these proteins, such as cyclin-dependent kinase 4 (Cdk4) (Bockstaele et al., 2006), chromosome alignment-maintaining phosphoprotein 1 (Champ1) (Itoh et al., 2011), minichromosome maintenance complex component 3 (Mcm3) (Lin, Aggarwal, and Diehl, 2008), kinesin family member 11 and 23 (Kif11, Kif23) (Rapley et al., 2008; Daigo et al., 2018), and nucleoporin Tpr (Rajanala et al., 2014), have been discovered to promote proliferation.

Moreover, Akt1 overactivation and enhanced availability were revealed in B cells of Eμ-*TCL1^{Akt-C}* mice, validating the Akt-mediated RT mouse model (**Fig.3.9A-C**). S100a4, a member of the Ca^{2+}-dependent S100 family, was identified as the most significantly up-regulated protein in Eμ-*TCL1^{Akt-C}* mice (12-times increased, **Fig.3.9A**) (Zimmer et al., 1995). The metastasis factor S100a4 correlates with poor prognosis in multiple solid tumors, including ovarian (Kikuchi et al., 2006; Link et al., 2019), prostate (Saleem et al., 2006; Siddique et al., 2013), and lung cancer (R. L. Stewart et al., 2016). In leukemia subtypes like AML, S100a4 has been shown to promote proliferation, cell cycle pro-

gression, and cell survival in transformed cells (Brenner and Bruserud, 2018; Alanazi et al., 2020).
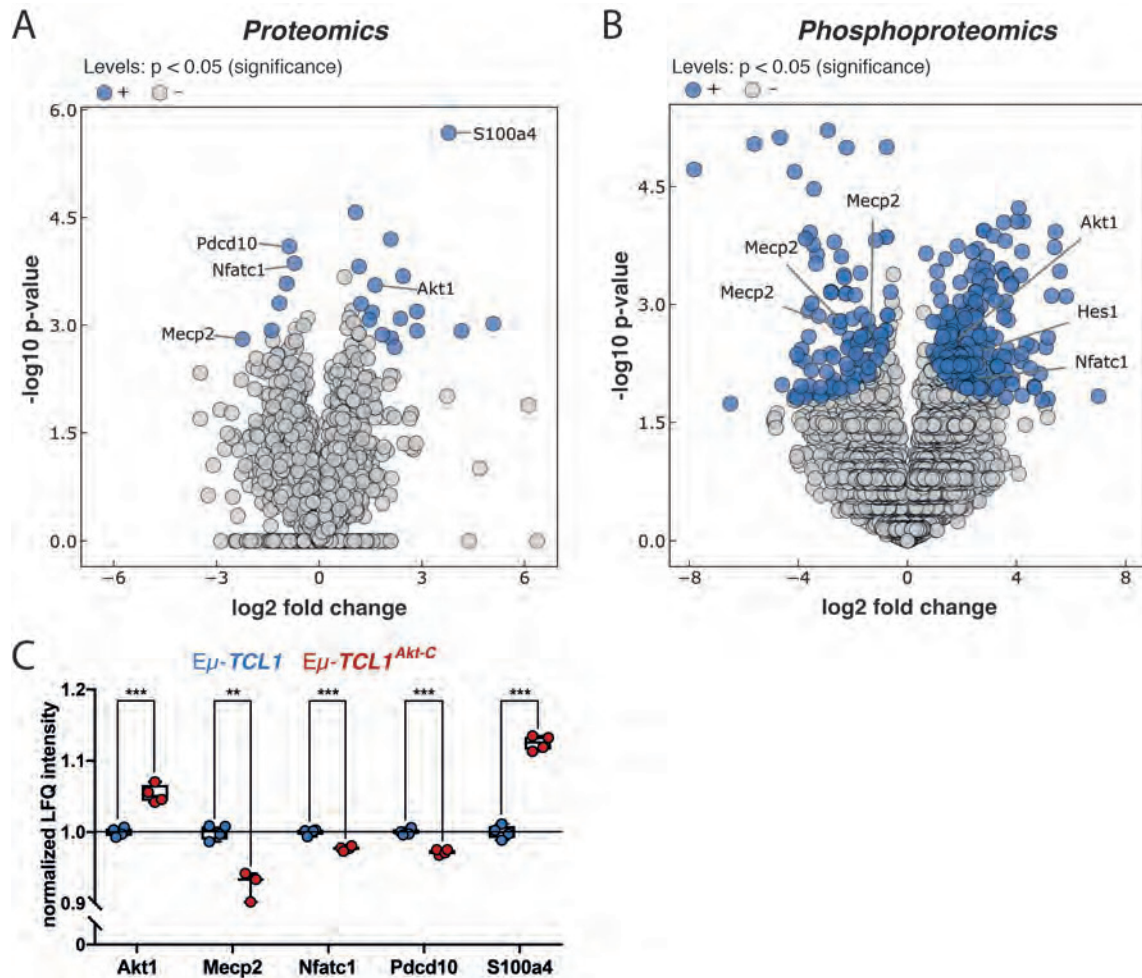
Fig. 3.9: Proteomics and Phosphoproteomics identify changes for S100a4, Mecp2, and Pdcd10, related to the Notch1 signaling. A,B Volcano blot of proteomics and phosphoproteomics of splenic B cells in comparison between Eμ-$TCL1^{Akt-C}$ vs. Eμ-$TCL1$ mice. Proteins with p < 0.05 were labeled as significant (blue colored). **C** Normalized label-free quantification (LFQ) intensity of indicated protein amounts (proteomics) of indicated mice. Data were normalized to the mean of Eμ-$TCL1$ mice. All data are presented as box with whiskers and median (**C**). **p ≤ 0.01 and ***p ≤ 0.001. Statistical analyses were performed using Student's t test (**C**).

A negative regulator of *s100a4* transcription, named Nfatc1, was reduced but more phosphorylated at Ser390 in Eμ-$TCL1^{Akt-C}$ mice (Bhattacharyya et al., 2011). In addition, methyl CpG binding protein 2 (Mecp2), a repressor of the Akt signaling and *Notch1,* was reduced and less phosphorylated at Ser70, Ser229, and Ser292 in RT cells (**Fig.3.9A,B**) (Li et al., 2014; W. Zhang et al., 2018). Furthermore, programmed cell

death 10 (Pdcd10) protein was reduced in RT cells of Eµ-*TCL1*$^{Akt-C}$ mice (**Fig.3.9A,C**). In accordance to this result, *Pdcd10* transcription has been reported to be repressed by Rbpj/Notch1, associated with tumoral cell proliferation (Lambertz et al., 2015). To investigate whether changed protein levels in Eµ-*TCL1*$^{Akt-C}$ mice are a consequence of altered gene expression, promoter regions (e.g. 2 kb upstream of transcription start) of significantly altered proteins were analyzed for transcription factor binding sites *via* Genomatix software. Akt regulates the activity of multiple transcription factors by phosphorylation. Mainly, Akt enhances the activity of Myc (R. Sears et al., 2000; R. C. Sears, 2004), Nfatc1 (Crabtree and Olson, 2002; Beurel, Grieco, and Jope, 2015), and Rbpj/Notch (Villegas et al., 2018) but represses FoxO1 (X. Zhang et al., 2011) and p53 (Ogawara et al., 2002) (**Fig.3.10A**). Significantly changed proteins exhibited variable transcription factor binding sites for FoxO1, Myc, Nfatc1, p53, and Rbpj (Notch) in their 2 kb upstream promoter region of corresponding genes, suggesting a direct transcriptional link between these transcription factors in *Akt-C*-expressing RT cells. In total, 13% of genes of changed proteins showed FoxO1 binding sites while 17%, 39%, and 43% of genes revealed binding sites for Myc, Nfatc1, and p53. The majority (65%) of significantly changed available proteins was identified as potential Rbpj/Notch target genes (**Fig.3.10B**).
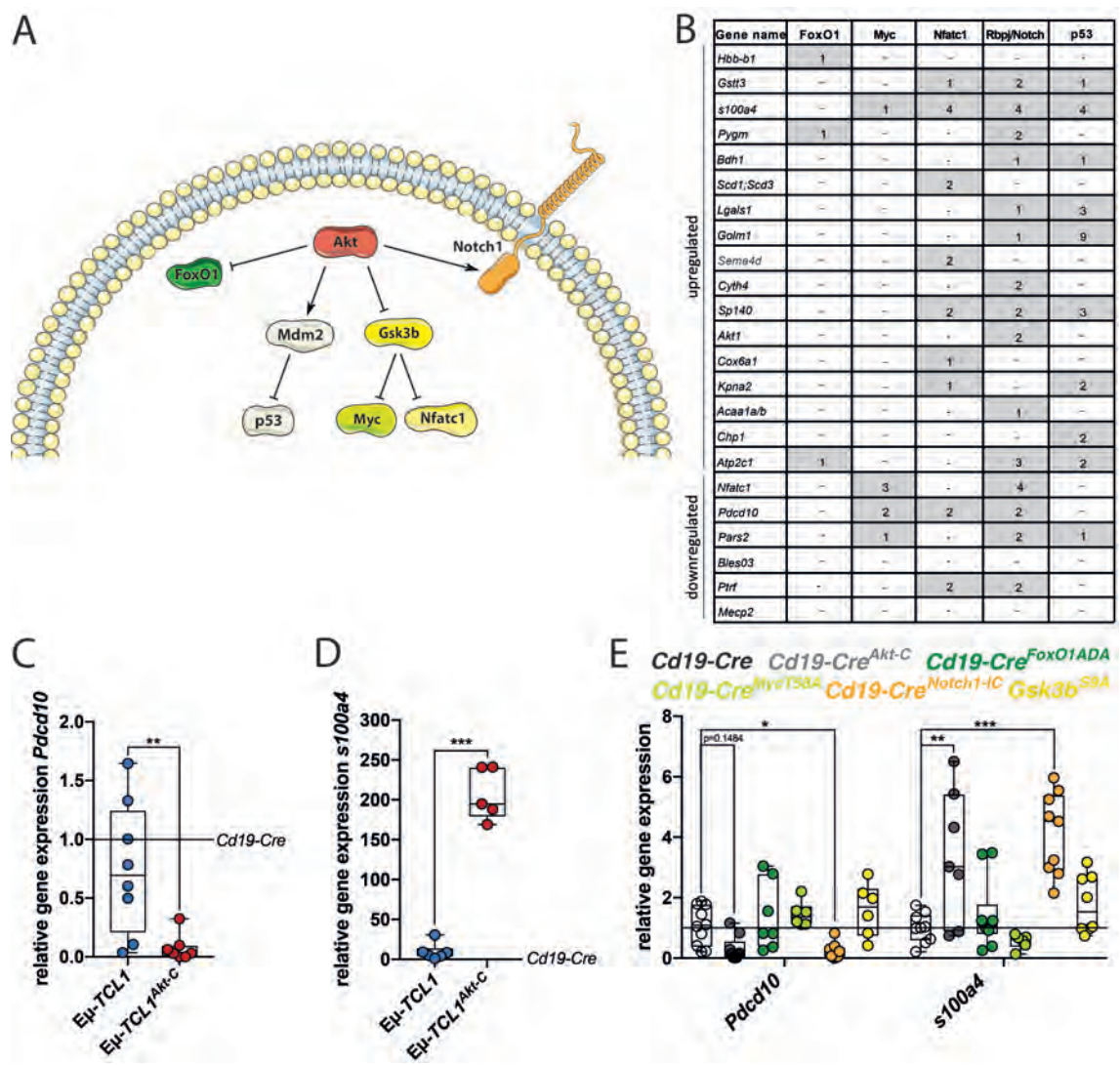
Fig. 3.10: Rbpj/Notch1-regulated transcriptional changes of *Pdcd10* and *s100a4* in Akt-initiated RT cells. A Scheme of downstream transcription factors of Akt. **B** Numbers of indicated transcription factor binding sites for significantly changed available proteins (proteomics) in comparison between Eµ-*TCL1*^Akt-C^ vs. Eµ-*TCL1* mice using Genomatix software. The transcription factors FoxO1, Myc, Nfatc1, Rbpj/Notch, and p53 were analyzed as effector of Akt. Proteins were sorted by values of the log2 fold change. **C-E** Relative gene expression of *Pdcd10* and *s100a4* relative to *Tbp* in splenic B cells of indicated mice at 7-8 months age *via* qPCR. Data were normalized to *Cd19-Cre* mice in **C-E**. All data are presented as box with whiskers and median (**C-E**). *p ≤ 0.05, **p ≤ 0.01, and ***p ≤ 0.001. Statistical analyses were performed using Student's t-test (**C-D**) and One-Way ANOVA plus Fisher's LSD test (**E**).

In accordance with proteomic data, increased *s100a4* expression was validated in B cells from Eµ-*TCL1*^Akt-C^ mice that revealed transcription factor binding sites for Myc, Nfatc1, p53, and Rbpj/Notch (**Fig.3.10D**). Using mouse models with conditional nuclear activation of FoxO1 (Cd19-Cre tg/wt; R26-fl-*FoxO1ADA*, termed *Cd19-Cre*^FoxO1ADA^),

Myc (Cd19-Cre tg/wt; R26-fl-*MycT58A*, termed *Cd19-Cre^MycT58A*), and Notch1 (Cd19-Cre tg/wt; R26-fl-*Notch1-IC*, termed *Cd19-Cre^Notch1-IC* mice, see chapter 3.3) or with indirect inhibition of Nfatc1 (Gsk3b^S9A, constitutive activation of Gsk3b kinase) in B cells, the transcriptional regulation of *s100a4* by Rbpj/Notch1 was verified (**Fig.3.10E**). Furthermore, *Pdcd10* expression was suppressed in Akt-mediated RT cells by Rbpj/Notch1 due to transcriptional repression in both Eµ-*TCL1^Akt-C* and *Cd19-Cre^Notch1-IC* mice (**Fig. 3.10C,E**). *Akt1* further showed transcription factor binding sites for Rbpj/Notch that is discussed in chapter 3.3.3.
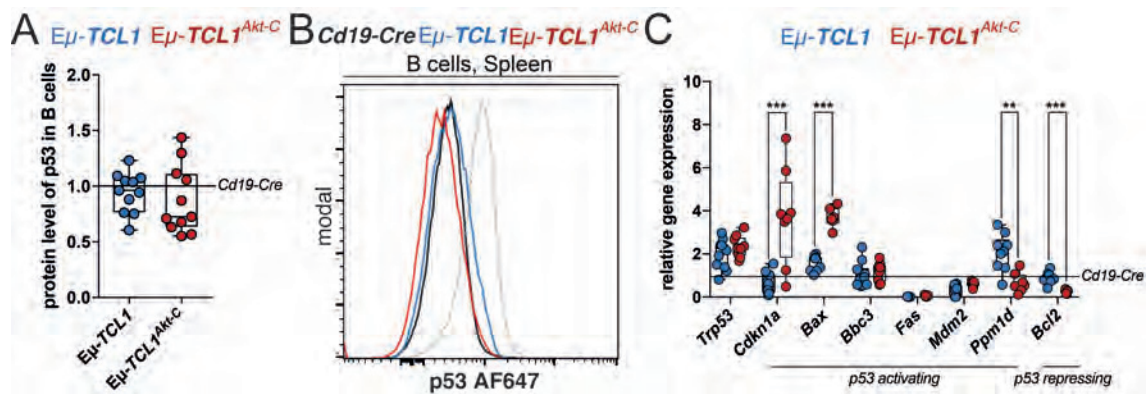
Fig. 3.11: Unaffected p53 activity in Akt-induced RT cells. A Relative protein quantification and **B** its representative blot of intracellular p53 AF647 in splenic B cells of indicated mice at 7-8 months age. **C** Relative gene expression of *Trp53* and common p53 target genes relative to *Tbp* in B cells of indicated mice at 7-8 months age. Data were previously gated for living (Aqua staining), single cells (FSC-A vs. FSC-H, SSC-A vs. SSC-H) in **B**. Data were normalized to *Cd19-Cre* mice in **A** and **C**. All data are presented as box with whiskers and median (**A,C**). **p ≤ 0.01 and ***p ≤ 0.001. Statistical analyses were performed using Student's t test (**A,C**). AF647: AlexaFluor 647.

In addition, despite the widely accepted Akt-mediated degradation of p53 (**Fig.3.10A**) (Ogawara et al., 2002), the protein level of the tumor suppressor p53 remained unchanged in transformed Eµ-*TCL1^Akt-C* mice compared to Eµ-*TCL1* and *Cd19-Cre* mice (**Fig.3.11A,B**). The transcriptional level of *Trp53* was also identical in both cancer mouse models but displayed upregulation compared to *Cd19-Cre* mice. Common target genes of p53 confirmed no tendency of expression pattern (**Fig.3.11C**) (Fischer, 2017). While some targets imply increased p53 activity (*Cdkn1a*, *Bax*, *Bcl2*), others implicate un-

changed or decreased activity (*Bbc3*, *Fas*, *Mdm2*, *Ppm1d*). Most p53 target genes are known to be additionally regulated by further transcription factors. For instance, *Cdkn1a* expression has been shown to be also regulated by Rbpj/Notch1 (Guo et al., 2009), p16 (Al-Khalaf and Aboussekhra, 2013), and Wnt/β-catenin (Xu et al., 2016). In summary, (phospho)proteomic profiling leads to the assumption that a potential cross-talk between Akt and Notch1 signaling increases the aggressiveness of CLL toward RT.

3.2.5 *Akt-C* Expression in RT Cells Results in Overactivation of the Notch1 Signaling

Human data indicate a possible link between gain-of-function mutations of the *NOTCH1* gene and augmented activation of AKT in patients with RT or an aggressive course of CLL (see chapter 3.1). In addition, changes on protein levels and their phosphory-lation states were identified in murine RT cells, associated with Rbpj/Notch1 activity (see chapter 3.2.4). Notch proteins act as cofactors for the transcription factor Rbpj by enhancing expression of genes involved in B cell development and proliferation (see chapter 1.4) (Kang, Kim, and Park, 2014; Francesca Arruga, Vaisitti, and Deaglio, 2018). *Notch1* and *Notch3* expression were significantly upregulated in RT cells of Eμ-*TCL1*$^{Akt-C}$ mice compared to CLL cells of Eμ-*TCL1* mice (**Fig.3.12A**). However, C_T (cycle threshold) values indicated low mRNA levels of *Notch3* in RT cells and ordinary levels compared to *Cd19-Cre* mice. Increased transcription of common target genes implicate enhanced Rbpj/Notch activity in RT cells of Eμ-*TCL1*$^{Akt-C}$ mice while CLL cells of Eμ-*TCL1* mice revealed unaffected expression levels of Rbpj/Notch target genes, similar to *Cd19-Cre* mice (**Fig.3.12B**) (Borggrefe and Oswald, 2009).
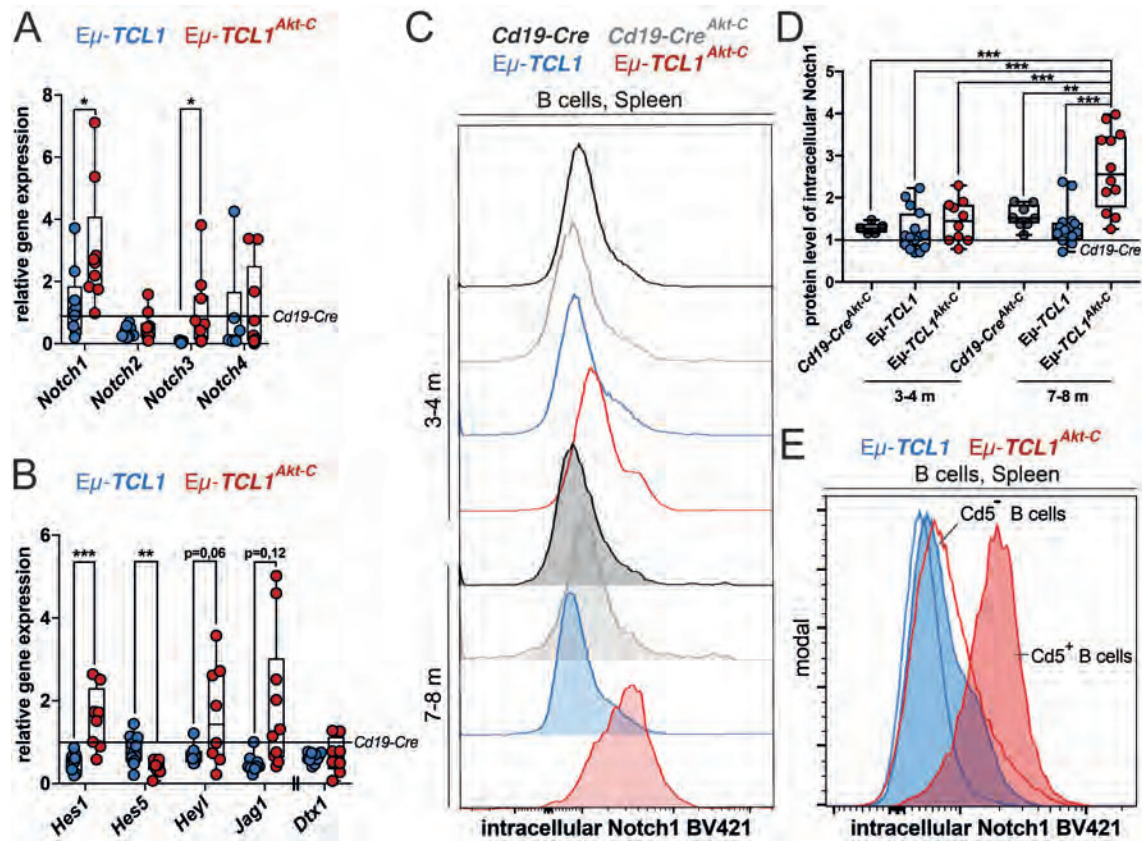
Fig. 3.12: Overactivation of the Notch1 signaling in Akt-induced RT cells. A Relative gene expression of Notch receptors and **B** common canonical (*Hes1*, *Hes5*, *Heyl*, and *Jag1*) as well as non-canonical (*Dtx1*) Rbpj/Notch target genes relative to *Tbp* in splenic B cells of indicated mice at 7-8 months age *via* qPCR. **C** Representative blot of intracellular Notch1 BV421 and **D** its relative protein quantification in splenic B cells of indicated mice at 3-4 (uncolored) and 7-8 months age (colored) *via* flow cytometry. **E** Representative blot of intracellular Notch1 BV421 in splenic Cd5⁻ (uncolored) and Cd5⁺ B cells (colored) of indicated mice at 7-8 months age *via* flow cytometry. Data were previously gated for living (Aqua staining), single cells (FSC-A vs. FSC-H, SSC-A vs. SSC-H) in **C** and **E**. Data were normalized to *Cd19-Cre* mice in **A**, **B**, and **D**. Data of mice at 3-4 months age represent the analysis before, at 7-8 months age the analysis after the transformation to RT in Eµ-*TCL1*^Akt-C^ mice. All data are presented as box with whiskers and median (**A,B,D**). *p ≤ 0.05, **p ≤ 0.01, and ***p ≤ 0.001. Statistical analyses were performed using Student's t-test (**A,B**) and Two-Way ANOVA plus Fisher's LSD test (**D**). BV421: Brilliant Violet 421.

Hes1 and *Dtx1* were selected as hallmark to distinguish between the activation of the canonical and non-canonical Notch signaling (F. Arruga et al., 2014). The unaltered *Dtx1* but enhanced *Hes1* expression demonstrated the restriction to the activation of the canonical Notch signaling. The expression-based data are in line with the transcriptional profile of RT cells of Eµ-*TCL1*^Akt-C^ mice compared to CLL cells of Eµ-*TCL1* mice *via* single cell RNA sequencing (scRNA-seq) in collaboration with Pallasch lab

(CECAD). scRNA-seq data demonstrated transcriptional upregulation of genes regulated by Rbpj/Notch1, such as *Hes1* and *s100a4* (Kohlhaas et al., 2020).

Strikingly, high protein levels of intracellular Notch1 were solely detected in RT cells of Eμ-*TCL1^{Akt-C}* mice. B cells of *Cd19-Cre^{Akt-C}* mice showed low levels of intracellular Notch1 in comparison to RT-transformed Eμ-*TCL1^{Akt-C}* mice but enhanced levels compared to *Cd19-Cre* mice. Contrariwise, CLL cells of Eμ-*TCL1* mice showed unaffected levels of intracellular Notch1 at any age in both Cd5$^+$ CLL and normal Cd5$^-$ B cells (**Fig.3.12C-E**). Besides, upregulation of intracellular Notch1 was restricted to Cd5$^+$ RT cells whereas normal Cd5$^-$ B cells of the same mouse showed low levels (**Fig.3.12E**). These data confirm the overactivation of the Notch1 pathway in murine Akt-mediated RT.

3.2.6 Splenic, Regulatory T cells Induce Overactivation of Notch1 Signaling in RT Cells by Presenting Dll1 Ligand

The transmembrane receptor Notch1 is activated through cleavage after binding to Jag or Dll ligands presented on adjacent cells to mediate changes of the microenvironment. CLL manifestation is influenced by bidirectional communication between leukemic cells and the TME through several crosstalk mechanisms by stimulating cell survival, proliferation, and metastasis (Quail and Joyce, 2013; Hacken and Jan A. Burger, 2016; Meurette and Mehlen, 2018). The marrow and SLO-located TME form the supportive structure to develop CLL and to progress to RT including macrophages (Galletti, Caligaris-Cappio, and Bertilaccio, 2016), monocyte-derived NLCs (J. A. Burger et al., 2000; Boissard et al., 2015), marrow stromal cells (Kurtova et al., 2009; Crompot et al., 2017), and several T cell subsets (Bagnara et al., 2011).
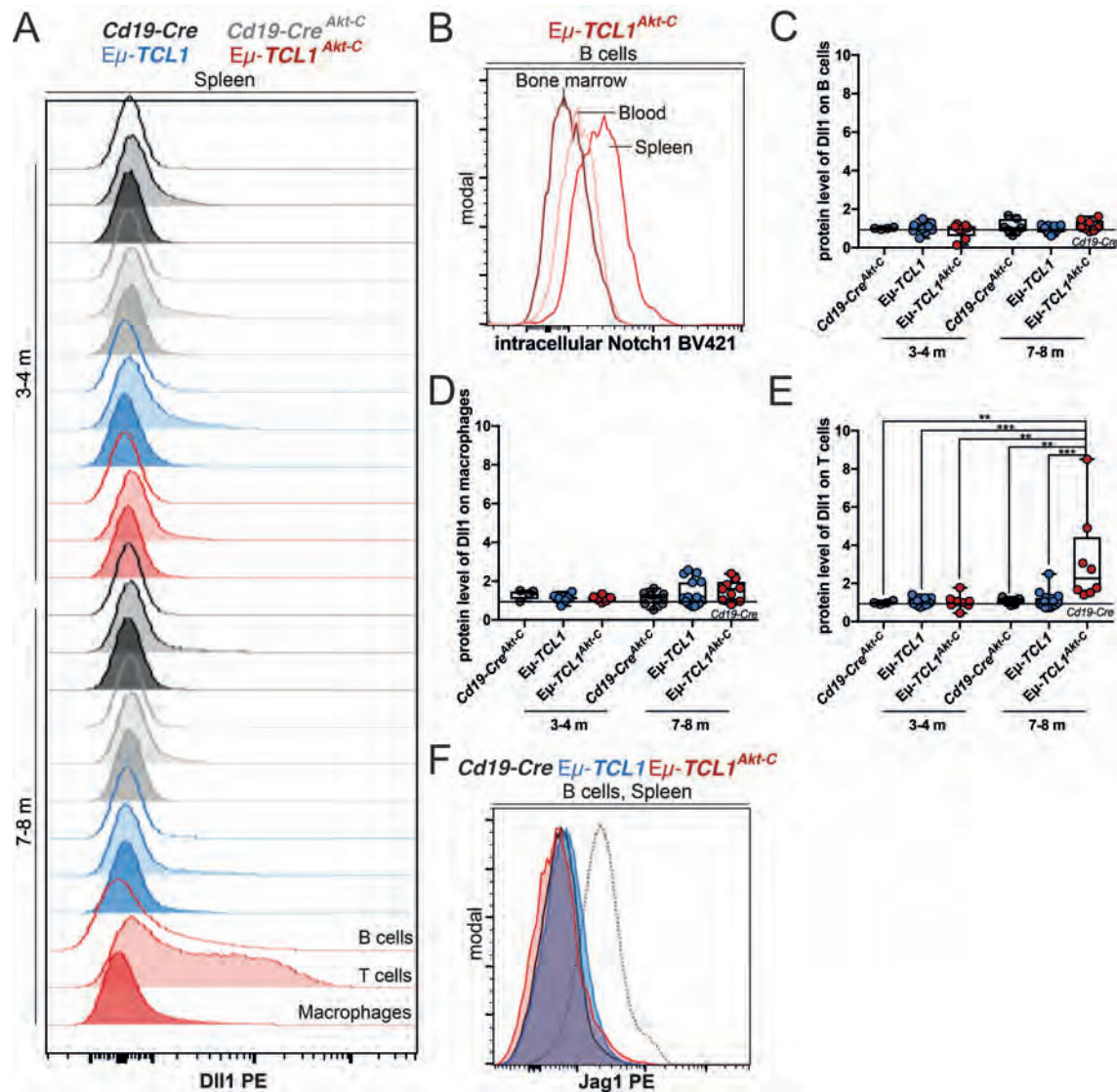
Fig. 3.13: Aberrant Dll1 on splenic T cells stimulates Notch1 signaling inAkt-induced RT.
A Representative blot of extracellular Dll1 PE on splenic B cells (uncolored), T cells (slightly colored), and macrophages (colored) of indicated mice at 3-4 and 7-8 months age *via* flow cytometry.
B Representative blot of intracellular Notch1 BV421 in blood (light red), splenic (red), and marrow (dark red) B cells of Eµ-*TCL1*$^{Akt-C}$ mice at 7-8 months age *via* flow cytometry. **C** Relative protein quantification of extracellular Dll1 PE on splenic B cells, **D** macrophages, and **E** T cells, of indicated mice at 3-4 and 7-8 months age *via* flow cytometry. **F** Representative blot of extracellular Jag1 PE on splenic B cells of indicated mice at 7-8 months age *via* flow cytometry. The dashed histogram represents a positive control. Data were previously gated for living (Aqua staining), single cells (FSC-A vs. FSC-H, SSC-A vs. SSC-H) in **A**, **B**, and **F**. Data were normalized to *Cd19-Cre* mice in **C-E**. Data of mice at 3-4 months age represent the analysis before, at 7-8 months age the analysis after the transformation to RT in Eµ-*TCL1*$^{Akt-C}$ mice. All data are presented as box with whiskers and median (**C-E**). **p ≤ 0.01 and ***p ≤ 0.001. Statistical analyses were performed using Two-Way ANOVA plus Fisher's LSD test (**C-E**). BV421: Brilliant Violet 421, PE: phycoerythrin.

Notch receptor - ligand interactions and their impact in RT progression have not been investigated so far. Tissue-specific analysis of intracellular Notch1 in transformed Eµ-*TCL1^{Akt-C}* mice indicates strongest Notch1 stimulation in splenic RT cells whereas marrow RT cells showed same levels as blood RT cells where cells are not in tight contact (**Fig.3.13B**). This result corresponds to human data evidencing that the transcriptional and protein-based upregulation of NOTCH1 was highest in SLO-derived CLL cells (F. Arruga et al., 2014). To specify ligand-presenting cells, protein levels of the prominent Notch1 ligand Dll1 were determined on the cell surface of splenic TME cells. Thereby, aberrant Dll1 was discovered on Cd90⁺ T cells in RT-transformed Eµ-*TCL1^{Akt-C}* mice. In contrast, T cells of Eµ-*TCL1^{Akt-C}* mice before transformation, Eµ-*TCL1* and *Cd19-Cre^{Akt-C}* mice showed unchanged Dll1 levels (**Fig.3.13A,E**). Simultaneously, Dll1 was unaltered presented on F4/80⁺ macrophages (**Fig.3.13D**). NLCs could not be identified in murine spleens.

In addition, RT cells of Eµ-*TCL1^{Akt-C}* mice showed low Dll1 levels (**Fig.3.13A,C**). Although another Notch1 ligand, named Jag1, has been identified as direct Rbpj/Notch1 target and was transcriptionally upregulated in RT-transformed Eµ-*TCL1^{Akt-C}* mice (**Fig. 3.12B**), Jag1 protein remained unchanged in RT cells (**Fig.3.13F**). These flow cytometry data are in line with previous studies showing the lack of DLL1 and DLL4 as well as unaltered JAG1 and JAG2 ligands in human CLL cells in both *NOTCH1* mutated and wildtype cases (F. Arruga et al., 2014). Furthermore, JAG1 expression and protein processing have been shown to associate with survival of CLL cells but not with NOTCH activation (De Falco et al., 2018). Here, low levels of Notch ligands on cancer cells confirm their inability to promote RT among each other but dependency on surrounding TME cells. The apoptotic bias of CLL and RT cells in absence of supportive TME cells is well accepted. As reported, only co-cultivation or supplementation of cytokines rescues leukemic cells from spontaneous apoptosis *ex vivo* (Ghamlouch et al., 2013).
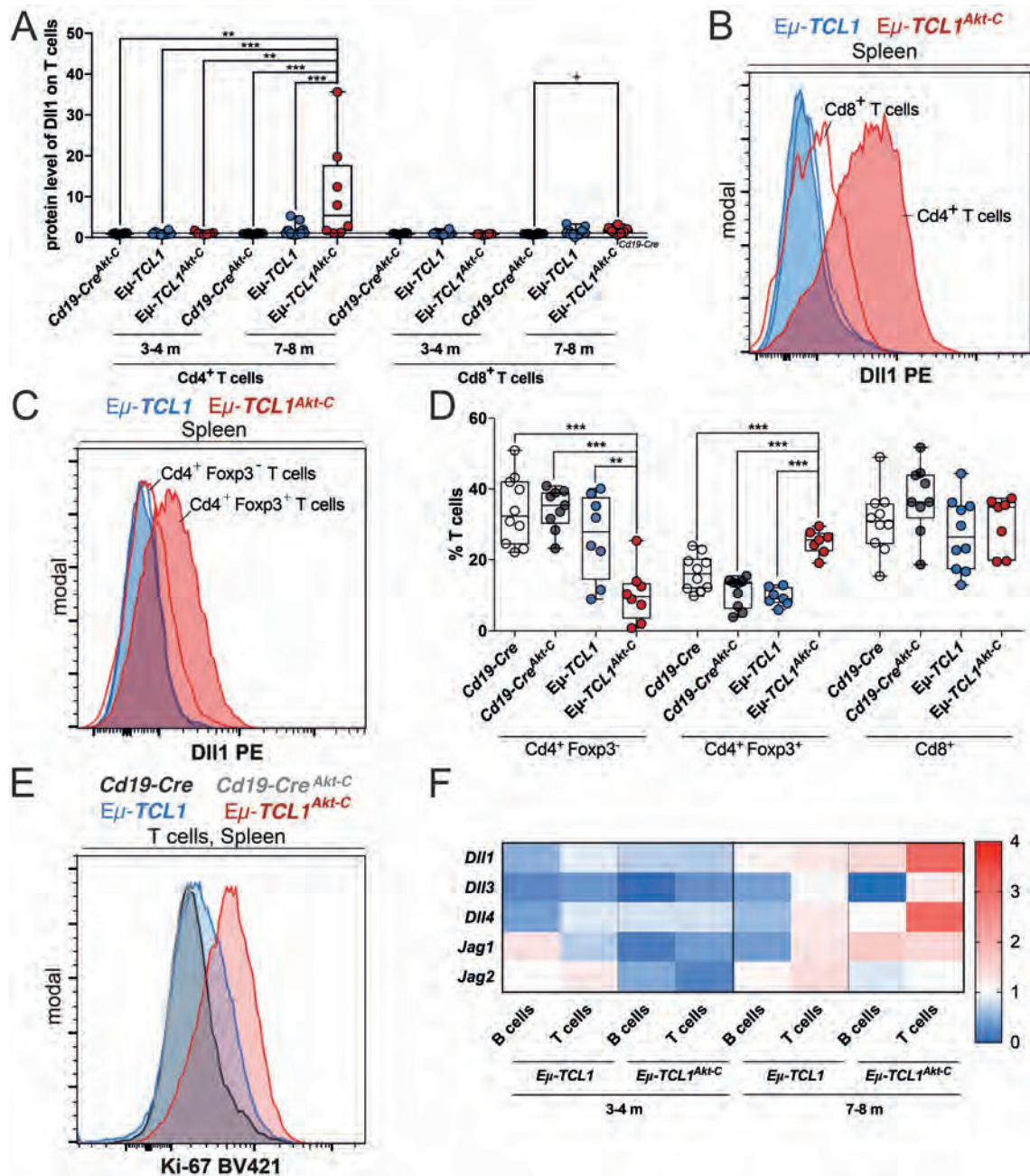
Fig. 3.14: Cell expansion and aberrant Dll1 on splenic, regulatory T cells stimulate Notch1 signaling in Akt-induced RT. A Relative protein quantification of extracellular Dll1 PE on splenic T cell subsets of indicated mice at 3-4 and 7-8 months age *via* flow cytometry. **B** Representative blot of extracellular Dll1 PE on splenic Cd4$^+$ (colored) and Cd8$^+$ T cells (uncolored) or on **C** Cd4$^+$ Foxp3$^-$ T helper cells (uncolored) and Cd4$^+$ Foxp3$^+$ regulatory T cells (colored) of indicated mice at 7-8 months age *via* flow cytometry. **D** Frequencies of splenic T cell subsets of indicated mice at 7-8 months age *via* flow cytometry. **E** Representative blot of nuclear Ki-67 BV421 in T cells of indicated mice at 7-8 months age *via* flow cytometry. **F** Relative gene expression of Notch ligands relative to *Tbp* in splenic B cells and T cells of indicated mice at 3-4 and 7-8 months age *via* qPCR. Data were previously gated for living (Aqua staining), single cells (FSC-A vs. FSC-H, SSC-A vs. SSC-H) in **B**, **C**, and **E**. Data were normalized to *Cd19-Cre* mice in **A** and **F**. Data of mice at 3-4 months age represent the analysis before, at 7-8 months age the analysis after the transformation to RT in Eμ-*TCL1*$^{Akt-C}$ mice. All data are presented as box with whiskers and median (**A**,**D**). *p ≤ 0.05, **p ≤ 0.01, and ***p ≤ 0.001. Statistical analyses were performed using One-Way (**D**) or Two-Way (**A**) ANOVA plus Fisher's LSD test. BV 421: Brilliant Violet 421, PE: phycoerythrin.

T cells are subdivided into Cd4$^+$ T helper or T$_{reg}$ cells as well as Cd8$^+$ cytotoxic T cells. Corresponding to the assumed CLL-promoting function of Cd4$^+$ T cells (Os et al., 2013), increased Dll1 levels were monitored on Cd4$^+$ T cells, especially Foxp3$^+$ T$_{reg}$ cells, in Eµ-*TCL1*$^{Akt-C}$ mice during RT. Dependent on the state of RT, the upregulation of Dll1 varied between a 1.8-times and a 35.6-times increase. Foxp3$^-$ T helper and Cd8$^+$ cytotoxic T cells revealed unchanged ligand levels. In contrast, Eµ-*TCL1*$^{Akt-C}$ mice before transformation, Eµ-*TCL1* and *Cd19-Cre*$^{Akt-C}$ mice showed low levels of Dll1 on diverse T cell subsets (**Fig.3.14A-C**). Furthermore, splenic T cells exhibited increased proliferation rates in RT-transformed Eµ-*TCL1*$^{Akt-C}$ mice by nuclear Ki-67 staining causing cell expansion (**Fig.3.14E**). As consequence, T$_{reg}$ cells expanded solely in Eµ-*TCL1*$^{Akt-C}$ mice with frequencies up to 28% of total T cells at the expense of T helper cells (**Fig.3.14D**). These observations matched with the scRNA-seq data of the splenic TME of RT-transformed Eµ-*TCL1*$^{Akt-C}$ mice which demonstrated an enrichment of Cd4$^+$ T cells with genes involved in pro-survival pathways, such as *Bcl2* (Kohlhaas et al., 2020). In accordance, increased frequencies of blood-derived T$_{reg}$ cells are reported in CLL patients with high accumulation in SLOs, associated with progressive outcome and unfavorable genetics (Weiss et al., 2011; Biancotto et al., 2012).

To investigate the cause of exaggerated Dll1 on T$_{reg}$ cells, the transcription of Notch ligands was determined. The transcription of *Dll1* and *Dll4* demonstrated a similar expression pattern, showing T cell-restricted overexpression in RT-transformed Eµ-*TCL1*$^{Akt-C}$ mice. *Dll3*, *Jag1*, and *Jag2* pointed unchanged expression in T cells of analyzed mice (**Fig.3.14F**). Presumably, upregulation of ligands in T$_{reg}$ cells occurred through transcriptional regulation during RT.

Consolidated, these data affirm the stimulation of the proto-oncogenic Notch1 signaling through splenic T$_{reg}$ cells by stringently presenting Notch1 ligands on the cell surface.

3.3   B Cell-Specific *Notch1-IC* Expression in Eμ-*TCL1* Transgenic CLL Mice Empowers the Transformation to RT

3.3.1   B Cell-Specific *Notch1-IC* Expression Drives RT in Eμ-*TCL1* Mice

Gain-of-function mutations of *NOTCH1* have been identified as the most frequently RT-promoting aberration (Puente et al., 2011; Fabbri, Rasi, et al., 2011). *NOTCH1* mutations regularly affect the C-terminal PEST domain by 2-bp (CT) frameshift deletions in human CLL and RT causing a premature stop codon (approximately 80% of cases) (Willander et al., 2013; Rosati et al., 2018). The PEST deletion, an initiator for the proteasomal degradation of NICD, prolongs half-life of activated NICD (Blain et al., 2017). Despite the assumed malignant effect of overactivated NOTCH1 in CLL, pathogenic NOTCH1 actions still remain unknown. Neither *in vivo*- nor *in vitro*-studies have been published so far to unravel the function of NOTCH1 causing an aggressive course of CLL.

To prove the significance of overactivated Notch1 in CLL *in vivo*, a Eμ-*TCL1* mouse model with a constitutive activated Notch1, named Notch1-IC, was generated. The tissue-specific expression of the *Notch1-IC* construct containing a loxP-flanked neo-STOP cassette was enabled by previous insertion into the ubiquitously expressed ROSA-26 locus between the coding sequence and the GT(ROSA)26Sor promoter (referred as R26-fl-*Notch1-IC*). R26-fl-*Notch1-IC*^fl/wt mice express Cre-dependent *eGFP* as reporter and the intracellular, active domain of the murine Notch1 receptor (encoding amino acids 1749-2293) without the PEST domain (**Fig.3.15A**) (Murtaugh et al., 2003). R26-fl-*Notch1-IC*^fl/wt mice were intercrossed with *Cd19-Cre* mice to receive *Cd19-Cre*^tg/wt; R26-fl-*Notch1-IC*^fl/wt mice (termed *Cd19-Cre*^Notch1-IC) with a B cell-specific expression of *Notch1-IC*. *Cd19-Cre*^Notch1-IC mice were further bred to Eμ-*TCL1* mice to receive experi-

mental Eµ-*TCL1*^tg/wt; *Cd19-Cre*^tg/wt; R26-fl-*Notch1-IC*^fl/wt mice (termed Eµ-*TCL1*^Notch1-IC,

Fig.3.15B).
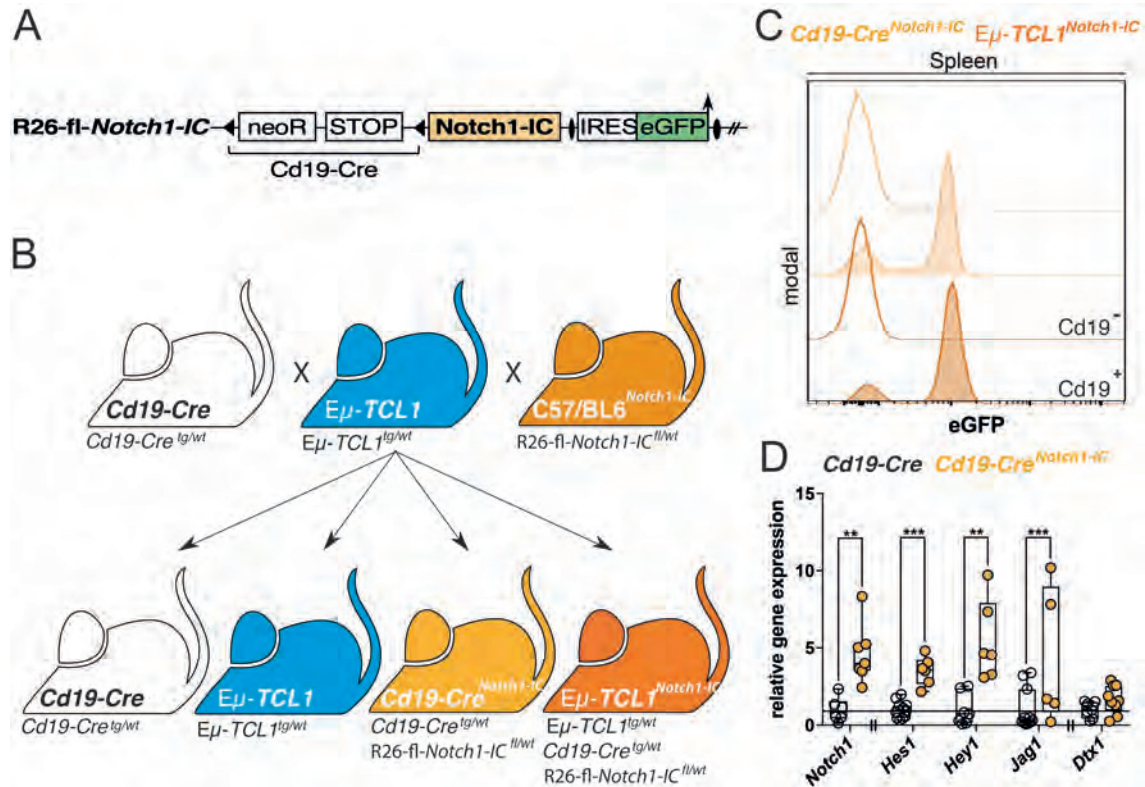
Fig. 3.15: Validation of the Notch1-IC construct expressed in B cells. A Scheme of the R26-fl-
Notch1-IC construct. **B** Scheme of the breeding strategy to receive experimental Eµ-*TCL1*^Notch1-IC
mice. **C** Representative blot of eGFP in Cd19⁻(uncolored) and Cd19⁺ (colored) splenocytes of
indicated mice at 3-5 months age *via* flow cytometry. **D** Relative gene expression of *Notch1* and
common canonical (*Hes1*, *Hey1, Jag1*) as well as non-canonical (*Dtx1*) Rbpj/Notch target genes
relative to *Tbp* in splenic B cells of indicated mice at 3-5 months age *via* qPCR. Data were previously
gated for living (Aqua staining), single cells (FSC-A vs. FSC-H, SSC-A vs. SSC-H) in **C**. Data were
normalized to *Cd19-Cre* mice in **D**. All data are presented as box with whiskers and median (**D**).
p ≤ 0.01, and ***p ≤ 0.001. Statistical analyses were performed using Student's t-test (D**). eGFP:
enhanced green fluorescent protein, IRES: internal ribosomal entry site, neoR: neomycin resistance,
Notch1-IC: constitutive active Notch1.

The B cell-restricted expression of *Notch1-IC* was verified by eGFP *via* flow cytometry

(**Fig.3.15C**). Both *Cd19-Cre*^Notch1-IC and Eµ-*TCL1*^Notch1-IC mice displayed eGFP expres-

sion specifically in Cd19⁺ B cells. Transcription of *Notch1* was further elevated in B cells

of *Cd19-Cre*^Notch1-IC mice. The augmented expression of common Rbpj/Notch target

genes validated increased canonical Notch1 activity and thus the functionality of the

mouse model (**Fig.3.15D**) (Borggrefe and Oswald, 2009; F. Arruga et al., 2014). *Dtx1*

as target for the non-canonical Notch pathway was slightly increased but not significant.
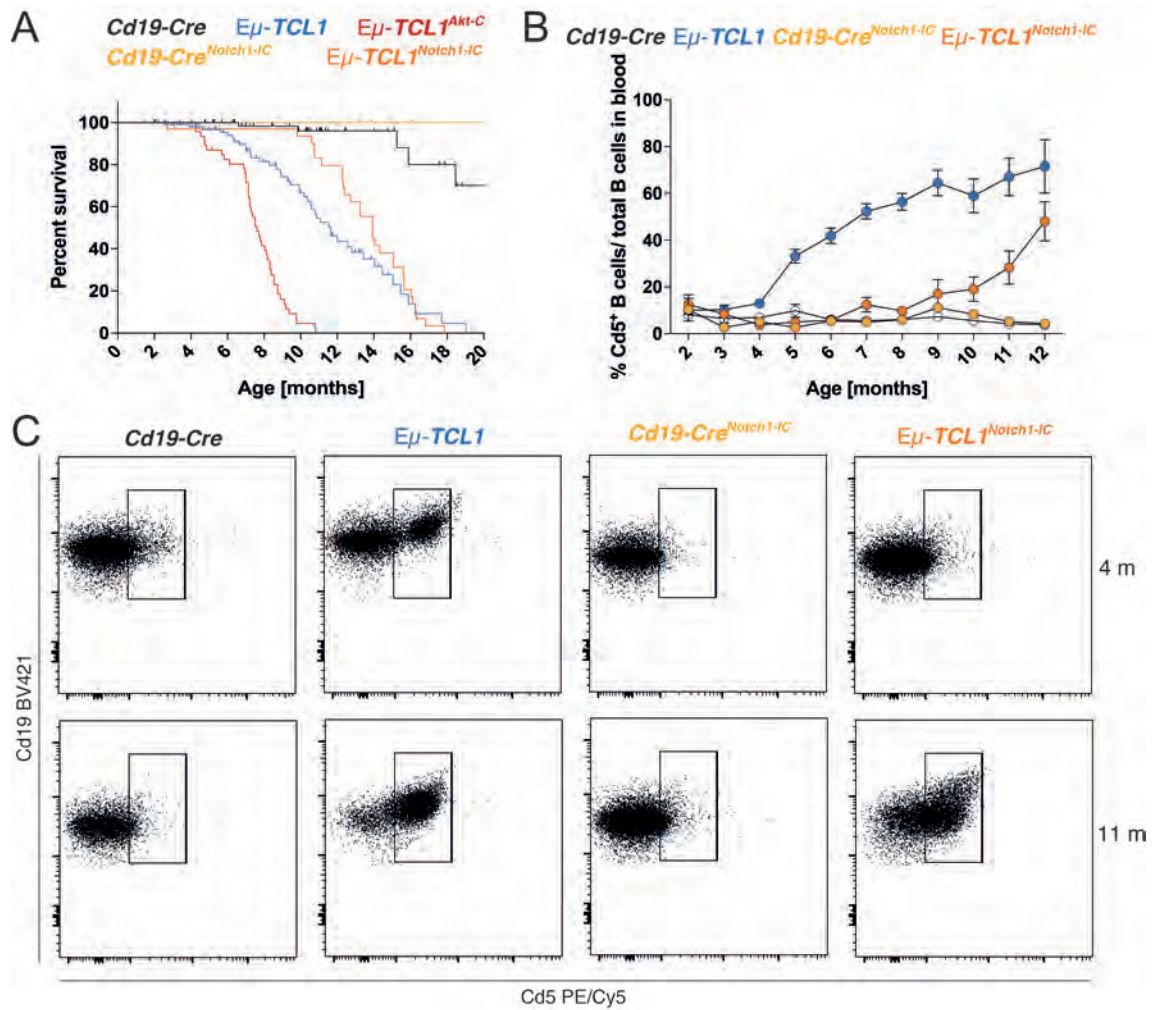
Fig. 3.16: B cell-specific *Notch1-IC* expression in Eμ-*TCL1* mice initiates CLL with a similar progression but a later outcome than in the Akt-induced RT mouse model. A Kaplan-Meyer survival curve of indicated mice. **B** Relative quantification (%) of Cd5$^+$ B cells in peripheral blood taken monthly from indicated mice (n=8-10 mice per genotype) *via* flow cytometry. **C** Representative blots of extracellular Cd5 PE/Cy5 and Cd19 BV421 in blood-derived samples of indicated mice at 4 and 11 months age *via* flow cytometry. The gating to define Cd5$^+$ B cells is shown and used for the quantification in **B**. Data were previously gated for living (Aqua staining), single cells (FSC-A vs. FSC-H, SSC-A vs. SSC-H) in **C**. Data are presented as box with means ± SEM (**B**). BV421: Brilliant Violet 421, FSC: forward scatter, PE/Cy5: tandem fluorochrome composed of phycoerythrin (PE) and cyanine 5 (Cy5).

The course of CLL was monitored by monthly screening of Cd5$^+$ B cells in peripheral blood. An increasing population of Cd5$^+$ B cells emerged in Eμ-*TCL1$^{Notch1-IC}$* mice with a similar progression but later outcome than in Eμ-*TCL1^{Akt-C}* mice. Cd5$^+$ leukemic B cells appeared in Eμ-*TCL1$^{Notch1-IC}$* mice from the age of 10 months (**Fig.3.16B,C**). The

survival capacity decreased markedly and similarly in both Eµ-*TCL1*[Notch1-IC] and Eµ-*TCL1*[Akt-C] mice but at different ages (median survival: 13.3 months for Eµ-*TCL1*[Notch1-IC] mice, **Fig.3.16A**). In opposition, reduced survival and leukemic cells lacked in *Cd19-Cre*[Notch1-IC] mice. Furthermore, a distinctive Cd5$^+$ B cell population was not detected in peripheral blood of *Cd19-Cre*[Notch1-IC] mice, similar to *Cd19-Cre* mice (**Fig.3.16C**).
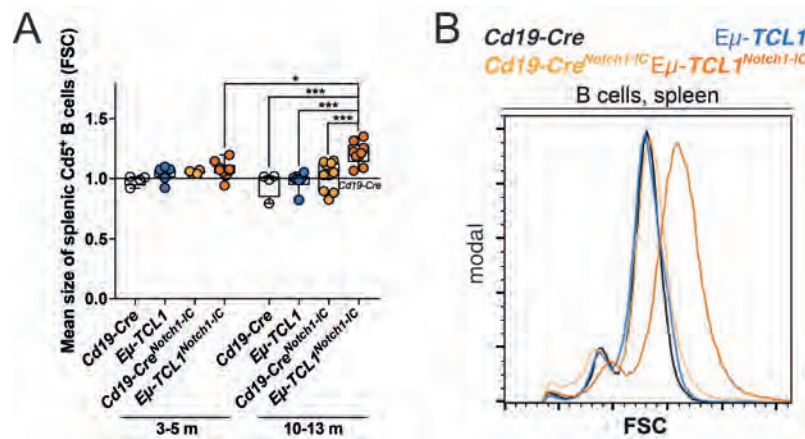
Fig. 3.17: B cell-specific *Notch1-IC* expression in Eµ-*TCL1* mice promotes enlarged cancer cells. A Relative cell size (FSC) of splenic Cd5$^+$ B cells of indicated mice at 3-5 and 10-13 months age. **B** Representative blots of FSC of splenic B cells of indicated mice at 10-13 months age. Data were previously gated for living (Aqua staining), single cells (FSC-A vs. FSC-H, SSC-A vs. SSC-H) in **B**. Data were normalized to *Cd19-Cre* mice in **A**. Data of mice at 3-5 months age represent the analysis before, at 10-13 months age the analysis after the transformation to RT in Eµ-*TCL1*[Notch1-IC] mice. Data are presented as box with whiskers and median (**A**). *p ≤ 0.05, and ***p ≤ 0.001. Statistical analyses were performed using Two-Way ANOVA plus Fisher's LSD test (**A**). FSC: forward scatter.

CLL and RT cells were distinguished by relative cell sizes (FSC) *via* flow cytometry. Splenic Cd5$^+$ B cells indicated enlarged cell sizes in Eµ-*TCL1*[Notch1-IC] mice at 10-13 months age, suggesting RT with a disease penetrance of 100%. In contrast, Eµ-*TCL1*[Notch1-IC] mice before transformation (3-5 months age) and *Cd19-Cre*[Notch1-IC] mice displayed normal cell sizes of Cd5$^+$-defined B cells (**Fig.3.17A,B**).
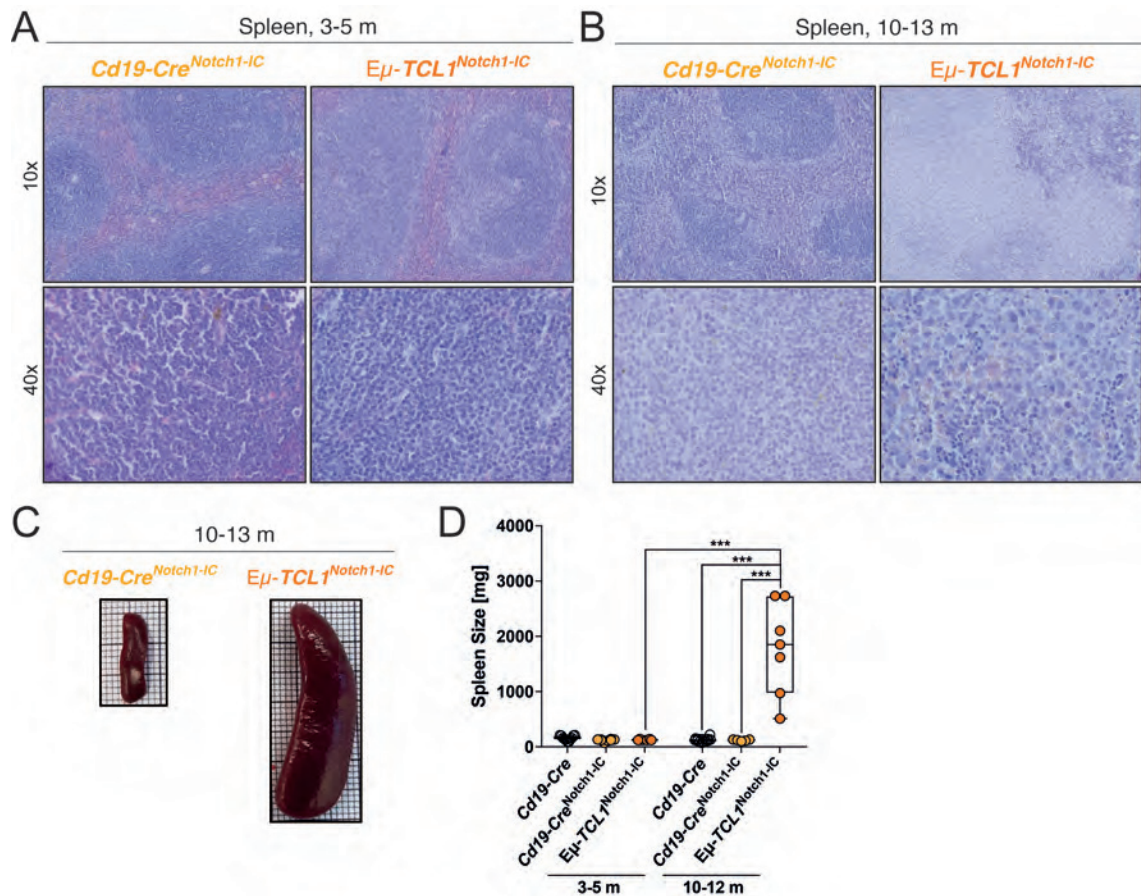
Fig. 3.18: B cell-specific *Notch1-IC* expression in Eµ-*TCL1* mice initiates RT. A,B Histological representatives (magnification: 10- and 40-times) of indicated mice at 3-5 and 10-13 months age using H&E staining. **C** Representative spleens and **D** its spleen sizes [mg] of indicated mice at 3-5 and 10-13 months age. Data of mice at 3-5 months age represent the analysis before, at 10-13 months age the analysis after the transformation to RT in Eµ-*TCL1*^Notch1-IC^ mice. Data are presented as box with whiskers and median (**D**). ***p ≤ 0.001. Statistical analyses were performed using Two-Way ANOVA plus Fisher's LSD test (**D**).

Moreover, H&E staining revealed DLBCL-like histomorphology with distorted splenic histoarchitecture in Eµ-*TCL1*^Notch1-IC^ mice at 10-13 months age. Splenocytes characterized enlarged, pleomorphic cells with abundant cytoplasm and multiple nucleoli, corresponding to human RT morphology (**Fig.3.18B**). *Cd19-Cre*^Notch1-IC^ and untransformed Eµ-*TCL1*^Notch1-IC^ mice exhibited inconspicuous splenic histomorphology in absence of enlarged splenocytes (**Fig.3.18A**). Considerably, Eµ-*TCL1*^Notch1-IC^ mice developed splenomegaly at 10-13 months age with spleen weights up to 2810 mg (23-times increase), indicating lymphomagenesis (**Fig.3.18C,D**). In contrast, *Cd19-Cre*^Notch1-IC^ and

untransformed Eµ-*TCL1*$^{Notch1-IC}$ mice featured ordinary spleen sizes.
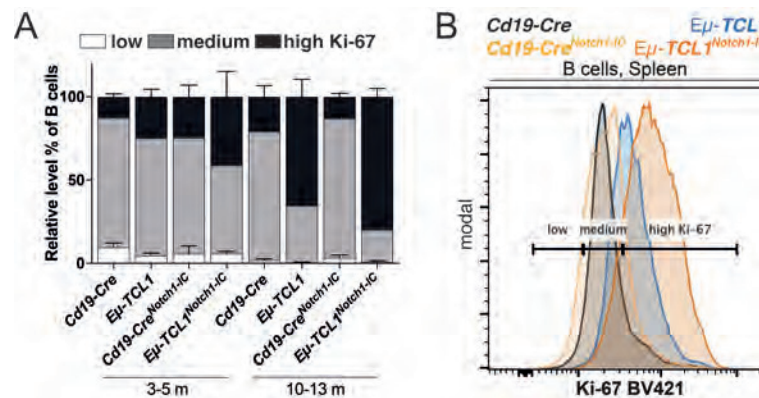
Fig. 3.19: Notch1-activated Eµ-*TCL1* mice display high proliferative capacity. A Relative level (%) of splenic B cells with low (white), medium (gray) or high (black) levels of nuclear Ki-67 BV421 of indicated mice at 3-5 and 10-13 months age (n=8-10 mice per genotype) *via* flow cytometry. **B** Representative blot of nuclear Ki-67 BV421 in total, splenic B cells of indicated mice at 10-13 months age *via* flow cytometry. Gating for "medium Ki-67" was defined based on the signal (50% of the maximal amplitude) of nuclear Ki-67 BV421 in *Cd19-Cre* mice. Augmented levels were defined as "high Ki-67", lower levels until the unstained peak (50% of the maximal amplitude) were defined as "low Ki-67". Data were previously gated for living (Aqua staining), single cells (FSC-A vs. FSC-H, SSC-A vs. SSC-H) in **B**. Data of mice at 3-5 months age represent the analysis before, at 10-13 months age the analysis after the transformation to RT in Eµ-*TCL1*$^{Notch1-IC}$ mice. Data are presented as box with means ± SEM (**A**). BV421: Brilliant Violet 421.

The proliferation rate associated with disease progression was determined using intracellular Ki-67 staining *via* flow cytometry. Proliferation was greatly augmented in splenic B cells of Eµ-*TCL1*$^{Notch1-IC}$ mice at any age. However, splenic RT cells revealed immoderate levels of nuclear Ki-67 in transformed Eµ-*TCL1*$^{Notch1-IC}$ mice, indicating high proliferative activity. On average, 79.8% of RT cells showed elevated Ki-67 levels in Eµ-*TCL1*$^{Notch1-IC}$ mice. In opposition, the proliferative activity of splenic B cells of *Cd19-Cre*$^{Notch1-IC}$ mice resembled the proliferation rate of *Cd19-Cre* mice (**Fig.3.19A,B**). Taken together, DLBCL-like RT occurred in Notch1-activated Eµ-*TCL1* mice with a disease penetrance of 100%, proving the oncogenic function of Notch1 *in vivo*.

3.3.2   B Cell-Specific *Notch1-IC* Expression in Eµ-*TCL1* Mice Drives RT In-

dependent of the Splenic TME

Due to the modified splenic TME in the Akt-mediated RT mouse model (see chapter 3.2.6), splenic TME and cancer cells of Eµ-*TCL1^{Notch1-IC}* mice were investigated for Notch1 ligands like Dll1 *via* flow cytometry. Splenic TME cells presented inconspicuous Dll1 levels on their cell surface (**Fig.3.20A**). Cd4$^+$ T cells in particular, including Foxp3$^+$ T$_{reg}$ cells, lacked plenty Dll1 (**Fig.3.20B**). In opposition to Akt-initiated RT, splenic T cells further exhibited ordinary proliferation rates alike *Cd19-Cre* mice (**Fig.3.20E**). Consequently, T cell frequencies, including T$_{reg}$ cells, were unaltered in RT-transformed Eµ-*TCL1^{Notch1-IC}* mice (**Fig.3.20D**). Summarized, the splenic TME of the RT-transformed Eµ-*TCL1^{Notch1-IC}* mouse model resembled the microenvironment of *Cd19-Cre* and *Cd19-Cre^{Notch1-IC}* mice. These data verify that the accumulation of Dll1 on the cell surface and the selective expansion of ligand-presenting TME cells are not regulated by Rbpj/Notch1 target genes but probably by direct interactions between the extracellular domains of Notch receptor and ligand. Furthermore, RT cells presented low levels of Notch1 ligands, such as Dll1 and Jag1 (**Fig.3.20A,F**).

Despite the low protein levels of Dll1 on TME cells, the transcription of *Dll1*, *Dll4*, and *Jag1* was upregulated in T cells of both Notch1-IC mouse models similar to Eµ-*TCL1^{Akt-C}* mice at which the upregulation was stronger in RT-transformed Eµ-*TCL1^{Notch1-IC}* mice compared to *Cd19-Cre^{Notch1-IC}* mice (**Fig.3.20G**). This result indicates that the T cell-restricted *Dll1* and *Dll4* expression are stimulated by Rbpj/Notch1 target genes of surrounding Notch1-activated B cells that are perhaps involved in cytokine production.
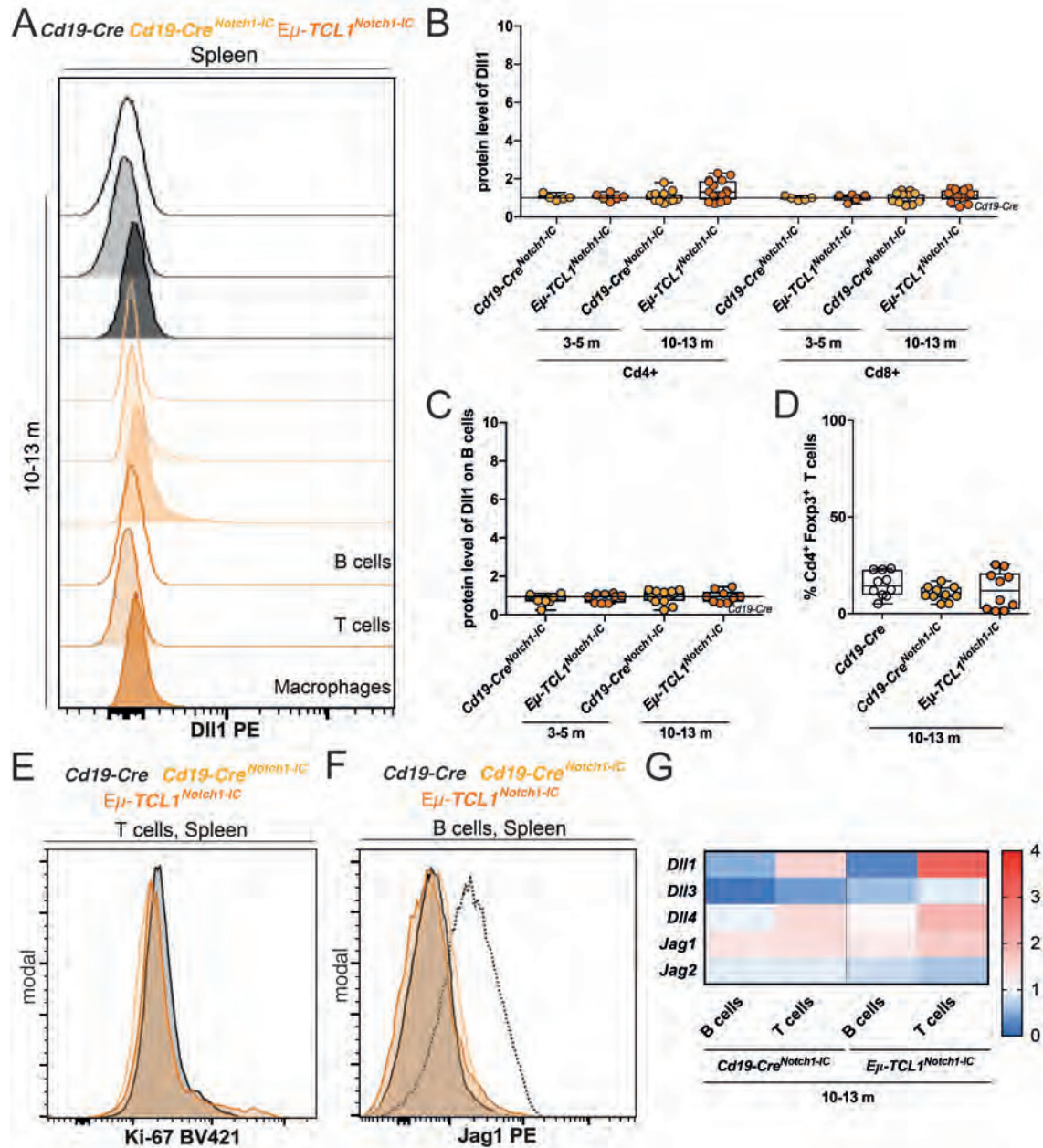
Fig. 3.20: Notch1-activated Eµ-*TCL1* mice develop RT independent of the splenic TME. **A** Representative blot of extracellular Dll1 PE on splenic B cells (uncolored), T cells (slightly colored), and macrophages (colored) of indicated mice at 10-13 months age *via* flow cytometry. **B** Relative quantification of extracellular Dll1 PE on splenic T cell subsets and **C** B cells of indicated mice at 3-5 and 10-13 months age *via* flow cytometry. **D** Relative numbers (%) of splenic Cd4$^+$ Foxp3$^+$ regulatory T cells in relation to total T cells of indicated mice at 10-13 months age *via* flow cytometry. **E** Representative blot of nuclear Ki-67 BV421 in splenic T cells of indicated mice at 10-13 months age *via* flow cytometry. **F** Representative blot of extracellular Jag1 PE on splenic B cells of indicated mice at 10-13 months age *via* flow cytometry. **G** Relative gene expression of Notch ligands relative to *Tbp* in splenic B cells and T cells of indicated mice at 10-13 months age *via* qPCR. BV421: Brilliant Violet 421, PE: phycoerythrin. Data of mice at 3-5 months age represent the analysis before, at 10-13 months age the analysis after the transformation to RT in Eµ-*TCL1*$^{Notch1-IC}$ mice. Data were previously gated for living (Aqua staining), single cells (FSC-A vs. FSC-H, SSC-A vs. SSC-H) in **A**, **E**, and **F**. Data were normalized to *Cd19-Cre* mice in **B**, **C**, and **G**. All data are presented as box with whiskers and median (**B-D**). Statistical analyses were performed using One-Way (**C**,**D**) or Two-Way (**B**) ANOVA plus Fisher's LSD test.

Collectively, these experiments demonstrate that the expression of the active domain of Notch1 in Eμ-*TCL1* CLL mice suffices to initiate RT, independent of the splenic TME. These findings strongly suggest the pivotal function of the co-overactivation of Akt and Notch1 during RT manifestation.

3.3.3 B Cell-Specific *Notch1-IC* Expression in Eμ-*TCL1* Mice Causes Over-activated Akt

The proteom of Akt-induced RT was characterized by the overexpression of the S100a4 oncogene and repression of the Pdcd10 tumor suppressor, both transcriptionally regulated by Rbpj/Notch1. In line with this, transformed Eμ-*TCL1*$^{Notch1-IC}$ mice showed Notch1-induced upregulation of *s100a4* and downregulation of *Pdcd10* transcription (**Fig.3.21A**). Consequently, Notch1 may exert its tumorigenic activity by regulating prominent canonical targets like *Hes1* but also *Pdcd10* and *s100a4* as effector genes. However, it might be that *vice versa* Notch1 increases Akt activity. To this end, *Akt1* gene revealed transcription factor binding sites for Rbpj/Notch in their 2 kb upstream promoter region using Genomatix software (**Fig.3.10B**). The transcription of *Akt1* was upregulated in both Notch1-IC mouse models and the protein levels of total Akt was enhanced in RT cells of Eμ-*TCL1*$^{Notch1-IC}$ mice compared to CLL cells of Eμ-*TCL1* mice (**Fig.3.21B,C**). In accordance with overactivated AKT in *NOTCH1* mutated RT patients (**Fig.3.1A,B**), Notch1-activated RT cells revealed Akt stimulation by Ser473 phosphorylation using Western blot (**Fig.3.21D,E**). As published for T cell acute lymphoblastic leukemia (T-ALL), Notch1 can promote Akt activity by silencing *Pten* expression *via Hes1* (Palomero, Dominguez, and Ferrando, 2008). Pten indirectly inhibits Akt actions as a PIP$_3$ phosphatase (Cantley and Neel, 1999; Georgescu, 2010; Carracedo and Pandolfi, 2008). Accordingly, *Pten* expression is repressed in both Notch1-activated

mouse models (**Fig.3.21B**).
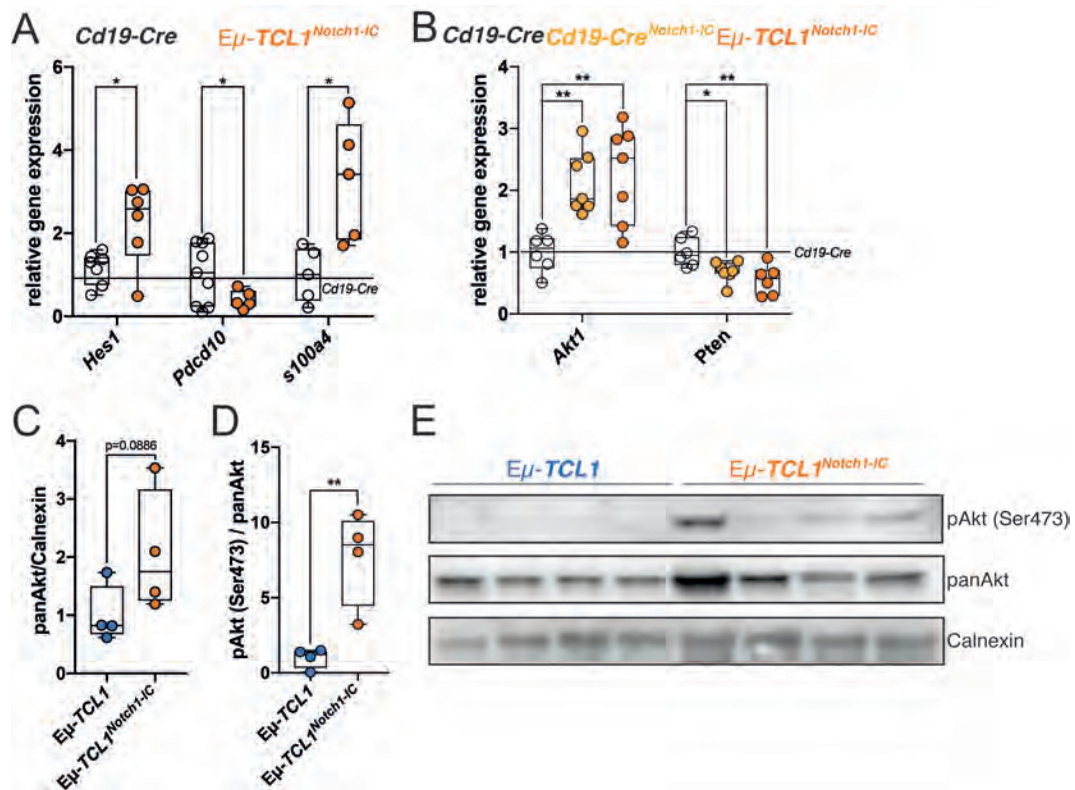
Fig. 3.21: Enhanced expression and activation of Akt in Notch1-induced RT cells. A Relative gene expression of *Hes1*, *Pdcd10*, and *s100a4* relative to *Tbp* in splenic B cells of indicated mice at 10-13 months age *via* qPCR. **B** Relative gene expression of *Akt1* and *Pten* relative to *Tbp* in splenic B cells of indicated mice at 10-13 months age *via* qPCR. **C** Relative protein quantification of panAkt normalized to Calnexin, **D** pAkt(Ser473) normalized to panAkt, and **E** its representative blot of pAkt (Ser 473) and panAkt of splenic B cells of indicated mice at 10-13 months age *via* Western blot. Calnexin was used as loading control. Data were normalized to Cd19-Cre mice in **A-B** or to Eµ-*TCL1* mice in **C**. Data of mice at 10-13 months age represent the analysis after the transformation to RT in Eµ-*TCL1*$^{Notch1-IC}$ mice. Data are presented as box with whiskers and median (**A-C**). *p ≤ 0.05 and **p ≤ 0.01. Statistical analyses were performed using Student's t test (**A,C**) or One-Way (**B**) ANOVA plus Fisher's LSD test.

These data suggest that Notch1 acts both up- and downstream of the Akt signaling to enable CLL progression to RT. These findings confirm a bidirectional co-overexpression and -activation of the Akt and Notch1 signaling during tumorigenesis in the Akt- and Notch1-mediated RT mouse models.

4 Discussion

CLL is the most frequent leukemia subtype in adults of developed countries accounting for approximately 30% of leukemia variants and defines a NHL of mature, long-lived B cells with a leukemic course (Simon, 2020). CLL describes a heterogeneous malignancy with a variable clinical outcome ranging from an indolent disease with a nearly normal life expectancy to an aggressive form depending on somatic aberrations. The majority of CLL patients evolves an indolent form that can last for decades initially without the need of any treatments (Rodríguez-Vicente, Díaz, and Hernández-Rivas, 2013). Nevertheless, up to 10% of CLL cases manifest a sudden aggressive course like RT with a markedly reduced survival of approximately 12 months (Y. Wang et al., 2020). Contrarily to CLL, RT commonly defines an aggressive NHL with histomorphological characteristics of a DLBCL (Richter, 1928; Parikh et al., 2013). Approximately 80% of DLBCL variants of RT cases are clonally related to the prior CLL disease and feature properties of both CLL and DLBCL (Mao et al., 2007).

In general, AKT kinase, as central node, is required for the activation, proliferation, and survival of mature B cells. Particularly in CLL, the involvement of PI3K/AKT is suggested as principal mediator of pro-survival signaling although gain-of-function mutations of members of the PI3K/AKT pathway are regularly not found (Schrader et al., 2014). However, several studies showed that extensive apoptosis of CLL cells occurred through specific inhibition of PI3K/AKT (Zhuang et al., 2010; Hofbauer et al.,

2011). Mainly, AKT can be activated by the BCR signaling which has been identified as the most prominent pathogenic pathway in CLL (Herishanu, Pérez-Galán, et al., 2011). Furthermore, BCR stimulation is known to highly correlate with worse prognosis of CLL (Rodríguez et al., 2007; Stevenson et al., 2011). In accordance, Wendel *et al* demonstrated in a lymphoma mouse model that Akt promotes tumorigenesis showing an aggressive course (Wendel et al., 2004). The dichotomy of the CLL course is still insufficiently understood, especially the impact of AKT actions. Due to the hypothesized correlation between PI3K/AKT signaling and worse prognosis of CLL, the questions arise how AKT downstream actions are involved in CLL pathogenesis and whether AKT activity correlates with an aggressive course, such as RT.

4.1 Active Akt Induces the Progression from CLL to RT by Over-activation of the Canonical Notch1 Signaling

4.1.1 Active Akt Drives the Transformation from CLL to RT

AKT kinase triggers B cell proliferation and activation through a multitude of downstream pathways including GSK3b (Alessi, James, et al., 1997), FOXO1 (Biggs et al., 1999; Brunet et al., 1999), and MDM2 (L. D. Mayo and Donner, 2001; Ogawara et al., 2002). In this thesis, the immunohistochemical study of human cancer biopsies confirms a correlation between activated AKT and RT development, especially for *TP53* and *NOTCH1* mutated cases. Contrarily, CLL and DLBCL biopsies lack active AKT in the majority of cases.

To solely focus on Akt actions in CLL pathogenesis *in vivo*, a B cell-specific, Akt-activated CLL mouse model was characterized. For this, the commonly studied Eµ-*TCL1* transgenic CLL mouse model was utilized possessing exogenous overexpression of the human *TCL1* gene specifically in B cells (Bichi et al., 2002). Under physiological condi-

tions, TCL1 is involved in the development of early B and T cells by mediating survival and growth signals (Teitell, 2005). Aberrant *TCL1* expression is known in about 90% of CLL patients and functions *inter alia* as coactivator of AKT, ATM, and heat shock protein 70 (HSP70) (Paduano et al., 2018). The mechanisms underlying overexpressed *TCL1* in B cell malignancies remain unsolved, probably a combination of transcriptional and epigenetic alterations initiated by TME-specific stimuli (Yuille et al., 2001; French et al., 2003; Sivina et al., 2012).

Active Akt initiates the spontaneous development of RT in Eμ-*TCL1* mice with a disease penetrance of 100%. The disease progression of the RT mouse model highly resembles the human RT outcome with an initial indolent course followed by sudden malignant transformation. In accordance with human RT, murine RT confirms an DLBCL-like histomorphology with enlarged, pleomorphic cells in absence of normal substructures and a distinctive lymphomatous phenotype including splenomegaly. Moreover, RT cells feature immoderate proliferative capacities and CLL/RT-typical immunophenotypic markers like CD5. The malignant effect of Akt is only observed in combination with overexpressed *TCL1*. Akt actions in absence of any oncogenic driver reveal an intrinsic phenotype but never drive leukemia/lymphomagenesis (Cox et al, submitted).

In line with the definition of RT, the genomic signature of the Akt-activated RT mouse model involves characteristic mutations of both CLL and DLBCL (Kohlhaas et al., 2020). The absence of recurrent mutations despite the identification of single RT-associated somatic alterations for individual mice, such as members of the BCR signaling or *Notch1*, confirms that murine RT exclusively occurs based on Akt actions as kinase. This finding indicates that Akt cooperates in the induction of aggressive CLL. Thereby, murine *in vivo*-studies of this thesis reveal the requirement of Akt actions on the transformation from CLL to RT.

4.1.2   Akt Promotes the Activation of the Notch1 Proto-oncogene in RT

Active AKT in *NOTCH1* mutated human cases with progressive CLL or RT suggests a correlation between AKT and NOTCH1 signaling in the aggressive course. In human biopsies, gain-of-function mutations in the *NOTCH1* gene occur in approximately 10% of CLL cases at diagnosis and 30% of RT cases (Fabbri, Rasi, et al., 2011; Puente et al., 2011). Hence, *NOTCH1* mutations represent the most RT-promoting aberration. *NOTCH1* somatic aberrations markedly reduce the overall survival of patients supposing a dismal prognosis and an unfavorable clinical outcome, similar to patients with *TP53* abnormalities (Rossi, Rasi, et al., 2012). Under physiological conditions, the evolutionary conserved NOTCH1 signaling promotes proliferation, maturation, and survival of B cells. NOTCH1 stimulation empowers the release of NICD as active moiety that translocates into the nucleus to regulate the transcription of target genes together with the transcription factor RBPJ (Andersson, Sandberg, and Lendahl, 2011). (Phospho)proteomic profiling of murine RT cells compared to CLL cells confirms changes for proteins associated with the Notch1 signaling. Thereby, more than half of significantly changed proteins exhibit transcription factor binding sites for Rbpj/Notch in promoter region of corresponding genes. For instance, S100a4 has been identified as the most upregulated protein in RT cells that was verified to be transcriptionally regulated by Rbpj/Notch1. Members of the Ca^{2+}-dependent S100 family highly correlate with metastasis, cell survival, and proliferation, implicating an aggressive course of cancer (Bresnick, Weber, and Zimmer, 2015; Brenner and Bruserud, 2018). In addition, Pdcd10 tumor suppressor is downregulated in the RT mouse model both at the transcriptional and protein level. Consistently, *Pdcd10* is accepted as a cancer-related target gene of Rbpj/Notch1 that represses the activation of Akt (Lambertz et al., 2015; Wan et al., 2020). Furthermore, Mecp2, a repressor of *Notch1* transcription and Akt

signaling, is decreased in murine RT cells (Li et al., 2014). In line with this, scRNA-seq data of the Akt-mediated RT mouse model in comparison to CLL mice reveal that the majority of differentially expressed genes in RT is regulated by Rbpj/Notch (Kohlhaas et al., 2020).

In further molecular investigations, augmented expression of prominent Rbpj/Notch target genes like *Hes1* approves Akt-initiated upregulation of the canonical Notch signaling. Notch1 is identified as the receptor involved in RT progression by enhanced expression and elevated protein levels of its intracellular, active moiety. In contrast, *TCL1*-driven CLL shows no alterations in Notch signaling. This study suggests that the co-overactivation of Akt and Notch1 signaling enables the malignant transformation to RT. In accordance, Akt/Notch interactions are assumed under physiological conditions in B cells. For instance, Akt/Notch2 cooperation empowers B cell differentiation toward MZ B cells in absence of any oncogenic driver including TCL1 (Cox et al, submitted). While concurrent activation of PI3K/Akt and Notch1 triggers tumorigenesis in melanoma (Bedogni et al., 2008) and ALL (Gutierrez and Look, 2007; Hales, Taub, and Matherly, 2014), a possible crosslink between Akt and Notch1 for CLL pathogenesis has not been reported so far. This study demonstrates for the first time that the overactivation of Akt increases the aggressiveness of CLL by activating the Notch1 pathway as a pivotal effector.

4.1.3 Regulatory T Cells Promote RT by Presenting Notch1 Ligands on the Cell Surface

Notch signaling needs external stimuli from the microenvironment *via* presentation of appropriate ligands, membrane-bound members of the Delta/Jagged family (LaFoya et al., 2016). Consequently, the Notch1 receptor needs the ligand-based activation to

evolute its proto-oncogenic effect. In CLL, dysregulated Notch activation is tissue- and microenvironment-dependent. Due to the highest upregulation of intracellular Notch1 in the spleen during RT, the splenic TME represents a potential source for Notch1 ligands like Dll1. This corresponds to the finding of Arruga *et al* which revealed highest expression and activation of NOTCH1 in human SLO-derived CLL cells (F. Arruga et al., 2014). Over the last decade, the central role of the TME in the pathogenesis of CLL and other B cell malignancies has been discovered but is still poorly understood.

This thesis shows abundant Dll1 ligand on splenic Cd4$^+$ T cells, especially on T$_{reg}$ cells, in Akt-mediated RT but not in CLL. In accordance, human BCR-activated CLL cells are known to instruct the migration of T cells toward SLOs *via* chemokines and to modify the TME to enable intercellular interactions (Attekum, Eldering, and Kater, 2017). This thesis further suggests that Notch1 activation in splenic RT cells promotes the expansion of ligand-presenting T$_{reg}$ cells. In concordance with the murine data of this thesis, CD4$^+$ T cells exhibit aberrant proliferation during human CLL (Palma et al., 2017). Furthermore, augmented frequencies of blood-derived T$_{reg}$ cells are reported in CLL patients with high accumulation in SLOs correlating with progressive outcome and unfavorable genetics (Weiss et al., 2011; Biancotto et al., 2012). In addition to Notch receptors, Notch ligands undergo proteolytic cleavage by Adam proteins and γ-secretase after binding to receptor to release an intracellular ligand domain (D'Souza, A. Miyamoto, and G. Weinmaster, 2008). Although the function of the proteolysis is not yet understood, an intrinsic activity is hypothesized which might support Notch activation and cell survival as a positive feedback mechanism (Zolkiewska, 2008). Nevertheless, the multiple modifications of SLO-located T cells enable Notch1 overactivation to drive murine RT.

In CLL patients, T cells are deregulated whereas the effect of various T cell subsets as pro- or anti-tumorigenic TME cells is still under discussion. Under physiological condi-

tions, T_{reg} cells reduce the activity of effector T cells as immunosuppressor to maintain peripheral tolerance and to limit autoimmune and chronic inflammatory diseases. The pathogenic effect of T_{reg} cells during CLL is still uncertain. Here, a pro-tumoral impact of T_{reg} cells is suggested.

Although RT describes an aggressive form of CLL, Akt-mediated RT cells highly depend on the TME. Despite the transcriptional regulation of Notch ligands like *Jag1* by Rbpj/Notch1, enhanced ligand proteins are absent on murine RT cells alluding to the inability of their mutual activation. These results are in line with previous studies that validate the absence of all NOTCH1 ligands (DLL1, DLL4, and JAG1) on human CLL cells in both *NOTCH1* mutated and wildtype cases (F. Arruga et al., 2014). JAG1 expression and protein processing correlate with survival of CLL cells but not with NOTCH activation (De Falco et al., 2018). Furthermore, NOTCH1 is known to be rapidly repressed in absence of TME-specific stimuli even in *NOTCH1*-mutated CLL cells (F. Arruga et al., 2014). This exhibits the requirement of consistent TME interactions for NOTCH1 signaling.

These findings verify the dependency of Akt-initiated RT cells from the splenic TME by the presentation of Notch1 ligands and the cellular expansion of ligand presenting T_{reg} cells. On the other hand, murine RT cells are shown here to adapt the surrounding TME toward a pro-tumoral behavior to ensure cancer progression.

4.2   The Active, Intracellular Domain of Notch1 Initiates RT Independent of the Splenic TME

4.2.1   Active Notch1 Drives the Transformation from CLL to RT

The most frequent *NOTCH1* mutations in CLL and RT patients affect the C-terminal PEST domain (approximately 80% of cases) (Rosati et al., 2018). Mutations consist of 2-bp (CT) frameshift deletions that cause a premature stop codon and the truncation of the PEST domain (Willander et al., 2013). The PEST domain promotes the proteasomal degradation of cleaved NICD. Consequently, PEST deletion prolongs the half-life of activated NICD (Blain et al., 2017). Although *NOTCH1* mutations predict the stabilization of its active form and dysregulated signaling, investigations of the functional effect of mutated NOTCH1 are still missing but vitally needed for the understanding of its pathogenic function in CLL.

To prove the transformative potential of activated Notch1 *in vivo,* a Eµ-*TCL1* transgenic CLL mouse model with a B cell-specific active Notch1 was characterized. For this purpose, only the intracellular, active domain of Notch1 without the PEST domain is expressed in the Eµ-*TCL1* CLL mouse model. Notch1 activation spontaneously drives RT in Eµ-*TCL1* mice with large tumor burden and disease penetrance of 100%. In accordance with the definition of human RT, Notch1-mediated RT affirms DLBCL-like histomorphology, CLL/RT-specific immunophenotypic characteristics, and splenomegaly. Notch1-caused RT further indicates an aggressive course by immoderate proliferation. Beside the various ages of incidence, the observed phenotype is nearly identical to the characterized Akt-initiated RT mouse model. The oncogenic function of Notch1 is only present in combination with overexpressed *TCL1*. In absence of any malignant driver, the activated Notch1 mouse model reveals an intrinsic phenotype but never develops

any B cell malignancies. Consolidated, this study confirms that the Notch1-activated RT mouse model imitates the biology of human RT. Overactivation of Notch1 promotes the progression of CLL toward RT.

4.2.2 Notch1 Acts as a Pivotal Upstream Oncogene of Akt during RT

This study suggests that Notch1 exerts its tumorigenic activity by acting downstream of the PI3K/Akt signaling. *Vice versa*, this thesis provides evidence that Notch1 also acts upstream of the PI3K/Akt pathway. *Akt1* is here verified as a direct target gene of Rbpj/Notch1 during RT. As published for T-ALL, Notch1 can indirectly promote Akt activity by silencing the *Pten* tumor suppressor gene *via Hes1* (Palomero, Dominguez, and Ferrando, 2008). Pten constitutes a major brake of the PI3K/Akt pathway by exerting enzymatic activity as a PIP_3 phosphatase (Cantley and Neel, 1999; Georgescu, 2010). In line with this, Notch1 drives Akt activation by reduced *Pten* expression in murine RT. This result corresponds to the data of patients with RT or aggressive CLL of this study that show anomalous AKT activation in *NOTCH1* mutated cases. In addition, studies about melanoma and metastatic colon cancer have reported that overexpressed *NOTCH1* increases the aggressiveness of cancer by activating the PI3K/AKT pathway which is reversed by NOTCH1 inhibition with γ-secretase inhibitors (GSIs) (Balint et al., 2005; Liu et al., 2006; Pal et al., 2018).

Consolidated, Akt and Notch1 activate each other in murine RT. This thesis demonstrates for the first time that bidirectional Notch1-PI3K/Akt interactions induce the transformation of CLL toward RT as key signaling.

4.2.3 Active Notch1 Drives RT Independent of the Splenic TME

Akt-induced RT empowers Notch1 actions by multiple modifications of the splenic TME, mainly *via* increased occurrence of Dll1-presenting T_{reg} cells. In contrast, the Notch1-mediated RT mouse model affirms the TME-independent development of RT with unchanged TME cell populations and absent Notch1 ligands on their cell surface. Presumably, the presentation of Notch ligands on the cell surface requires the extracellular domain of Notch receptors that is lacking in the Notch1-IC-induced RT mouse model. Nevertheless, Notch1-activated RT cells empower ligand expression in surrounding T cells maybe by pro-tumorigenic cytokine production, regulated by Rbpj/Notch1 target genes (Colombo et al., 2018).

This study demonstrates that the expression of the intracellular, active domain of Notch1 induces RT, uncoupled from the SLO-derived TME. This strongly evidences the importance of the oncogenic Notch1 signaling in RT and proves the driving force of Notch1 in aggressive CLL pathogenesis.

4.3 Conclusions

This thesis shows the transformative central function of bidirectional Akt/Notch1 signaling in the development of RT in both human sections and murine *in vivo*-studies. Notch1 activation is mediated by splenic, ligand-presenting T_{reg} cells (**Fig.4.1**). The upregulation of Notch1 ligands in T_{reg} cells requires both the expression of Rbpj/Notch1 target genes and the extracellular domain of the Notch1 receptor in RT cells. Thereby, this study indicates that the expression of Notch1 ligands in T cells is induced by Rbpj/Notch1 target genes of RT cells whereas the enhanced presentation of ligands as well as the expansion of TME subsets might require the possible binding to the extracellular moiety of the Notch receptor. This illustrates the potential 'manipulative'

effect of RT cells on the TME to promote disease progression.
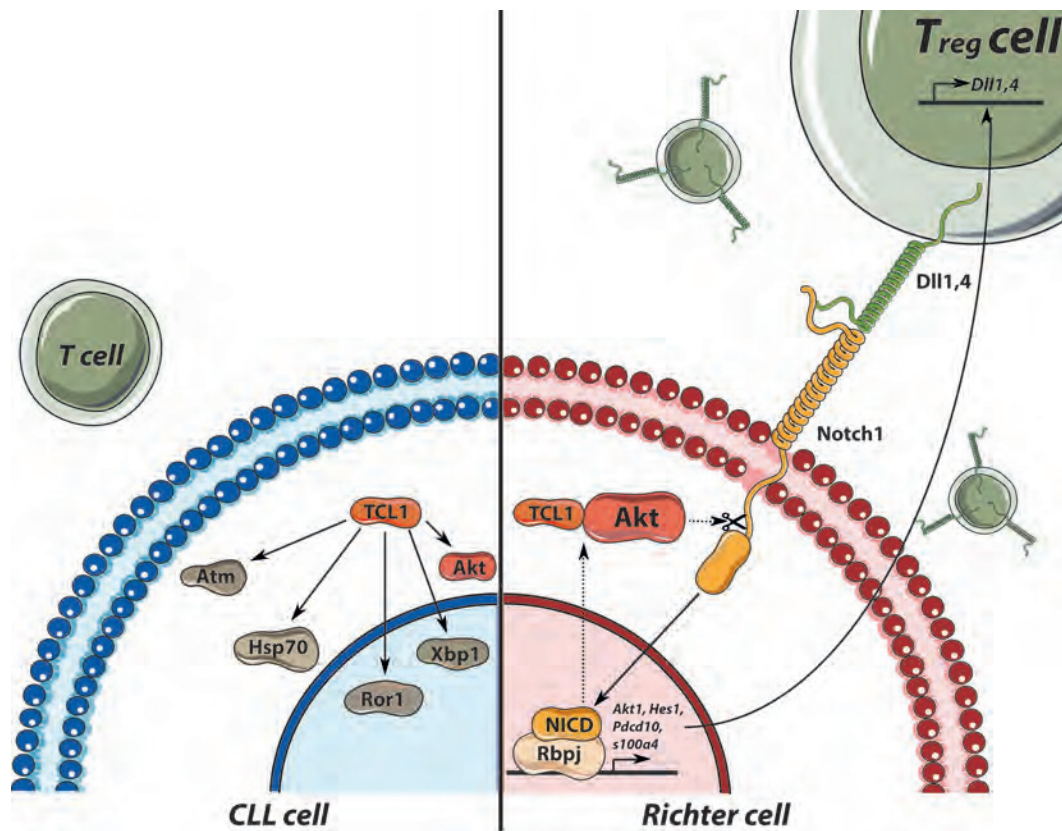
Fig. 4.1: Bidirectional overactivation of Akt and Notch1 in *TCL1*-overexpressed CLL promotes RT. During CLL, TCL1 regulates downstream proteins including Akt, Atm, Ror1, and Hsp70 (Paduano *et al*, 2018; left side). During RT, overactivated Akt enhances the stimulation of the canonical Notch1 signaling by promoting the expression of Rbpj/Notch1 target genes. Notch1 activation is caused by ligand-presenting regulatory T (T_{reg}) cells. Activated Notch1 induces further Notch1 ligand presentation and cell expansion of T_{reg} cells. Rbpj/Notch1 target genes are *inter alia* involved in the transcriptional upregulation of *Dll1* and *Dll4* in T_{reg} cells. Identified target genes during RT include *Akt1*, *Hes1*, *Pdcd10*, and *s100a4*. *Vice versa*, Notch1 enhances Akt actions by promoting phosphorylation (right side). The illustration was created using Servier Medical Art. CLL: chronic lymphocytic leukemia, Dll1,4: Delta-like protein 1,4, Hes1: Hairy enhancer of split 1, Hsp70: Heat shock protein 70, NICD: Notch1 intracellular domain, Pdcd10: Programmed cell death 10, Rbpj: Recombination signal binding protein for immunoglobulin kappa J region, Ror1: Receptor tyrosine kinase like orphan receptor 1, s100a4: S100 calcium-binding protein A4, TCL1: T cell leukemia/lymphoma protein 1, Xbp1: X-box binding protein 1.

This thesis supports further studies to develop PI3K/AKT- and NOTCH1-targeted therapies for aggressive CLL and RT. Kinase inhibitors of the BCR signaling have become attractive alternatives to chemotherapeutic treatments for leukemia/lymphoma, such as ibrutinib and idelalisib (Wiestner, 2012; Wiestner, 2015; Maharaj, Sahakian, and Pinilla-

Ibarz, 2017). Due to the multiple physiological functions of PI3K/AKT and NOTCH1 in various cell types, severe and lasting side effects are conceivable during systemic inhibition of both pathways. To minimize side effects, treatments that are directed to oncogenic AKT/NOTCH1 mediators or interaction partners are more selective and recommended. For instance, S100A4 is a newly identified RBPJ/NOTCH1 target in CLL that comes more and more into focus for novel therapies. A recent study records first successes of an anti-S100A4 antibody therapy in aggressive cancer (Ganaie et al., 2020). However, because of the high correlation between active AKT/NOTCH1 and poor outcome, pAKT and NICD may function as novel prognostic tools for human CLL patients.

5 References

Alanazi, Bader et al. (2020). "Integrated nuclear proteomics and transcriptomics identifies S100A4 as a therapeutic target in acute myeloid leukemia." In: *Leukemia*. ISSN: 14765551. DOI: 10.1038/s41375-019-0596-4.

Alessi, Dario R., F. Barry Caudwell, et al. (1996). "Molecular basis for the substrate specificity of protein kinase B; comparison with MAPKAP kinase-1 and p70 S6 kinase." In: *FEBS Letters*. ISSN: 00145793. DOI: 10.1016/S0014-5793(96)01370-1.

Alessi, Dario R., Stephen R. James, et al. (1997). "Characterization of a 3-phosphoinositide-dependent protein kinase which phosphorylates and activates protein kinase Bα." In: *Current Biology*. ISSN: 09609822. DOI: 10.1016/s0960-9822(06)00122-9.

Allan, John N and Richard R Furman (2018). "Current trends in the management of Richter's syndrome." In: *International Journal of Hematologic Oncology*. ISSN: 2045-1393. DOI: 10.2217/ijh-2018-0010.

Álvarez-Garcia, Virginia et al. (2019). *Mechanisms of PTEN loss in cancer: It's all about diversity*. DOI: 10.1016/j.semcancer.2019.02.001.

Andersson, Emma R, Rickard Sandberg, and Urban Lendahl (2011). "Notch signaling: simplicity in design, versatility in function." In: *Development* 138.17, pp. 3593–3612.

Arruga, F. et al. (2014). "Functional impact of NOTCH1 mutations in chronic lymphocytic leukemia." In: *Leukemia*. ISSN: 14765551. DOI: 10.1038/leu.2013.319.

Arruga, Francesca, Tiziana Vaisitti, and Silvia Deaglio (2018). *The NOTCH pathway and its mutations in mature B cell malignancies*. DOI: 10.3389/fonc.2018.00550.

Attekum, Martijn H.A. van, Eric Eldering, and Arnon P. Kater (2017). *Chronic lymphocytic leukemia cells are active participants in microenvironmental cross-talk*. DOI: 10.3324/haematol.2016.142679.

Bagnara, Davide et al. (2011). "A novel adoptive transfer model of chronic lympho-cytic leukemia suggests a key role for T lymphocytes in the disease." In: *Blood*. ISSN: 00064971. DOI: `10.1182/blood-2010-12-324210`.

Balint, Klara et al. (2005). "Activation of Notch1 signaling is required for β-catenin-mediated human primary melanoma progression." In: *Journal of Clinical Investigation*. ISSN: 00219738. DOI: `10.1172/JCI25001`.

Bedogni, Barbara et al. (2008). "Notch1 is an effector of Akt and hypoxia in melanoma development." In: *Journal of Clinical Investigation*. ISSN: 00219738. DOI: `10.1172/JCI36157`.

Bertrand, F. E. et al. (2000). "Notch-1 and Notch-2 exhibit unique patterns of expression in human B-lineage cells." In: *Leukemia*. ISSN: 08876924. DOI: `10.1038/sj.leu.2401942`.

Beurel, Eleonore, Steven F. Grieco, and Richard S. Jope (2015). *Glycogen synthase kinase-3 (GSK3): Regulation, actions, and diseases*. DOI: `10.1016/j.pharmthera.2014.11.016`.

Beyer, Marc et al. (2005). "Reduced frequencies and suppressive function of CD4+CD25 hi regulatory T cells in patients with chronic lymphocytic leukemia after therapy with fludarabine." In: *Blood*. ISSN: 00064971. DOI: `10.1182/blood-2005-02-0642`.

Bhattacharyya, Sankar et al. (2011). "NFATc1 affects mouse splenic B cell function by controlling the calcineurin-NFAT signaling network." In: *Journal of Experimental Medicine*. ISSN: 15409538. DOI: `10.1084/jem.20100945`.

Biancotto, Angélique et al. (2012). "Phenotypic complexity of T regulatory subsets in pa-tients with B-chronic lymphocytic leukemia." In: *Modern Pathology*. ISSN: 08933952. DOI: `10.1038/modpathol.2011.164`.

Bichi, Roberta et al. (2002). "Human chronic lymphocytic leukemia modeled in mouse by targeted TCL1 expression." In: *Proceedings of the National Academy of Sciences of the United States of America*. ISSN: 00278424. DOI: `10.1073/pnas.102181599`.

Biggs, William H. et al. (1999). "Protein kinase B/Akt-mediated phosphorylation promotes nuclear exclusion of the winged helix transcription factor FKHR1." In: *Proceedings of the National Academy of Sciences of the United States of America*. ISSN: 00278424. DOI: `10.1073/pnas.96.13.7421`.

Binet, J. L. et al. (1981). "A new prognostic classification of chronic lymphocytic leukemia derived from a multivariate survival analysis." In: *Cancer*. ISSN: 10970142. DOI: `10.1002/1097-0142(19810701)48:1<198::AID-CNCR2820480131>3.0.CO;2-V`.

Biran, Anat et al. (2019). "Deciphering the Role of Locally Disordered DNA Methylation on CLL Development In Vivo." In: *Blood*. ISSN: 0006-4971. DOI: `10.1182/blood-2019-130744`.

Blain, Jennifer et al. (2017). "C-terminal deletion of NOTCH1 intracellular domain (N1ICD) increases its stability but does not amplify and recapitulate N1ICD-dependent signalling /631/67 /631/80/86 /13 /13/95 /38 /38/109 /96 article." In: *Scientific Reports*. ISSN: 20452322. DOI: `10.1038/s41598-017-05119-0`.

Bockstaele, Laurence et al. (2006). "Regulated Activating Thr172 Phosphorylation of Cyclin-Dependent Kinase 4(CDK4): Its Relationship with Cyclins and CDK "Inhibitors"." In: *Molecular and Cellular Biology*. ISSN: 0270-7306. DOI: `10.1128/mcb.02006-05`.

Boissard, Frédéric et al. (2015). "Nurse like cells: Chronic lymphocytic leukemia associated macrophages." In: *Leukemia and Lymphoma*. DOI: `10.3109/10428194.2014.991731`.

Borggrefe, T. and F. Oswald (2009). *The Notch signaling pathway: Transcriptional regulation at Notch target genes*. DOI: `10.1007/s00018-009-8668-7`.

Bosch, Francesc and Riccardo Dalla-Favera (2019). *Chronic lymphocytic leukaemia: from genetics to treatment*. DOI: `10.1038/s41571-019-0239-8`.

Bozkulak, Esra Cagavi and Gerry Weinmaster (2009). "Selective Use of ADAM10 and ADAM17 in Activation of Notch1 Signaling." In: *Molecular and Cellular Biology*. ISSN: 0270-7306. DOI: `10.1128/mcb.00406-09`.

Bray, Freddie et al. (2018). "Global cancer statistics 2018: GLOBOCAN estimates of incidence and mortality worldwide for 36 cancers in 185 countries." In: *CA: A Cancer Journal for Clinicians*. ISSN: 1542-4863. DOI: `10.3322/caac.21492`.

Bray, Sarah J. (2006). *Notch signalling: A simple pathway becomes complex*. DOI: `10.1038/nrm2009`.

Brenner, Annette K. and Øystein Bruserud (2018). *S100 Proteins in Acute Myeloid Leukemia*. DOI: `10.1016/j.neo.2018.09.007`.

Bresnick, Anne R., David J. Weber, and Danna B. Zimmer (2015). *S100 proteins in cancer*. DOI: `10.1038/nrc3893`.

Brognard, John and Alexandra C. Newton (2008). *PHLiPPing the switch on Akt and protein kinase C signaling*. DOI: `10.1016/j.tem.2008.04.001`.

Brognard, John, Emma Sierecki, et al. (2007). "PHLPP and a Second Isoform, PHLPP2, Differentially Attenuate the Amplitude of Akt Signaling by Regulating Distinct Akt Isoforms." In: *Molecular Cell*. ISSN: 10972765. DOI: `10.1016/j.molcel.2007.02.017`.

Bruey, Jean Marie et al. (2010). "Circulating Ki-67 index in plasma as a biomarker and prognostic indicator in chronic lymphocytic leukemia." In: *Leukemia Research*. ISSN: 01452126. DOI: `10.1016/j.leukres.2010.03.010`.

Brunet, Anne et al. (1999). "Akt promotes cell survival by phosphorylating and inhibiting a forkhead transcription factor." In: *Cell*. ISSN: 00928674. DOI: `10.1016/S0092-8674(00)80595-4`.

Burger, J. A. et al. (2000). "Blood-derived nurse-like cells protect chronic lymphocytic leukemia B cells from spontaneous apoptosis through stromal cell-derived factor-1." In: *Blood*. ISSN: 00064971. DOI: `10.1182/blood.v96.8.2655`.

Burger, Jan A. (2010). *Chemokines and chemokine receptors in chronic lymphocytic leukemia (CLL): From understanding the basics towards therapeutic targeting*. DOI: `10.1016/j.semcancer.2010.09.005`.

Burger, Jan A. and Nicholas Chiorazzi (2013). *B cell receptor signaling in chronic lymphocytic leukemia*. DOI: `10.1016/j.it.2013.07.002`.

Buschle, Michael et al. (1993). "Interferon γ inhibits apoptotic cell death in B cell chronic lymphocytic leukemia." In: *Journal of Experimental Medicine*. ISSN: 15409538. DOI: `10.1084/jem.177.1.213`.

Calamito, Marco et al. (2010). "Akt1 and Akt2 promote peripheral B-cell maturation and survival." In: *Blood*. ISSN: 00064971. DOI: `10.1182/blood-2009-09-241638`.

Caligaris-Cappio, F. et al. (1993). "The nature of the B lymphocyte in B-chronic lymphocytic leukemia." In: *Blood Cells*.

Campo, Elias et al. (2018). *TP53 aberrations in chronic lymphocytic leukemia: An overview of the clinical implications of improved diagnostics*. DOI: `10.3324/haematol.2018.187583`.

Cantley, Lewis C. and Benjamin G. Neel (1999). *New insights into tumor suppression: PTEN suppresses tumor formation by restraining the phosphoinositide 3-kinase/AKT pathway*. DOI: `10.1073/pnas.96.8.4240`.

Carracedo, A. and P. P. Pandolfi (2008). *The PTEN-PI3K pathway: Of feedbacks and cross-talks*. DOI: `10.1038/onc.2008.247`.

Castel, David et al. (2013). "Dynamic binding of RBPJ is determined by notch signaling status." In: *Genes and Development*. ISSN: 08909369. DOI: `10.1101/gad.211912.112`.

Charalambous, Andreas and Panagiota Vasileiou (2012). *Risk factors for childhood leukemia: A comprehensive literature review*.

Cimmino, Amelia et al. (2005). "miR-15 and miR-16 induce apoptosis by targeting BCL2." In: *Proceedings of the National Academy of Sciences of the United States of America*. ISSN: 00278424. DOI: 10.1073/pnas.0506654102.

CNI, National Cancer Institute (2019). "NCI Dictionary of Cancer Terms." In: *National Cancer Institute*.

Col, Jessica Dal et al. (2008). "Distinct functional significance of Akt and mTOR constitutive activation in mantle cell lymphoma." In: *Blood*. ISSN: 00064971. DOI: 10.1182/blood-2007-07-103481.

Colombo, Michela et al. (2018). *Cancer cells exploit notch signaling to redefine a supportive cytokine milieu*. DOI: 10.3389/fimmu.2018.01823.

Crabtree, Gerald R. and Eric N. Olson (2002). *NFAT signaling: Choreographing the social lives of cells*. DOI: 10.1016/S0092-8674(02)00699-2.

Crompot, Emerence et al. (2017). "Extracellular vesicles of bone marrow stromal cells rescue chronic lymphocytic leukemia B cells from apoptosis, enhance their migration and induce gene expression modifications." In: *Haematologica*. ISSN: 15928721. DOI: 10.3324/haematol.2016.163337.

D'Souza, B., A. Miyamoto, and G. Weinmaster (2008). *The many facets of Notch ligands*. DOI: 10.1038/onc.2008.229.

Daigo, Kayo et al. (2018). "Characterization of KIF11 as a novel prognostic biomarker and therapeutic target for oral cancer." In: *International Journal of Oncology*. ISSN: 17912423. DOI: 10.3892/ijo.2017.4181.

Dancescu, M. et al. (1992). "Interleukin 4 protects chronic lymphocytic leukemic b cells from death by apoptosis and upregulates bcl-2 expression." In: *Journal of Experimental Medicine*. ISSN: 15409538. DOI: 10.1084/jem.176.5.1319.

De Falco, Filomena et al. (2018). "IL-4-dependent Jagged1 expression/processing is associated with survival of chronic lymphocytic leukemia cells but not with Notch activation." In: *Cell Death and Disease*. ISSN: 20414889. DOI: `10.1038/s41419-018-1185-6`.

Dong, Ying et al. (2020). "Leukemia incidence trends at the global, regional, and national level between 1990 and 2017." In: *Experimental Hematology and Oncology*. ISSN: 21623619. DOI: `10.1186/s40164-020-00170-6`.

Esau, Daniel (2017). *Viral Causes of Lymphoma: The History of Epstein-Barr Virus and Human T-Lymphotropic Virus 1*. DOI: `10.1177/1178122X17731772`.

Fabbri, Giulia and Riccardo Dalla-Favera (2016). *The molecular pathogenesis of chronic lymphocytic leukaemia*. DOI: `10.1038/nrc.2016.8`.

Fabbri, Giulia, Silvia Rasi, et al. (2011). "Analysis of the chronic lymphocytic leukemia coding genome: Role of NOTCH1 mutational activation." In: *Journal of Experimental Medicine*. ISSN: 00221007. DOI: `10.1084/jem.20110921`.

Faridi, Jesika et al. (2003). "Akt promotes increased mammalian cell size by stimulating protein synthesis and inhibiting protein degradation." In: *American Journal of Physiology - Endocrinology and Metabolism*. ISSN: 01931849. DOI: `10.1152/ajpendo.00239.2003`.

Ferrari, Simona et al. (2007). "Mutations of the Igβ gene cause agammaglobulinemia in man." In: *Journal of Experimental Medicine*. ISSN: 00221007. DOI: `10.1084/jem.20070264`.

Fischer, M. (2017). *Census and evaluation of p53 target genes*. DOI: `10.1038/onc.2016.502`.

Fonseka, Lakshan N and Carlos A Tirado (2015). "C-MYC Involvement in Chronic Lymphocytic Leukemia (CLL): A Molecular and Cytogenetic Update." In: *Journal of the Association of Genetic Technologists*. ISSN: 1523-7834.

Francia Di Celle, Paola et al. (1996). "Intereukin-8 induces the accumulation of B-cell chronic lymphocytic leukemia cells by prolonging survival in an autocrine fashion." In: *Blood*. ISSN: 00064971. DOI: `10.1182/blood.v87.10.4382.bloodjournal87104382`.

French, Samuel W. et al. (2003). "Sp1 transactivation of the TCL1 oncogene." In: *Journal of Biological Chemistry*. ISSN: 00219258. DOI: `10.1074/jbc.M207166200`.

Frenzel, Lukas P. et al. (2011). "Sustained NF-kappaB activity in chronic lymphocytic leukemia is independent of genetic and epigenetic alterations in the TNFAIP3 (A20) locus." In: *International Journal of Cancer*. ISSN: 00207136. DOI: `10.1002/ijc.25579`.

Fresno Vara, Juan Ángel et al. (2004). *P13K/Akt signalling pathway and cancer*. DOI: `10.1016/j.ctrv.2003.07.007`.

Galletti, G., F. Caligaris-Cappio, and M. T.S. Bertilaccio (2016). *B cells and macrophages pursue a common path toward the development and progression of chronic lymphocytic leukemia*. DOI: `10.1038/leu.2016.261`.

Ganaie, Arsheed A. et al. (2020). "Anti-S100A4 antibody therapy is efficient in treating aggressive prostate cancer and reversing immunosuppression: Serum and biopsy S100A4 as a clinical predictor." In: *Molecular Cancer Therapeutics*. ISSN: 15388514. DOI: `10.1158/1535-7163.MCT-20-0410`.

Gaudio, Eugenio et al. (2012). "Tcl1 interacts with Atm and enhances NF-κB activation in hematologic malignancies." In: *Blood*. ISSN: 00064971. DOI: `10.1182/blood-2011-08-374561`.

Gauld, Stephen B. and John C. Cambier (2004). *Src-family kinases in B-cell development and signaling*. DOI: `10.1038/sj.onc.1208075`.

Georgescu, Maria Magdalena (2010). *Pten tumor suppressor network in PI3K-Akt pathway control*. DOI: `10.1177/1947601911407325`.

Ghamlouch, Hussein et al. (2013). "A Combination of Cytokines Rescues Highly Purified Leukemic CLL B-Cells from Spontaneous Apoptosis In Vitro." In: *PLoS ONE*. ISSN: 19326203. DOI: `10.1371/journal.pone.0060370`.

Ghosh, Asish K. et al. (2010). "Circulating microvesicles in B-cell chronic lymphocytic leukemia can stimulate marrow stromal cells: Implications for disease progression." In: *Blood*. ISSN: 00064971. DOI: `10.1182/blood-2009-09-242719`.

Giné, Eva et al. (2010). "Expanded and highly active proliferation centers identify a histological subtype of chronic lymphocytic leukemia ("accelerated" chronic lymphocytic leukemia) with aggressive clinical behavior." In: *Haematologica*. ISSN: 03906078. DOI: `10.3324/haematol.2010.022277`.

Gold, M R et al. (1999). "The B cell antigen receptor activates the Akt (protein kinase B)/glycogen synthase kinase-3 signaling pathway via phosphatidylinositol 3-kinase." In: *Journal of immunology (Baltimore, Md. : 1950)*. ISSN: 0022-1767.

Gonzalez, Eva and Timothy E. McGraw (2009). *The Akt kinases: Isoform specificity in metabolism and cancer*. DOI: `10.4161/cc.8.16.9335`.

Gregory, Mark A., Ying Qi, and Stephen R. Hann (2003). "Phosphorylation by Glycogen Synthase Kinase-3 Controls c-Myc Proteolysis and Subnuclear Localization." In: *Journal of Biological Chemistry*. ISSN: 00219258. DOI: `10.1074/jbc.M310722200`.

Guo, Dongmei et al. (2009). "Notch-1 regulates Akt signaling pathway and the expression of cell cycle regulatory proteins cyclin D1, CDK2 and p21 in T-ALL cell lines." In: *Leukemia Research*. ISSN: 01452126. DOI: `10.1016/j.leukres.2008.10.026`.

Gutierrez, Alejandro and A. Thomas Look (2007). *NOTCH and PI3K-AKT Pathways Intertwined*. DOI: `10.1016/j.ccr.2007.10.027`.

Hacken, Elisa ten and Jan A. Burger (2016). *Microenvironment interactions and B-cell receptor signaling in Chronic Lymphocytic Leukemia: Implications for disease pathogenesis and treatment*. DOI: `10.1016/j.bbamcr.2015.07.009`.

Hales, Eric C., Jeffrey W. Taub, and Larry H. Matherly (2014). *New insights into Notch1 regulation of the PI3K-AKT-mTOR1 signaling axis: Targeted therapy of γ-secretase inhibitor resistant T-cell acute lymphoblastic leukemia*. DOI: `10.1016/j.cellsig.2013.09.021`.

Hallek, Michael et al. (2018). "iwCLL guidelines for diagnosis, indications for treatment, response assessment, and supportive management of CLL." In: *Blood*. ISSN: 15280020. DOI: `10.1182/blood-2017-09-806398`.

Hampel, Franziska et al. (2011). "CD19-independent instruction of murine marginal zone B-cell development by constitutive Notch2 signaling." In: *Blood*. ISSN: 00064971. DOI: `10.1182/blood-2010-12-325944`.

Heinig, Kristina et al. (2014). "Access to follicular dendritic cells is a pivotal step in murine chronic lymphocytic leukemia b-cell activation and proliferation." In: *Cancer Discovery*. ISSN: 21598290. DOI: `10.1158/2159-8290.CD-14-0096`.

Herishanu, Yair, Ben Zion Katz, et al. (2013). *Biology of Chronic Lymphocytic Leukemia in Different Microenvironments. Clinical and Therapeutic Implications*. DOI: `10.1016/j.hoc.2013.01.002`.

Herishanu, Yair, Patricia Pérez-Galán, et al. (2011). "The lymph node microenvironment promotes B-cell receptor signaling, NF-κB activation, and tumor proliferation in chronic lymphocytic leukemia." In: *Blood*. ISSN: 00064971. DOI: `10.1182/blood-2010-05-284984`.

Herling, M. et al. (2006). "TCL1 shows a regulated expression pattern in chronic lymphocytic leukemia that correlates with molecular subtypes and proliferative state." In: *Leukemia*. ISSN: 14765551. DOI: `10.1038/sj.leu.2404017`.

Herling, Marco et al. (2009). "High TCL1 levels are a marker of B-cell receptor pathway responsiveness and adverse outcome in chronic lymphocytic leukemia." In: *Blood* 114.21, pp. 4675–4686.

Hofbauer, J. P. et al. (2011). "Development of CLL in the TCL1 transgenic mouse model is associated with severe skewing of the T-cell compartment homologous to human CLL." In: *Leukemia*. ISSN: 08876924. DOI: 10.1038/leu.2011.111.

Howlader, N et al. (2012). "SEER Cancer statistics review 1975-2010." In: *Journal of National Cancer Institute*.

Hsieh, James J.D. et al. (1999). "CIR, a corepressor linking the DNA binding factor CBF1 to the histone deacetylase complex." In: *Proceedings of the National Academy of Sciences of the United States of America*. ISSN: 00278424. DOI: 10.1073/pnas. 96.1.23.

Ianni, Mauro Di et al. (2009). *A new genetic lesion in B-CLL: A NOTCH1 PEST domain mutation*. DOI: 10.1111/j.1365-2141.2009.07816.x.

Itoh, Go et al. (2011). "CAMP (C13orf8, ZNF828) is a novel regulator of kinetochore-microtubule attachment." In: *EMBO Journal*. ISSN: 02614189. DOI: 10.1038/emboj. 2010.276.

Jain, Preetesh and Susan O'Brien (2012). *Richter's transformation in chronic lympho-cytic leukemia*. DOI: 10.1016/j.leukres.2004.09.008.

Kang, Jung Ah, Woo Seok Kim, and Sung Gyoo Park (2014). "Notch1 is an important mediator for enhancing of B-cell activation and antibody secretion by Notch ligand." In: *Immunology*. ISSN: 13652567. DOI: 10.1111/imm.12333.

Kao, Hung Ying et al. (1998). "A histone deacetylase corepressor complex regulates the Notch signal transduction pathway." In: *Genes and Development*. ISSN: 08909369. DOI: 10.1101/gad.12.15.2269.

Al-Khalaf, Huda H. and Abdelilah Aboussekhra (2013). "P16INK4A Positively Regulates p21WAF1 Expression by suppressing AUF1-dependent mRNA decay." In: *PLoS ONE*. ISSN: 19326203. DOI: 10.1371/journal.pone.0070133.

Kikuchi, Norihiko et al. (2006). "Nuclear expression of S100A4 is associated with aggressive behavior of epithelial ovarian carcinoma: An important autocrine/paracrine factor in tumor progression." In: *Cancer Science*. ISSN: 13479032. DOI: `10.1111/j.1349-7006.2006.00295.x`.

Kikushige, Yoshikane and Toshihiro Miyamoto (2014). *Hematopoietic stem cell aging and chronic lymphocytic leukemia pathogenesis*. DOI: `10.1007/s12185-014-1651-6`.

Kitada, Shinichi et al. (1999). "Bryostatin and CD40-ligand enhance apoptosis resistance and induce expression of cell survival genes in B-cell chronic lymphocytic leukaemia." In: *British Journal of Haematology*. ISSN: 00071048. DOI: `10.1046/j.1365-2141.1999.01642.x`.

Klein, Ulf et al. (2010). "The DLEU2/miR-15a/16-1 Cluster Controls B Cell Proliferation and Its Deletion Leads to Chronic Lymphocytic Leukemia." In: *Cancer Cell*. ISSN: 15356108. DOI: `10.1016/j.ccr.2009.11.019`.

Knittel, Gero et al. (2016). "B-cell-specific conditional expression of Myd88p.L252P leads to the development of diffuse large B-cell lymphoma in mice." In: *Blood*. ISSN: 15280020. DOI: `10.1182/blood-2015-11-684183`.

Kohlhaas, Vivien et al. (2020). "Active AKT signaling triggers CLL towards Richter's transformation via over-activation of Notch1." In: *Blood*. ISSN: 0006-4971.

Kuo, Yi Chun et al. (2008). "Regulation of phosphorylation of Thr-308 of Akt, cell proliferation, and survival by the B55α regulatory subunit targeting of the protein phosphatase 2A holoenzyme to Akt." In: *Journal of Biological Chemistry*. ISSN: 00219258. DOI: `10.1074/jbc.M709585200`.

Kurtova, Antonina V. et al. (2009). "Diverse marrow stromal cells protect CLL cells from spontaneous and drug-induced apoptosis: Development of a reliable and reproducible system to assess stromal cell adhesion-mediated drug resistance." In: *Blood*. ISSN: 00064971. DOI: `10.1182/blood-2009-07-233718`.

LaFoya, Bryce et al. (2016). *Notch: A multi-functional integrating system of microenvironmental signals*. DOI: `10.1016/j.ydbio.2016.08.023`.

Laine, Jarmo et al. (2000). "The protooncogene TCL1 is an Akt kinase coactivator." In: *Molecular cell* 6.2, pp. 395–407.

Lambertz, Nicole et al. (2015). "Downregulation of programmed cell death 10 is associated with tumor cell proliferation, hyperangiogenesis and peritumoral edema in human glioblastoma." In: *BMC Cancer*. ISSN: 14712407. DOI: `10.1186/s12885-015-1709-8`.

Landau, Dan A et al. (2015). "Mutations driving CLL and their evolution in progression and relapse." In: *Nature* 526.7574, p. 525.

Landau, Dan A. et al. (2013). "Evolution and impact of subclonal mutations in chronic lymphocytic leukemia." In: *Cell*. ISSN: 00928674. DOI: `10.1016/j.cell.2013.01.019`.

Latronico, Michael V.G. et al. (2004). "Regulation of cell size and contractile function by AKT in cardiomyocytes." In: *Annals of the New York Academy of Sciences*. DOI: `10.1196/annals.1302.021`.

Li, Hongda et al. (2014). "Cell cycle-linked MeCP2 phosphorylation modulates adult neurogenesis involving the Notch signalling pathway." In: *Nature Communications*. ISSN: 20411723. DOI: `10.1038/ncomms6601`.

Liao, Yong and Mien Chie Hung (2010). *Physiological regulation of Akt activity and stability*.

Lin, Douglas I., Priya Aggarwal, and J. Alan Diehl (2008). "Phosphorylation of MCM3 on Ser-112 regulates its incorporation into the MCM2-7 complex." In: *Proceedings of the National Academy of Sciences of the United States of America*. ISSN: 00278424. DOI: `10.1073/pnas.0800077105`.

Link, Theresa et al. (2019). "Clinical relevance of circulating MACC1 and S100A4 transcripts for ovarian cancer." In: *Molecular Oncology*. ISSN: 18780261. DOI: `10.1002/1878-0261.12484`.

Lionetti, Marta et al. (2014). "High-throughput sequencing for the identification of NOTCH1 mutations in early stage chronic lymphocytic leukaemia: Biological and clinical implications." In: *British Journal of Haematology*. ISSN: 13652141. DOI: `10.1111/bjh.12800`.

Liu, Zhao Jun et al. (2006). "Notch1 signaling promotes primary melanoma progression by activating mitogen-activated protein kinase/phosphatidylinositol 3-kinase-Akt pathways and up-regulating N-cadherin expression." In: *Cancer Research*. ISSN: 00085472. DOI: `10.1158/0008-5472.CAN-05-3589`.

Lutzny, Gloria et al. (2013). "Protein Kinase C-β-Dependent Activation of NF-κB in Stromal Cells Is Indispensable for the Survival of Chronic Lymphocytic Leukemia B Cells In Vivo." In: *Cancer Cell*. ISSN: 15356108. DOI: `10.1016/j.ccr.2012.12.003`.

M.K., McKenna et al. (2017). "Splenic microenvironment is important in the survival and growth of Chronic Lymphocytic Leukemia in mice." In: *Journal of Immunology*. ISSN: 1550-6606.

Mackus, Wendelina J.M. et al. (2003). "Expansion of CMV-specific CD8+CD45RA+CD27-T cells in B-cell chronic lymphocytic leukemia." In: *Blood*. ISSN: 00064971. DOI: `10.1182/blood-2003-01-0182`.

Maharaj, Kamira, Eva Sahakian, and Javier Pinilla-Ibarz (2017). *Emerging role of BCR signaling inhibitors in immunomodulation of chronic lymphocytic leukemia*. DOI: `10.1182/bloodadvances.2017006809`.

Mao, Zhengrong et al. (2007). "IgVH mutational status and clonality analysis of Richter's transformation: Diffuse large B-cell lymphoma and hodgkin lymphoma in association with B-cell chronic lymphocytic leukemia (B-CLL) represent 2 different pathways of

disease evolution." In: *American Journal of Surgical Pathology*. ISSN: 01475185. DOI: `10.1097/PAS.0b013e31804bdaf8`.

Martel, Véronique et al. (1997). "De novo methylation of tumour suppressor genes CDKN2A and CDKN2B is a rare finding in B-cell chronic lymphocytic leukaemia." In: *British Journal of Haematology*. ISSN: 00071048. DOI: `10.1046/j.1365-2141.1997.3953209.x`.

Mayo, Lindsey D. and David B. Donner (2001). "A phosphatidylinositol 3-kinase/Akt pathway promotes translocation of Mdm2 from the cytoplasm to the nucleus." In: *Proceedings of the National Academy of Sciences of the United States of America*. ISSN: 00278424. DOI: `10.1073/pnas.181181198`.

Mayo, Marty W. et al. (2002). "PTEN blocks tumor necrosis factor-induced NF-κB-dependent transcription by inhibiting the transactivation potential of the p65 subunit." In: *Journal of Biological Chemistry*. ISSN: 00219258. DOI: `10.1074/jbc.M108670200`.

Meurette, Olivier and Patrick Mehlen (2018). *Notch Signaling in the Tumor Microenvironment*. DOI: `10.1016/j.ccell.2018.07.009`.

Miranda-Filho, Adalberto et al. (2018). "Epidemiological patterns of leukaemia in 184 countries: a population-based study." In: *The Lancet Haematology*. ISSN: 23523026. DOI: `10.1016/S2352-3026(17)30232-6`.

Moon, Jang Bae et al. (2012). "Akt Induces Osteoclast Differentiation through Regulating the GSK3β/NFATc1 Signaling Cascade." In: *The Journal of Immunology*. ISSN: 0022-1767. DOI: `10.4049/jimmunol.1101254`.

Murtaugh, L. Charles et al. (2003). "Notch signaling controls multiple steps of pancreatic differentiation." In: *Proceedings of the National Academy of Sciences of the United States of America*. ISSN: 00278424. DOI: `10.1073/pnas.2436557100`.

Nakae, Jun, Valarie Barr, and Domenico Accili (2000). "Differential regulation of gene expression by insulin and IGF-1 receptors correlates with phosphorylation of a single

amino acid residue in the forkhead transcription factor FKHR." In: *EMBO Journal*. ISSN: 02614189. DOI: `10.1093/emboj/19.5.989`.

Negro, Roberto et al. (2012). "Overexpression of the autoimmunity-associated phosphatase PTPN22 promotes survival of antigen-stimulated CLL cells by selectively activating AKT." In: *Blood*. ISSN: 00064971. DOI: `10.1182/blood-2012-01-403162`.

Nolte, Hendrik et al. (2018). "Instant Clue: A Software Suite for Interactive Data Visualization and Analysis." In: *Scientific Reports*. ISSN: 20452322. DOI: `10.1038/s41598-018-31154-6`.

Ogawara, Yoko et al. (2002). "Akt enhances Mdm2-mediated ubiquitination and degradation of p53." In: *Journal of Biological Chemistry*. ISSN: 00219258. DOI: `10.1074/jbc.M109745200`.

Oppezzo, P. and G. Dighiero (2013). *Role of the B-cell receptor and the microenvironment in chronic lymphocytic leukemia*. DOI: `10.1038/bcj.2013.45`.

Os, Audun et al. (2013). "Chronic lymphocytic leukemia cells are activated and proliferate in response to specific T helper cells." In: *Cell reports* 4.3, pp. 566–577.

Osaki, M., M. Oshimura, and H. Ito (2004). "PI3K-Akt pathway: Its functions and alterations in human cancer." In: *Apoptosis*. ISSN: 13608185. DOI: `10.1023/B:APPT.0000045801.15585.dd`.

Paduano, Francesco et al. (2018). "T-Cell Leukemia/Lymphoma 1 (TCL1): An oncogene regulating multiple signaling pathways." In: *Frontiers in Oncology*. ISSN: 2234943X. DOI: `10.3389/fonc.2018.00317`.

Pal, Deeksha et al. (2018). "Suppression of Notch1 and AKT mediated epithelial to mesenchymal transition by Verrucarin J in metastatic colon cancer." In: *Cell Death and Disease*. ISSN: 20414889. DOI: `10.1038/s41419-018-0810-8`.

Palacios, F. et al. (2015). "Activation of the PI3K/AKT pathway by microRNA-22 results in CLL B-cell proliferation." In: *Leukemia*. ISSN: 14765551. DOI: 10.1038/leu.2014. 158.

Palamarchuk, Alexey et al. (2012). "Tcl1 protein functions as an inhibitor of de novo DNA methylation in B-cell chronic lymphocytic leukemia (CLL)." In: *Proceedings of the National Academy of Sciences of the United States of America*. ISSN: 00278424. DOI: 10.1073/pnas.1200003109.

Palma, Marzia et al. (2017). "T cells in chronic lymphocytic leukemia display dysregulated expression of immune checkpoints and activation markers." In: *Haematologica*. ISSN: 15928721. DOI: 10.3324/haematol.2016.151100.

Palomero, Teresa, Maria Dominguez, and Adolfo A. Ferrando (2008). *The role of the PTEN/AKT pathway in NOTCH1-induced leukemia*. DOI: 10.4161/cc.7.8.5753.

Panin, Vladislav M. et al. (2002). "Notch ligands are substrates for protein O-fucosyltransferase-1 and Fringe." In: *The Journal of biological chemistry*. ISSN: 00219258. DOI: 10.1074/jbc.M204445200.

Parikh, Sameer A. et al. (2013). "Diffuse large B-cell lymphoma (Richter syndrome) in patients with chronic lymphocytic leukaemia (CLL): A cohort study of newly diagnosed patients." In: *British Journal of Haematology*. ISSN: 00071048. DOI: 10.1111/bjh. 12458.

Pascutti, Maria Fernanda et al. (2013). "IL-21 and CD40L signals from autologous T cells can induce antigen-independent proliferation of CLL cells." In: *Blood*. ISSN: 15280020. DOI: 10.1182/blood-2012-11-467670.

Patel, Satish et al. (2008). "Tissue-Specific Role of Glycogen Synthase Kinase 3β in Glucose Homeostasis and Insulin Action." In: *Molecular and Cellular Biology*. ISSN: 0270-7306. DOI: 10.1128/mcb.00763-08.

Pekarsky, Y. (2000). "Tcl1 enhances Akt kinase activity and mediates its nuclear translocation." In: *Proceedings of the National Academy of Sciences*. ISSN: 00278424. DOI: `10.1073/pnas.040557697`.

Pekarsky, Yuri et al. (2008). "Tcl1 functions as a transcriptional regulator and is directly involved in the pathogenesis of CLL." In: *Proceedings of the National Academy of Sciences of the United States of America*. ISSN: 00278424. DOI: `10.1073/pnas.0810965105`.

Puente, Xose S. et al. (2011). "Whole-genome sequencing identifies recurrent mutations in chronic lymphocytic leukaemia." In: *Nature*. ISSN: 14764687. DOI: `10.1038/nature10113`.

Quail, Daniela F. and Johanna A. Joyce (2013). *Microenvironmental regulation of tumor progression and metastasis*. DOI: `10.1038/nm.3394`.

Rai, K. R. et al. (1975). "Clinical staging of chronic lymphocytic leukemia." In: *Blood*. ISSN: 00064971. DOI: `10.1182/blood.v46.2.219.bloodjournal462219`.

Rajanala, Kalpana et al. (2014). "Phosphorylation of nucleoporin Tpr governs its differential localization and is required for its mitotic function." In: *Journal of Cell Science*. ISSN: 14779137. DOI: `10.1242/jcs.149112`.

Rapley, Joseph et al. (2008). "The NIMA-family kinase Nek6 phosphorylates the kinesin Eg5 at a novel site necessary for mitotic spindle formation." In: *Journal of Cell Science*. ISSN: 00219533. DOI: `10.1242/jcs.035360`.

Rawlings, David J. et al. (2017). *Altered B cell signalling in autoimmunity*. DOI: `10.1038/nri.2017.24`.

Richter, Maurice N (1928). "Generalized reticular cell sarcoma of lymph nodes associated with lymphatic leukemia." In: *The American journal of pathology* 4.4, p. 285.

Rickert, Robert C., Jürgen Roes, and Klaus Rajewsky (1997). "B lymphocyte-specific, Cre-mediated mutagenesis in mice." In: *Nucleic Acids Research*. ISSN: 03051048. DOI: 10.1093/nar/25.6.1317.

Rodríguez, A. et al. (2007). "Molecular heterogeneity in chronic lymphocytic leukemia is dependent on BCR signaling: Clinical correlation." In: *Leukemia*. ISSN: 14765551. DOI: 10.1038/sj.leu.2404831.

Rodríguez-Vicente, Ana E., Marcos González Díaz, and Jesús M. Hernández-Rivas (2013). *Chronic lymphocytic leukemia: A clinical and molecular heterogenous disease*. DOI: 10.1016/j.cancergen.2013.01.003.

Roessner, Philipp M. and Martina Seiffert (2020). *T-cells in chronic lymphocytic leukemia: Guardians or drivers of disease?* DOI: 10.1038/s41375-020-0873-2.

Rosati, Emanuela et al. (2018). *NOTCH1 aberrations in Chronic lymphocytic leukemia*. DOI: 10.3389/fonc.2018.00229.

Rossi, Davide, Silvia Rasi, et al. (2012). "Mutations of NOTCH1 are an independent predictor of survival in chronic lymphocytic leukemia." In: *Blood*. ISSN: 00064971. DOI: 10.1182/blood-2011-09-379966.

Rossi, Davide, Valeria Spina, Michaela Cerri, et al. (2009). "Stereotyped B-cell receptor is an independent risk factor of chronic lymphocytic leukemia transformation to richter syndrome." In: *Clinical Cancer Research*. ISSN: 10780432. DOI: 10.1158/1078-0432.CCR-08-3266.

Rossi, Davide, Valeria Spina, Clara Deambrogi, et al. (2011). "The genetics of Richter syndrome reveals disease heterogeneity and predicts survival after transformation." In: *Blood* 117.12, pp. 3391–3401.

Rozman, Ciril and Emilio Monserrat (1995). "Current Concepts, Chronic Lymphocytic Leukemia." In: *The New England Journal of Medicine*. ISSN: 02671700.

Rudelius, Martina et al. (2006). "Constitutive activation of Akt contributes to the pathogenesis and survival of mantle cell lymphoma." In: *Blood*. ISSN: 00064971. DOI: 10.1182/blood-2006-04-015586.

Saito, Toshiki et al. (2003). "Notch2 is preferentially expressed in mature B cells and indispensable for marginal zone B lineage development." In: *Immunity*. ISSN: 10747613. DOI: 10.1016/S1074-7613(03)00111-0.

Saleem, Mohammad et al. (2006). "S100A4 accelerates tumorigenesis and invasion of human prostate cancer through the transcriptional regulation of matrix metalloproteinase 9." In: *Proceedings of the National Academy of Sciences of the United States of America*. ISSN: 00278424. DOI: 10.1073/pnas.0606747103.

Santos, Margarida Almeida et al. (2007). "Notch1 engagement by Delta-like-1 promotes differentiation of B lymphocytes to antibody-secreting cells." In: *Proceedings of the National Academy of Sciences of the United States of America*. ISSN: 00278424. DOI: 10.1073/pnas.0702891104.

Sarbassov, Dos D. et al. (2005). "Phosphorylation and regulation of Akt/PKB by the rictor-mTOR complex." In: *Science*. ISSN: 00368075. DOI: 10.1126/science.1106148.

Al-Sawaf, Othman, Barbara Eichhorst, and Michael Hallek (2020). "Chronic lymphocytic leukemia." In: *Onkologe*. ISSN: 14330415. DOI: 10.1007/s00761-020-00769-8.

Scharenberg, Andrew M. et al. (1998). "Phosphatidylinositol-3,4,5-trisphosphate (PtdIns-3,4,5-P3)/Tec kinase-dependent calcium signaling pathway: A target for SHIP-mediated inhibitory signals." In: *EMBO Journal*. ISSN: 02614189. DOI: 10.1093/emboj/17.7.1961.

Schrader, Alexandra et al. (2014). "AKT-pathway Inhibition in Chronic Lymphocytic Leukemia Reveals Response Relationships Defined by TCL1." In: *Current Cancer Drug Targets*. ISSN: 15680096. DOI: 10.2174/1568009614666141028101711.

Sears, Rosalie et al. (2000). "Multiple Ras-dependent phosphorylation pathways regulate Myc protein stability." In: *Genes and Development*. ISSN: 08909369. DOI: `10.1101/gad.836800`.

Sears, Rosalie C. (2004). *The life cycle of c-Myc: From synthesis to degradation*. DOI: `10.4161/cc.3.9.1145`.

Seth, Rachna and Amitabh Singh (2015). *Leukemias in Children*. DOI: `10.1007/s12098-015-1695-5`.

Siddique, Hifzur R. et al. (2013). "The S100A4 Oncoprotein Promotes Prostate Tumorigenesis in a Transgenic Mouse Model: Regulating NFκB through the RAGE Receptor." In: *Genes and Cancer*. ISSN: 19476019. DOI: `10.1177/1947601913492420`.

Siegel, Rebecca L. et al. (2021). "Cancer Statistics, 2021." In: *CA: A Cancer Journal for Clinicians*. ISSN: 0007-9235. DOI: `10.3322/caac.21654`.

Simon (2020). "Cancer Facts & Figures 2020." In: *CA: A Cancer Journal for Clinicians*.

Sivina, M. et al. (2012). "Stromal cells modulate TCL1 expression, interacting AP-1 components and TCL1-targeting micro-RNAs in chronic lymphocytic leukemia." In: *Leukemia*. ISSN: 08876924. DOI: `10.1038/leu.2012.63`.

Stambolic, Vuk et al. (1998). "Negative regulation of PKB/Akt-dependent cell survival by the tumor suppressor PTEN." In: *Cell*. ISSN: 00928674. DOI: `10.1016/S0092-8674(00)81780-8`.

Stankovic, Tatjana and Anna Skowronska (2014). *The role of ATM mutations and 11q deletions in disease progression in chronic lymphocytic leukemia*. DOI: `10.3109/10428194.2013.829919`.

Stevenson, Freda K. et al. (2011). *B-cell receptor signaling in chronic lymphocytic leukemia*. DOI: `10.1182/blood-2011-06-338855`.

Stewart, Rachel L. et al. (2016). "S100A4 drives non-small cell lung cancer invasion, associates with poor prognosis, and is effectively targeted by the FDAapproved anti-

helminthic agent niclosamide." In: *Oncotarget*. ISSN: 19492553. DOI: `10.18632/oncotarget.8969`.

Stokoe, David et al. (1997). "Dual role of phosphatidylinositol-3,4,5-trisphosphate in the activation of protein kinase B." In: *Science*. ISSN: 00368075. DOI: `10.1126/science.277.5325.567`.

Swerdlow, Steven H. et al. (2016). *The 2016 revision of the World Health Organization classification of lymphoid neoplasms*. DOI: `10.1182/blood-2016-01-643569`.

Tadmor, Tamar et al. (2014). "Richter's transformation to diffuse large B-cell lymphoma: a retrospective study reporting clinical data, outcome, and the benefit of adding rituximab to chemotherapy, from the Israeli CLL Study Group." In: *American journal of hematology*. ISSN: 10968652. DOI: `10.1002/ajh.23826`.

Takata, Minoru and Tomohiro Kurosaki (1996). "A role for Bruton's tyrosine kinase in B cell antigen receptor-mediated activation of phospholipase C-γ2." In: *Journal of Experimental Medicine*. ISSN: 00221007. DOI: `10.1084/jem.184.1.31`.

Teitell, Michael A. (2005). *The TCL1 family of oncoproteins: Co-activators of transformation*. DOI: `10.1038/nrc1672`.

Ten Hacken, Elisa and Jan A. Burger (2014). "Molecular pathways: Targeting the microenvironment in chronic lymphocytic leukemia-focus on the B-cell receptor." In: *Clinical Cancer Research*. ISSN: 10780432. DOI: `10.1158/1078-0432.CCR-13-0226`.

Thomas, Matthew et al. (2007). "Notch activity synergizes with B-cell-receptor and CD40 signaling to enhance B-cell activation." In: *Blood*. ISSN: 00064971. DOI: `10.1182/blood-2006-09-046698`.

Tresckow, Julia von et al. (2019). "Behandlung der chronischen lymphatischen Leukämie." In: *Deutsches Arzteblatt International*. ISSN: 18660452. DOI: `10.3238/arztebl.2019.0041`.

Villegas, Santiago Nahuel et al. (2018). "PI3K/Akt Cooperates with Oncogenic Notch by Inducing Nitric Oxide-Dependent Inflammation." In: *Cell Reports.* ISSN: 22111247. DOI: `10.1016/j.celrep.2018.02.049`.

Vollbrecht, Claudia et al. (2015). "Comprehensive analysis of disease-related genes in chronic lymphocytic leukemia by multiplex PCR-based next generation sequencing." In: *PloS one* 10.6, e0129544.

Wan, Xueyan et al. (2020). "PDCD10-Deficiency Promotes Malignant Behaviors and Tumor Growth via Triggering EphB4 Kinase Activity in Glioblastoma." In: *Frontiers in Oncology*. ISSN: 2234943X. DOI: `10.3389/fonc.2020.01377`.

Wang, Xiaoyan et al. (2011). "Phosphorylation regulates c-Myc's oncogenic activity in the mammary gland." In: *Cancer Research*. ISSN: 00085472. DOI: `10.1158/0008-5472.CAN-10-1032`.

Wang, Yucai et al. (2020). "Clinical characteristics and outcomes of Richter transformation: Experience of 204 patients from a single center." In: *Haematologica*. ISSN: 15928721. DOI: `10.3324/haematol.2019.224121`.

Wąsik-Szczepanek, Ewa et al. (2018). "Richter syndrome: A rare complication of chronic lymphocytic leukemia or small lymphocytic lymphoma." In: *Advances in Clinical and Experimental Medicine*. ISSN: 24512680. DOI: `10.17219/acem/75903`.

Weiss, Lukas et al. (2011). "Regulatory T cells predict the time to initial treatment in early stage chronic lymphocytic leukemia." In: *Cancer*. ISSN: 0008543X. DOI: `10.1002/cncr.25752`.

Wendel, Hans Guido et al. (2004). "Survival signalling by Akt and eIF4E in oncogenesis and cancer therapy." In: *Nature*. ISSN: 00280836. DOI: `10.1038/nature02369`.

Wendtner, C.-M. et al. (2012). *Chronic Lymphocytic Leukemia Guideline*.

Werner, Markus, Elias Hobeika, and Hassan Jumaa (2010). *Role of PI3K in the generation and survival of B cells*. DOI: `10.1111/j.1600-065X.2010.00934.x`.

Wierda, W. G. et al. (2000). "CD40-ligand (CD154) gene therapy for chronic lymphocytic leukemia." In: *Blood*. ISSN: 00064971. DOI: `10.1182/blood.v96.9.2917.h8002917_2917_2924`.

Wiestner, Adrian (2012). *Emerging role of kinase-targeted strategies in chronic lymphocytic leukemia*. DOI: `10.1182/blood-2012-05-423194`.

– (2015). "The role of b-cell receptor inhibitors in the treatment of patients with chronic lymphocytic leukemia." In: *Haematologica*. ISSN: 15928721. DOI: `10.3324/haematol.2014.119123`.

Willander, Kerstin et al. (2013). "NOTCH1 mutations influence survival in chronic lymphocytic leukemia patients." In: *BMC Cancer*. ISSN: 14712407. DOI: `10.1186/1471-2407-13-274`.

World Health Organization (2020). "Globocan 2020." In: *International Agency for research*.

Xu, Jinhua et al. (2016). "β-catenin regulates c-Myc and CDKN1A expression in breast cancer cells." In: *Molecular Carcinogenesis*. ISSN: 10982744. DOI: `10.1002/mc.22292`.

Yamamoto, Shinya, Wu Lin Charng, and Hugo J. Bellen (2010). *Endocytosis and intracellular trafficking of notch and its ligands*. DOI: `10.1016/S0070-2153(10)92005-X`.

Yang, Jianying and Michael Reth (2015). "Receptor dissociation and B-cell activation." In: *Current Topics in Microbiology and Immunology*. ISSN: 21969965. DOI: `10.1007/82_2015_482`.

Yeh, Yuh Ying et al. (2015). "Characterization of CLL exosomes reveals a distinct microRNA signature and enhanced secretion by activation of BCR signaling." In: *Blood*. ISSN: 15280020. DOI: `10.1182/blood-2014-12-618470`.

Yuille, Martin R. et al. (2001). "TCL1 is activated by chromosomal rearrangement or by hypomethylation." In: *Genes Chromosomes and Cancer*. ISSN: 10452257. DOI: `10.1002/gcc.1099`.

Zhang, Qingxiu and Francois X. Claret (2012). *Phosphatases: The new brakes for cancer development?* DOI: `10.1155/2012/659649`.

Zhang, Wei et al. (2018). "MeCP2 deficiency promotes cell reprogramming by stimulating IGF1/AKT/mTOR signaling and activating ribosomal protein-mediated cell cycle gene translation." In: *Journal of Molecular Cell Biology*. ISSN: 17594685. DOI: `10.1093/jmcb/mjy018`.

Zhang, Xinbo et al. (2011). *Akt, FoxO and regulation of apoptosis*. DOI: `10.1016/j.bbamcr.2011.03.010`.

Zhu, Zilu et al. (2019). "The AKT isoforms 1 and 2 drive B cell fate decisions during the germinal center response." In: *Life Science Alliance*. ISSN: 25751077. DOI: `10.26508/lsa.201900506`.

Zhuang, Jianguo et al. (2010). "Akt is activated in chronic lymphocytic leukemia cells and delivers a pro-survival signal: The therapeutic potential of Akt inhibition." In: *Haematologica*. ISSN: 03906078. DOI: `10.3324/haematol.2009.010272`.

Zimmer, Danna B. et al. (1995). "The S100 protein family: History, function, and expression." In: *Brain Research Bulletin*. ISSN: 03619230. DOI: `10.1016/0361-9230(95)00040-2`.

Zolkiewska, A. (2008). *ADAM proteases: Ligand processing and modulation of the Notch pathway*. DOI: `10.1007/s00018-008-7586-4`.

Zurli, Vanessa et al. (2017). "Ectopic ILT3 controls BCR-dependent activation of Akt in B-cell chronic lymphocytic leukemia." In: *Blood*. ISSN: 15280020. DOI: `10.1182/blood-2017-03-775858`.

6 Danksagung

An dieser Stelle möchte ich mich herzlich bei all den Personen bedanken, die auf vielfältige Art und Weise zum Erfolg dieser Arbeit beigetragen und mich auf meinem Weg der Promotion begleitet haben:

- **PD Dr. F. Thomas Wunderlich**, der mich in seiner Arbeitsgruppe aufgenommen und mir die Anfertigung dieser Dissertation ermöglicht hat. Dadurch wurde mir die Möglichkeit geboten, an einem faszinierendem Thema zu forschen. Während der gesamten Zeit hat seine aufgeschlossene Einstellung zur Wissenschaft eine großartige Arbeitsatmosphäre geschaffen, in der ich meine Forschungsideen frei entwickeln und mit ihm wissenschaftlich diskutieren konnte.

- **PD Dr. F. Thomas Wunderlich, Prof. Dr. Lutz Schmitt** und **Prof. Dr. Jörg Pietruszka** für die Bereitschaft meine Doktorarbeit als Gutachter bzw. Mentor zu unterstützen.

- **Prof. Dr. Jens Brüning**, den Direktor des Max-Planck-Instituts für Stoffwechselforschung, für die freundliche Aufnahme an dem Institut.

- **Patrick Jankowski, Lisa Böcking, Pia Scholl, Nadine Spenrath, Anke Lietzau** und **Heike Krämer** für die Unterstützung im Labor als technische Assistent*innen.

- **Eddie O'Brien** und **Christina Strassner** für die Versorgung meiner Mäuse.

- **AG Wunderlich** für die sehr gute Zusammenarbeit und angenehme Atmosphäre.

- **AG Brüning, AG Steculorum, AG Fenselau** und **AG Backes** für die schöne Zeit als Kolleg*innen und die regen Diskussionen.

- **Mitarbeiter*innen** des Max-Planck-Instituts für Stoffwechselforschung für die stete Hilfsbereitschaft und Zusammenarbeit.

- **Dr. Mona al-Maarri, Dr. Stuart Blakemore, Prof. Dr. Christian Pallasch, Dr. Nadine Hövelmeyer, Dr. Janica Wiederstein** und **Prof. Dr. Marcus Krüger** für die guten Kollaborationen.

- **Philipp Mülheims** für seinen Rückhalt und uneingeschränktes Vertrauen, sowie die Unterstützung in den letzten 4 Jahren, die sich nicht in Worte fassen lässt.

- **Meine Familie** und **Freunde**, die immer an mich glauben und unterstützen.

Vielen Dank!

7   Versicherung

Ich versichere, dass ich die von mir vorgelegte Dissertation selbständig angefertigt, die benutzten Quellen und Hilfsmittel vollständig angegeben und die Stellen der Arbeit - einschließlich Tabellen, Karten und Abbildungen -, die anderen Werken im Wortlaut oder dem Sinn nach entnommen sind, als Entlehnung kenntlich gemacht habe; dass diese Dissertation noch keiner anderen Fakultät oder Universität zur Prüfung vorgelegen hat; dass sie - abgesehen von oben angegebenen Teilpublikationen - noch nicht veröffentlicht worden ist sowie, dass ich eine solche Veröffentlichung vor Abschluss des Promotionsverfahrens nicht vornehmen werde. Die Bestimmungen dieser Promotionsordnung sind mir bekannt. Die von mir vorgelegte Dissertation ist von PD Dr. F. Thomas Wunderlich betreut worden.

.

Vivien Kohlhaas

(Köln, den 02.03.2021)

Curriculum Vitae

Personal Information

Name	Vivien Kohlhaas
Date of Birth	April 4th, 1994
Place of Birth	Witten, Germany
Mail	Vivien.Kohlhaas@sf.mpg.de

Further Education

2017-2021	**PhD** under supervision of Habil. T. Wunderlich, PhD; MPI for Metabolism Research, Cologne Heinrich-Heine-University, Düsseldorf
2015-2016	**Master Study** ‚Biochemistry', Fast Track Heinrich-Heine-Universität, Düsseldorf
2012-2015	**BSc** ‚Biochemistry' (ECTS: A) Heinrich-Heine-Universität, Düsseldorf
	'The Analysis of Interorgan Lipid Handling in Mouse Models with Tissue-Specific Overexpression of SREBP-1c' under supervision of Habil. Michael Roden, PhD; German Diabetes Center (DDZ), Düsseldorf

Academic Fellowship

2013-2016	Grant 'Deutschlandstipendium Chancen Nutzen'

Publications

Cox, EM, El Behi, M, (submitted), **AKT activity orchestrates marginal zone B cell development in mouse and human**. *Journal of Experimental Medicine.*

Kohlhaas, V, Blakemore, SJ, Al-Maarri, M, (2020), **Active Akt signaling triggers CLL toward Richter transformation** *via* **overactivation of Notch1**. *Blood*. 137 (5):646–660.

Jelenik, T, Fjögel, U, Alvarez-Hermandez, E, (2018), **Insulin resistance and vulnerability to cardiac ischemia**, *Diabetes*. 67(12) 2695-2702

Conferences, Seminar

2021	*Lecturer ReSi Seminar, Cologne*
2020	Cell Press – New Horizons in B Cell Biology Conference, Shanghai
2018	Global Health Conference ‚World Health Summit', invited by ‘Melinda & Bill Gates Foundation', Berlin

Extracurricular Experience

Lecturer	-biomedical and biotechnological academies at the ‘Science College Overbach' (since 2017)
	-mathematics academies of the ‘Landesverband Mathematikwettbewerbe NRW e. V.' (until 2016)
	-scientific talk about ‚Non-destructive testing of materials', invited by the German Research Foundation (DFG) and ‚Ministerium für Familie, Kinder, Jugend, Kultur und Sport des Landes Nordrhein-Westfalen' (2012)
Juror	-‚Jugend forscht' for biology and chemistry (since 2016)
Membership	-STEM ambassador at ‚MINT Zukunft schaffen' (since 2016)
	-Member of the GBM